Foundations: Shallow and deep foundations, unsaturated conditions, heave and collapse, monitoring and proof testing

1 author:

António Viana Da Fonseca
University of Porto

8

Foundations: Shallow and deep foundations, unsaturated conditions, heave and collapse, monitoring and proof testing

A. Viana da Fonseca
University of Porto, Portugal

S. Buttling
Senior Principal Geotechnical Engineer, GHD, Brisbane, Australia

R.Q. Coutinho
Federal University of Pernambuco, Brazil

8.1 INTRODUCTION

Many aspects of foundation design and construction in tropical soils are the same as those in sedimented soils, about which many text books have already been written. We have therefore tried to emphasise those aspects of foundation engineering on tropical soils which are unconventional, based on our combined experiences in many regions of the world where tropical residual soils exist.

In many parts of the engineering world, limit state design methods are now being used for geotechnical designs. In some places, for example Australia, they have been around for 15 years already. In others, such as Europe, they have only recently been implemented. In the past, when considering shallow foundations on cohesive soils, an adequate factor of safety (probably 3) on ultimate bearing capacity failure was considered enough to also provide a limit on settlement. On cohesionless soils, the ultimate bearing capacities were generally well in excess of what might be required, and allowable settlement would control the design. Hence, the charts produced by Terzaghi which showed the bearing pressure that would lead to 25 mm (1 inch) of settlement for a range of soil densities (SPT N values). Now it is again found that, in many circumstances, the ultimate limit state can be designed for without difficulty, and it is the serviceability limit state which governs. To adequately satisfy this limit state requires a reasonable knowledge of foundation performance, and particularly foundation stiffness. Much of this chapter is devoted to discussing methods of predicting foundation behaviour.

8.2 DIRECT (SHALLOW) FOUNDATIONS

8.2.1 Solutions to foundations on residual soils – factors that affect the concept

Foundations in residual soils might be considered as one more aspect of the broad range of foundation engineering. However, what makes residual soils special is that they contain the characteristics of all the main soil groups (fine or coarse materials, cohesive or granular soils etc.), and they fit in between soils and rock masses in what can be classified as "Intermediate Geotechnical Material" (IGM), see Figure 8.1. As a result, foundation performance can be very variable and designs can often be based on adaptations of designs suited to either soils or rocks. Regional practice and local experience can help to find satisfactory solutions, generally empirical, but they are no substitute for detailed soil investigation of heterogeneities, and monitoring of foundation construction (e.g. by automated pile construction monitoring).

8.2.2 Particular conditions in residual soils

Microstructure, non-linear stiffness, small and large strain anisotropy, weathering and its effects on structure, consolidation characteristics and strain rate dependency

Figure 8.1 Uncertainties due to heterogeneities of residual profiles (*After* Milititsky *et al.*, 2005)

(Schnaid, 2005) are all very important factors in assessing the mechanical characteristics of natural soils, therefore new techniques of measuring soil properties or, better still, new interpretation methods (Viana da Fonseca and Coutinho, 2008) are required. Most of the soils are unsaturated, and need to be dealt with carefully. Since bonded geomaterials, such as residual soils, are highly variable, the interpretation of their mechanical behaviour is complex. Because of the variability, one suitable solution involves cross-correlation of multiple measurements from different tests, but it is even better to have more measurements in one test.

Igneous rocks, like granite, are composed mainly of quartz, feldspar and mica. Quartz is resistant to chemical decomposition, while feldspar and mica are transformed mainly into clay minerals during the weathering process. The effects of temperature, drainage and topography have reduced the rocks in place to residual soils that range from clays to sandy silts and silty sands, grading with depth into saprolite and partially weathered rocks. As weathering proceeds, the reduction in vertical stress as a result of the removal of overburden accelerates the rate of exfoliation (stress release jointing) and the alternate wetting and drying processes in the underlying fresh rock (Viana da Fonseca and Coutinho, 2008). These processes increase the surface area of rock on which weathering can proceed, which leads to deeper weathering profiles (Irfan, 1988; Ng and Leung, 2007b).

Depending on the degree of alteration, some residual soils lose all the features of the parent rock, while others, as illustrated in Figure 8.2, have clear relict structure (Rocha Filho, 1986; Costa Filho *et al.*, 1989; Viana da Fonseca, 2003). Examples of relict structures include evidence of bonding or dissolved bond features, as well as cracks and fissures from the original fractured rock mass (Mayne and Brown, 2003).

Degree of weathering: topographic complexities and characteristics of profiles

Looking at the weathering profile from the bottom upwards, one can find materials grading all the way from fresh rock, through slightly and moderately weathered rock, to soil which retains the characteristics of rock (called young residual or saprolitic soil), to the upper horizon where no remaining rock characteristics can be seen (known as mature residual or lateritic soil). The upper layers may be mixed with transported soil,

Figure 8.2 Parent rock with potentially unstable weak features (Porto, Portugal)

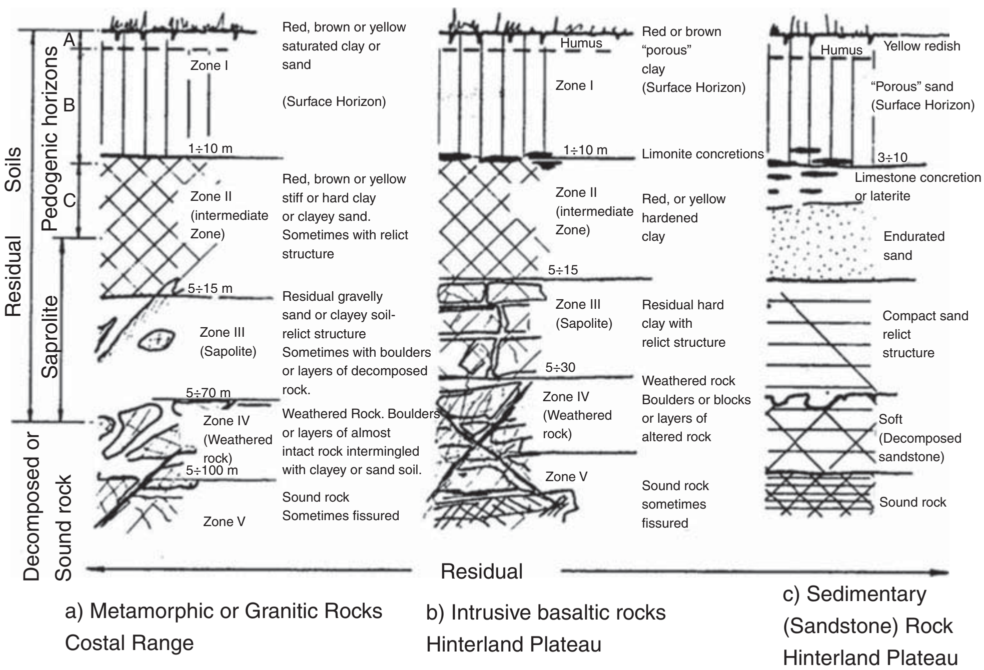

Figure 8.3 Typical profiles of Brazilian residual soils – some zones may be absent (*After* Vargas, 1985)

such as colluvium, which may be difficult to distinguish from the true residual soils. Figure 8.3 presents a proposal for the classification of such profiles. Unfortunately, the sequence is exactly the opposite of that of weathering grades proposed by Dearman (1976), in which Grade I represents Fresh Rock, and Grade VI Residual Soil. Therefore, the term Zone will be used as in the diagram in Figure 8.3.

Zone II (lateritic soil) is usually formed under hot and humid conditions involving high permeability profiles, resulting in a bond structure with high contents of oxides and hydroxides of iron and aluminium (laterisation). Not all soils belonging to this horizon develop enough pedogenetic evolution for laterisation. The Zone III (saprolitic soil) can show a high level of heterogeneity both vertically and laterally as well as a complex structural arrangement which retains the characteristics of the parent rock. The texture and mineralogy of these soils can vary considerably with the degree of weathering and leaching. In a tropical region the weathering profile often shows a very narrow or inexistent Zone V, while in temperate climates this zone can be reasonably thick.

Mitchell and Coutinho (1991), Lacerda and Almeida (1995), and Clayton and Serratrice (1998) each present a general view of many soils which are called unusual soils (Schnaid *et al.*, 2004; Coutinho *et al.*, 2004a), including bonded soils, granitic saprolitic soil and lateritic soils, and unsaturated collapsible soils. Bonding and structure are important components of shear strength in residual soils, since they have a major impact on the cohesive-frictional response (characterised by c' and ϕ'). Anisotropy, derived from relict structures of the parent rock, can also be a characteristic of a residual soil. In those conditions, the structure formed during the weathering process can become very sensitive to external loads, requiring special sampling techniques in order to preserve it. This topic of sampling representativeness is very sensitive in these materials and is discussed in Viana da Fonseca and Coutinho (2008). The effects of sampling on the behaviour of soft clays, stiff clays, and sands, is described in Hight (2000) as well as the improvements that have been made to more common methods of sampling, which have enabled higher quality samples to be obtained. Residual soils are too variable to index them as clays or sands, or as intermediate materials, but certainly their behaviour is very much dependent on their macro- and micro-interparticle bonded structure, which has to be preserved both when they are weak (sensitive to induced strains) or stronger (less weathered profiles). Conventional rotary core sampling and block sampling are considered suitable techniques to obtain sufficiently intact samples for determining shear strength and stiffness of soils derived from *in situ* rock decomposition. In Portugal, as in Hong Kong, the Mazier core-barrel is becoming common for soil sampling (Viana da Fonseca and Coutinho, 2008). When a soil sample with the least possible disturbance is required, the block sampling technique can be applied.

Local experience in Hong Kong has found the Mazier technique to be the most suitable sampling method available for weathered granular materials at depths (Ng and Leung, 2007a). However, comparable studies between samples recovered by this method and block samples, carried out in the University of Porto (Ferreira *et al.*, 2002), have proved that the Mazier technique is very sensitive to the execution process, particularly for the pressure, flow volume and type of drilling fluid, putting the natural structure at risk for the more weathered and granular profiles. Some results are presented in Figure 8.4. In Ng and Leung (2007a), and again in Ng and Leung (2007b), the authors note that the shear-wave velocities of the block specimens were an average 27% higher than those of the Mazier specimens.

Usually, the void ratio and density of a residual soil are not directly related to its stress history, unlike the case of sedimentary clayey soils (Vaughan, 1985; Vaughan *et al.*, 1988; GSEGWP, 1990; Viana da Fonseca, 2003). The presence of some kind of bonding, even weak, usually implies the existence of a peak shear strength envelope, showing a cohesion intercept and a yield stress which marks a discontinuity in stress-strain behaviour. The structure in natural soil has two "faces": the "fabric"

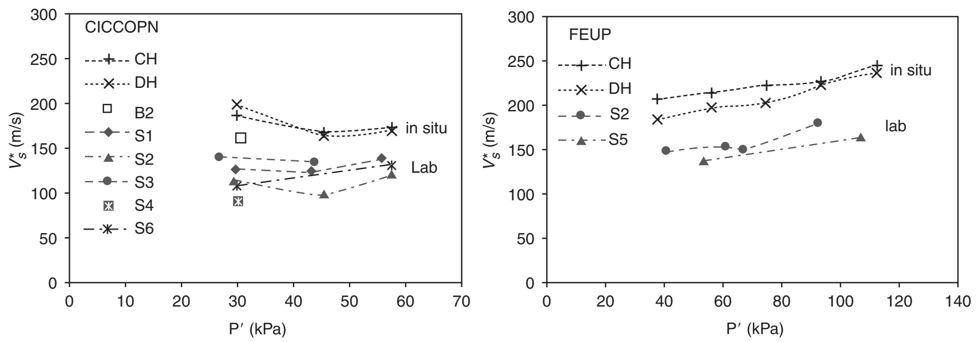

Sampler: B2 – Block; S1 – GMPV; S2 – ST85; S3 – NT81; S4 - Mazier; S5 – Osterberg; S6 – Shelby
CH – Crosshole; DH – Downhole

Figure 8.4 Normalised shear wave velocities, for different types of samplers used in residual soil from granite in two experimental sites in Porto (*After* Ferreira *et al.*, 2004)

that represents the spatial arrangement of soil particles and inter-particle contacts, and "bonding" between particles, which can be progressively destroyed during plastic straining (leading to the term "destructuration"). Most, if not all, geomaterials are structured, but the mechanical response of naturally bonded soils is dominated by this effect (Leroueil and Vaughan, 1990). Here the cohesive component due to cementation can dominate soil shear strength, especially in engineering applications involving low stress levels (Schnaid, 2005) or in specific stress-paths where this component is relevant, such as cut slopes.

Trying not to make the wrong choice of foundation type

Residual masses generally exhibit stronger heterogeneity than deposited soils, changing their characteristics gradually both laterally and vertically, especially with regard to their mechanical properties. As a result, it is common to have to adopt different foundation types, such as shallow foundations (footings and mats) and deep foundations (piles), within very limited areas, depending upon the consistency of the overburden soils and the depth to parent rock (Figure 8.5). An accurate mapping of the spatial variability of the mechanical properties, essential for geotechnical design, is very challenging although the situation has improved recently by the use of geophysical methods (Viana da Fonseca *et al.*, 2006). Several *in situ* testing methodologies, such as Standard Penetration Testing (SPT), Cone Penetrometer Testing (CPT), Dilatometer Testing (DMT), Pressuremeter Testing (PMT) and Self Boring Pressuremeter Testing (SBPT), and geophysical survey, surface and borehole seismic tests, electrical resistivity and Ground Penetrating Radar (GPR), have been used to assess the mechanical properties of these particular soils, with varying degrees of success (Figure 8.6).

The water table is in many cases deep in the profile; hence there is a significant layer of unsaturated soil. In this case, the role of matrix suction and its effect on soil behaviour has to be recognised and considered in the interpretation of *in situ* tests. The main difference between saturated soils and unsaturated soils is the existence of

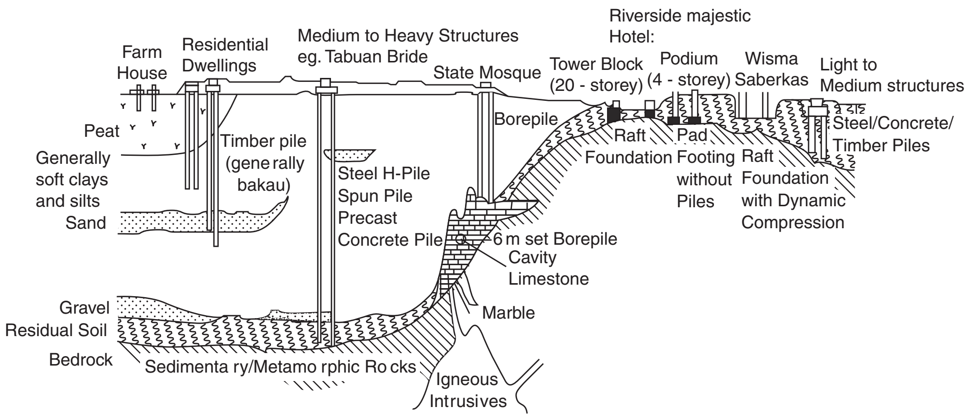

Figure 8.5 Different foundations and relationships to the rockline (*After* Yogeswaran, 1995; Singh *et al.*, 2006)

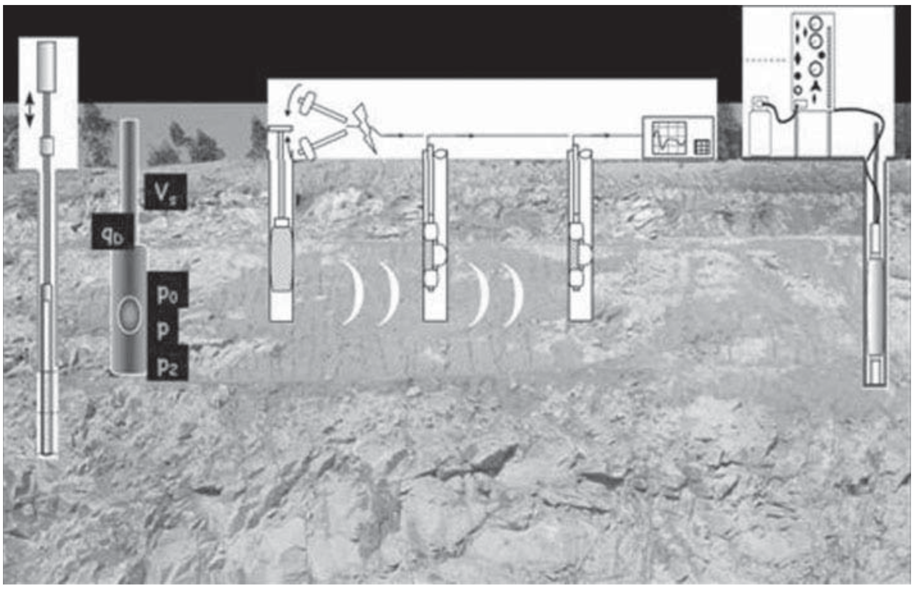

Figure 8.6 Multiple solutions for *in situ* testing of characterisation in complex and highly heterogeneous weathered rocks and/or residual soils (*After* Viana da Fonseca, 2006)

negative porewater pressures, largely known as suction, which tends to increase the effective stresses and hence the strength and stiffness of the soil.

Residual soils derived from a wide variety of parent rocks can also be collapsible, which has serious consequences for foundation behaviour. Collapsible residual soils have a metastable state characterised by a honeycomb structure and partially saturated condition that can develop after a parent rock has been thoroughly decomposed or

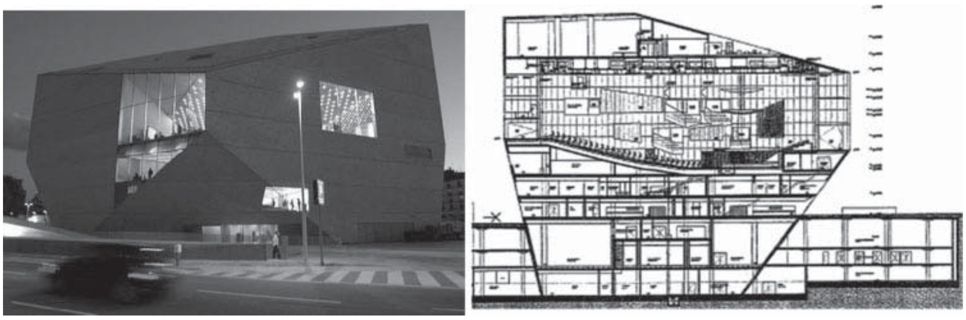

Figure 8.7 View and section through building and car park (*After* Gaba *et al.*, 2004)

while the decomposition is continuing (Vargas, 1971). Commonly, collapsible residual soils form under conditions of heavy concentrated rainfalls in short periods of time, followed by long dry periods, high temperature, high evaporation rates, and flat slopes, so that leaching of material can occur. There are two mechanisms of bonding in the metastable soil structure: soil water suction and cementation by clay or other types of fine particles. Collapsible residual soils usually have low activity and low plasticity. Colluvial deposits (or mature residual soils) can become collapsible in environments where the climate is characterised by alternating wet and dry seasons that cause a continuous process of leaching of the soluble salts and colloidal particles much like residuals soils (Mitchell and Coutinho, 1991).

8.2.3 Main demands for the guarantee of structural limit state conditions

Differential settlements caused by heterogeneity in plan and depth

Foundation displacements can be considered both in terms of displacement of the entire foundation, and differential displacements of parts of the foundation. As well stated in structural codes such as EN1997-1, to ensure the avoidance of a serviceability limit state, assessment of differential settlements and relative rotations shall take account of both the distribution of loads and the possible variability of the ground, unless they are prevented by the stiffness of the structure. Because of the heterogeneity inherent in weathered rock masses and residual soils,as discussed above, where the state of weathering, decomposition and fracturing of the rock may vary considerably in depth and plan, this conditions the design of spread foundations or other mixed solutions.

Foundations for special projects, such as that described by Gaba *et al.* (2004), have to be developed in a way that they ensure strict settlement control. In this case history, the ground investigation, interpretation and foundation design and construction for the Casa da Música do Porto, Portugal, is described. The overall project comprised detailed multi-disciplinary design of the structure, foundations and building services for a 20,000 m^2, high quality concert hall (Figure 8.7).

The ground investigation included boreholes, with SPT and dynamic probing (DPSH and jet grout probing) correlated to be used in the foundation design.

A shallow foundation option, with a methodological improvement of specific zones by jet-grouting, was considered.

Boreholes identified a sequence of residual soil overlying completely decomposed granite (Grade V) over highly and moderately weathered granites (Grade IV and III) below final formation. Grade III granite or better was considered to be competent rock, and a suitable founding material. The boundary between Grade IV and Grade III granite was therefore selected as "engineering rock head" (ERH) for design purposes. The thickness of each weathering grade above this level was found to vary significantly across the site, especially the Grade V granite, presenting potential problems with differential settlements across the structure. Probing was therefore carried out to investigate this variability in more detail. In order to determine the elevation of the ERH with a greater degree of certainty, "jet grout probes" were made (Figure 8.8a). This probing was carried out by drilling through the residual soil and weathered rock using a jet-grouting rig until it met refusal. This technique was chosen because of the ready availability of appropriate plant on site and the relative speed with which the probing could be carried out in comparison with drilling boreholes. This meant that a large number of locations could be probed in a short period of time and the ERH level defined in an expeditious way (Figure 8.8b). The probing was carried out along the lines of load bearing walls and at column locations within the building footprint.

The design of the building used the soil stiffness derived from the penetration tests, and the loading of each zone was modelled using the *Oasys* computer program VDISP (Oasys, 2001). From these analyses, spring stiffness values for each zone were derived and input into a structural model of the building in order to assess the bearing pressures and anticipated settlements. The foundations were represented in the structural analysis as "slab on Winkler soil" finite elements. The design criteria required limits on total and differential settlement. The structural analysis demonstrated that it was not feasible to satisfy the settlement criteria using a shallow foundation scheme, even with ground improvement. A piled solution was therefore adopted, in which end bearing and shaft friction in a socket extending 1 m below ERH provided sufficient geotechnical load capacity for the piles and a stiff loading response, and resulted in the structural capacity of the concrete being the limiting factor in pile design. An allowable working concrete stress of 5 MPa was adopted.

In order to ensure satisfactory construction of the piles, construction controls and acceptance criteria were applied. These included specifying target foundation depths and maximum pile bore penetration rates at the founding level. Integrity testing confirmed that the piles were sound and of good quality construction.

There are several other case histories reported in the literature, where the spatial development of the weathered rock and residual soils is highly irregular and erratic. In the city of Porto, the design and construction of the Metro was based on weathering grades and structural features which were used for the derivation of the design parameters (Babendererde *et al.*, 2004). The highly variable nature of the deeply weathered Porto granite posed significant challenges in the driving of around 7 km of tunnels in largely populated urban areas, involving a large number of underground stations. The change from one weathered zone to another is neither progressive nor transitional (Viana da Fonseca, 2003; Babendererde *et al.*, 2004; Marques *et al.*, 2004), moving abruptly from a fresh granitic mass to a very weathered soil-like mass. The thickness of the weathered parts varies very quickly from several meters to zero. Blocks of sound

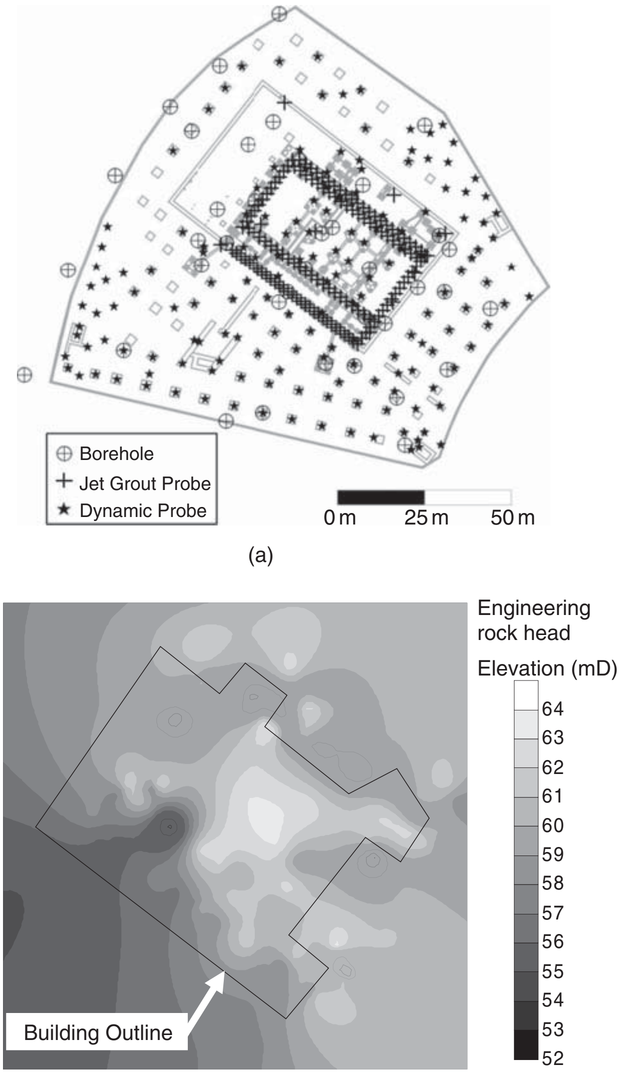

(b)

Figure 8.8 (a) Plan of the ground investigation; (b) Contours of engineering rock head within building footprint (*After* Gaba *et al*., 2004)

rock (boulders or corestones), of various dimensions can "float" inside completely decomposed granite. Weathered material, either transported or *in situ*, also occurs in discontinuities. A particularly striking feature is that, due to the erratic weathering of the granite, weathered zones of considerable size, well beyond the size of typical "boulders", can be found under zones of sound granite. A typical case of this is illustrated in Figure 8.9 showing the appearance of Porto granite in the face of an excavation for

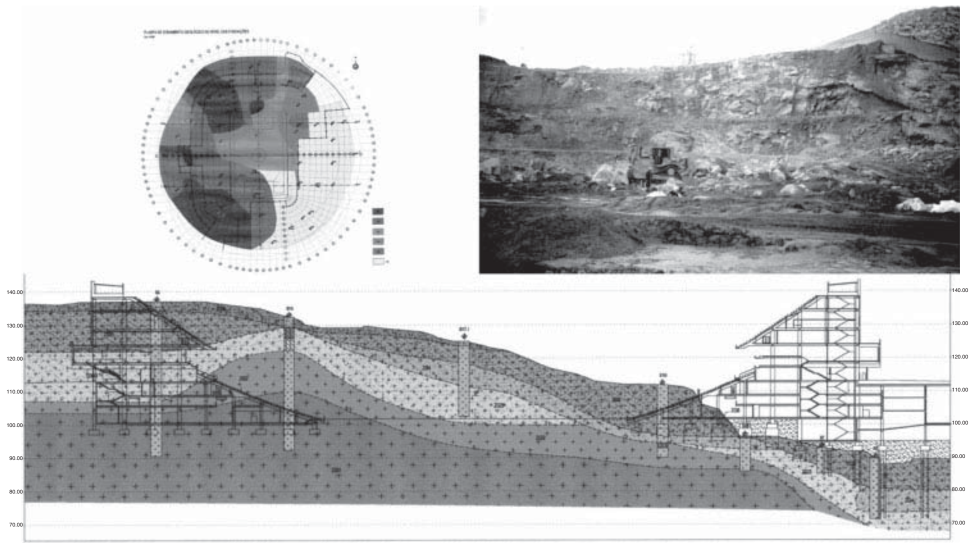

Figure 8.9 Appearance of Porto granite in the face of an excavation (Babendererde *et al.*, 2004) for the new football F. C. Porto stadium and distinct foundations solutions as designed by Campos e Matos *et al.* (2004)

the new football stadium of F. C. Porto. Fracturing of the rock mass and heterogeneity in weathering is obvious.

Load tests on residual soil and settlement prediction on shallow foundation

Semi-empirical methods, based on linear and non-linear behaviour models, mainly for settlement prediction purposes, are often used for the design of shallow foundations. Viana da Fonseca (1996 and 2001) discussed the applicability of such methods, by analyzing the results obtained at an experimental site on a fairly homogeneous saprolitic soil derived from granite. This included *in situ* and laboratory tests, together with a full-scale load test on circular concrete footings. The information obtained in terms of strength and stiffness was combined, with the aim of refining some of the approaches based on the Theory of Elasticity. Emphasis was especially given to semi-empirical methods based on results of *in situ* tests (SPT, CPT, PLT, PMT, DMT and Seismic Cross-Hole tests), but also on the use of results from very precise triaxial tests on high quality samples. Some of the well established methods (Parry, 1978; Burland and Burbidge, 1985; Anagnastopoulos *et al.*, 1991; Schmertmann *et al.*, 1978; Robertson, 1990, 1991; Ghionna *et al.*. 1991; or Wahls and Gupta, 1994 – see below) were tested and some adaptations to parameters and methods were suggested that gave a better fit to the observed behaviour.

Experimental site and analysis of the loading tests

The experimental work was carried out at a site (around 50 m × 30 m) in which a homogeneous saprolitic soil 6 m thick had been identified by a previous site investigation.

Figure 8.10 Overview of the weathered profile revealed in a fresh cutting on the experimental site

Geologically, the parent rock is representative of the granite from Porto region (Viana da Fonseca, 2003). Figure 8.10, taken at the end of the experimental investigation and prior to the construction of a new building for a District Hospital, gives a clear overview of the general saprolitic profile developing with depth.

Apart from the natural spatial variation of the relict structure and fabric of these residual soils, there is evidence of a reasonably homogeneous geotechnical profile, as revealed by results obtained from specimens taken with the SPT sampler and from blocks. A detailed description of the extensive testing programme is given in Viana da Fonseca (2003). Only the results of SPT, CPT and DMT tests and the values of the maximum shear modulus, G_0, obtained from CH tests are shown here in Figure 8.11. It is observed that the CPT cone resistance, q_c, the N_{60} from SPT and p_0 and p_1 from DMT, show a nearly linear increase with depth (or vertical effective stress, σ'_{v0}), whilst G_0 appears to be almost constant.

The loading test of a full scale circular concrete footing, with a diameter of 1.20 m and fully instrumented, was carried out (Figure 8.12a), and is described in detail in Viana da Fonseca (2001). The resulting complete pressure-settlement curve shows a clear increase of the settlement rate with load for pressure values exceeding around 125 kPa (Figure 8.12b).

The time for settlement stabilisation at each load step significantly increased above this pressure, representing a transition from an essentially elastic behaviour, confirmed by the small difference between the inclination of the first loading curve and that of the first unload-reload cycle, to a phase in which the cemented structure of the soil was substantially damaged. Serviceability limit state pressure, applying the criterion proposed by Décourt (1992), is defined by a settlement of 0.75% of the diameter

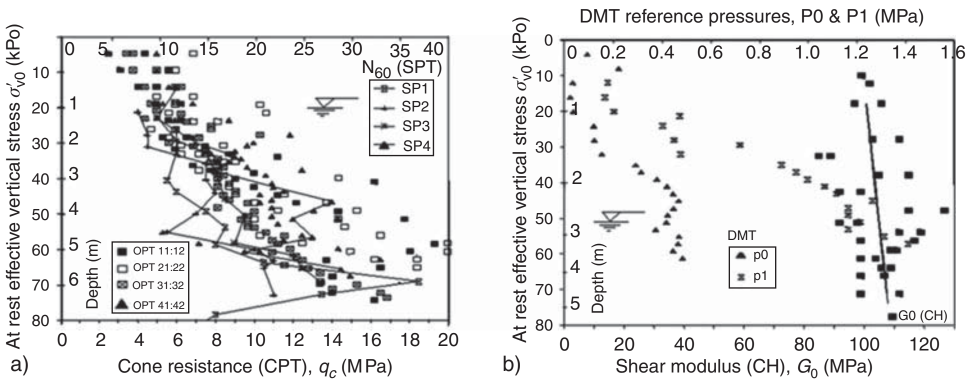

Figure 8.11 *In situ* test results: (a) SPT and CPT; (b) CH and DMT

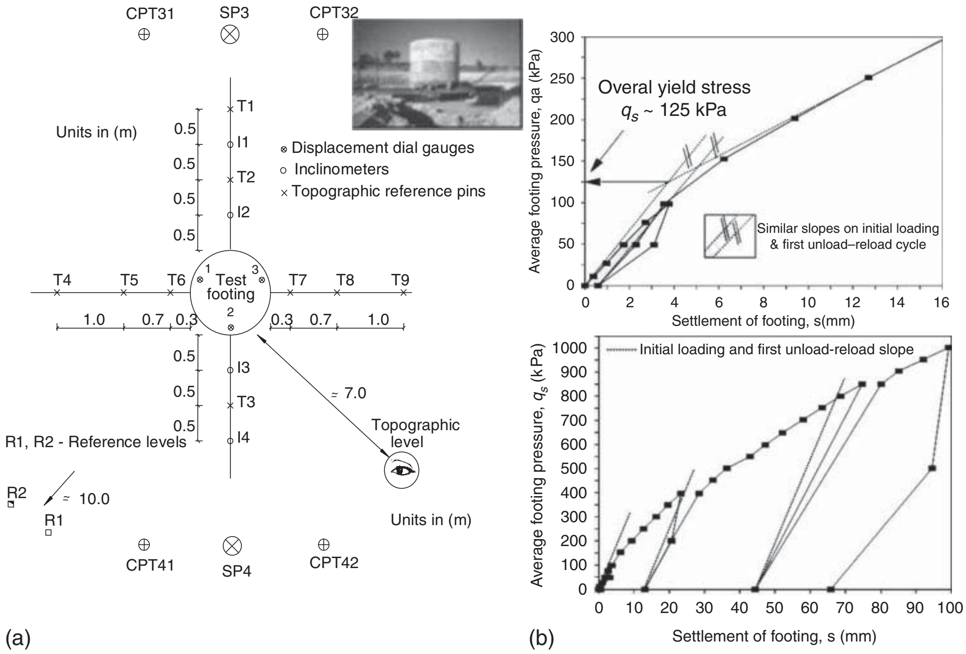

Figure 8.12 (a) Plan of the experimental area; (b) pressure-settlement curve of the footing loading test – general picture and enlargement for $q_s \leq 300$ kPa (*After* Viana da Fonseca, 2001)

of the loading surface, which corresponds to an applied pressure of about 195 kPa. Viana da Fonseca *et al.* (1997) discussed the strain distribution under the centre of the footing obtained from a simplified nonlinear elastic analysis, for applied pressures of 100, 200 and 400 kPa, corresponding to a value near to the serviceability limit state pressure, and to half and twice that value; strain values exceed 10^{-3} only in a restricted zone adjacent to the footing. These results corroborate evidence (Jardine *et al.*, 1986; Burland, 1989; Tatsuoka and Kohata, 1995) of the rather low strain

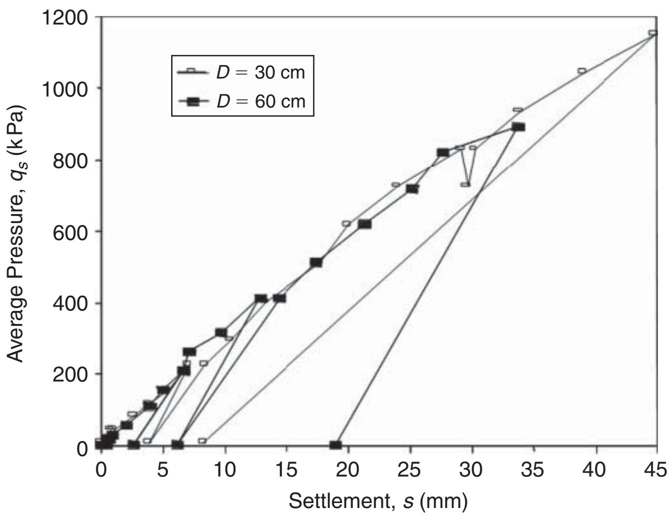

Figure 8.13 Pressure-settlement curve of the plate loading tests ($D = 30$ and 60 cm)

levels involved in a number of soil-structure interaction problems, including shallow foundations, under working conditions. The analysis of vertical displacement of the ground surface around the footing, and the horizontal displacements at the surface and in the ground in its vicinity were also discussed by Viana da Fonseca (2001). Based on the evidence presented, it can be stated that the applicability of elasticity theory to a settlement analysis under service conditions, is reasonable from a practical point of view. In residual soils, the bearing capacity is due to strength factors related to friction and cohesive components of the stressed ground. Reliable results for these can only be determined by two or more *in situ* loading tests, using different sizes and over a homogeneous space.

The execution of more than one loading test to define failure patterns has the advantage of allowing an integrated analysis of different pressure-displacement curves, enabling the importance of both stiffness and depth of influence to be studied. On the same homogeneous soil zone as the footing loading test, two more surfaces were prepared for testing smaller plates of 30 and 60 cm diameter (Figure 8.13). An analysis of punching type failures in these residual soils has been made and from those failure loads (Viana da Fonseca *et al.*, 1997), in the bearing capacity formulation (EN 1997-1), taking account of the water level position, three equations are obtained. These can be optimised to get a range for the two Mohr-Coulomb strength parameters. The derived values were: $c' \cong 7$ kPa and $\phi' \cong 37°$, revealing a fair agreement with the results obtained from extensive laboratory testing of undisturbed samples (Viana da Fonseca, 1998) and from *in situ* testing (Viana da Fonseca *et al.*, 1998).

Deformability characteristics evaluated from loading tests

The common interpretation of the results taken from loading tests on three different sized loaded areas was done by considering Young's modulus constant with depth,

Table 8.1 Ratios between *in situ* tests parameters (*After* Viana da Fonseca *et al.*, 2001, 2003, 2006)

q_c/P_L	N_{60}/P_L (MPa^{-1})	N_{60}/E_{PMT} (MPa^{-1})	E_{PMT}/P_L	E_{PMTUR}/E_{PMT}	E_D/E_{PMT}
4–6	14.6	1.4	10–12	1.4–1.9	$\cong 1.5$

N_{60} – 0 number of blows in SPT for an energy ratio of 60%; q_c – CPT cone resistance; E_{PMT}, E_{PMTUR} – pressuremeter modulus ("elastic" and unload/reload); E_D – Dilatometer modulus; P_L – Net limit pressure of PMT

and by assuming an increase in stiffness with depth (Viana da Fonseca, 1999; Viana da Fonseca and Cardoso, 1999). From these analyses, the trend of increasing values of Young's modulus with the loading area is clear. Therefore, the first conclusion to be drawn is that an increase in stiffness with depth is to be expected and has an obvious relation to the results of penetration testing with depth (more than the very smooth increase of the dynamic modulus, G_0). The position of the settlement centre, z_I (Carrier and Christian, 1973), for circular foundations, was determined to be $z_I \cong B$.

It is interesting to note that, considering the results of the CID triaxial tests (details below) under a consolidation effective stress corresponding to a depth similar to the footing diameter, the tangent Young's modulus for the K_0 shear stress level was found to be $E_{tK0} \cong 8$ MPa. The use of such a modulus in an elastic analysis of the footing loading test would lead to a crude overestimation of the observed settlement. However, if E_{tK0} is multiplied by a factor of "sampling representativeness" (G_0/G_{el}) one obtains a value that would provide a good prediction of the settlement for typical working conditions (the methodology is thoroughly discussed in Viana da Fonseca *et al.*, 1997). This observation suggests that the application of a design methodology that corrects the values of the deformation modulus from triaxial tests by factors referenced to field tests (Cross-Hole tests or similar) may give good results.

Correlations between in situ test parameters

Viana da Fonseca *et al.* (2001, 2003, 2006) made an analysis of two experimental sites on Porto granite saprolitic soils, including derived ratios between PMT and SPT or CPT parameters. Some correlations are included in Table 8.1.

Ratios between distinct values of Young's moduli inferred from the investigations conducted have the obvious interest of fulfilling the needs of geotechnical designers to obtain data from different origins for each specific purpose.

Viana da Fonseca *et al.* (2001, 2003) and Topa Gomes (2009) reported some interesting correlations from data available in local sites: (i) values of Young's moduli determined directly, with no empirical treatment, or without deriving assumptions; (ii) common constant ratios that are assumed to correlate SPT (DP) or CPT parameters with Young's modulus, comparing them with transported soils; (iii) relative values of moduli can be summarised in the way that is expressed in Table 8.2a, while some relations could be pointed out between *in situ* tests, as expressed in Table 8.2b.

It is interesting to note that, for most designs, Sabatini *et al.* (2002) state that the elastic modulus corresponding to 25 percent of failure stress, E_{25}, may be used. In Piedmont residual soils, the use of the dilatometer modulus, E_D, as equal to E_{25} has been shown to provide reasonably accurate predictions of settlement (Mayne and

Table 8.2a Ratios between deformability (Young and Shear) modulus (*After* Viana da Fonseca *et al*., 1998a, 2001, 2003; Topa Gomes, *2009*)

$E_0(CH)/E_{s1\%}(PLT)$	$E_0(CH)/E_{ur}(PLT)$	$E_0(CH)/E_m$	$G_0(CH)/G_{ur}(SBP)$
$\cong$8–15	$\cong$2–3	$\cong$20–30	$\cong$1.7–3

CH – seismic cross-hole tests; PLT – plate load tests

Table 8.2b Average ratios between Young's modulus and *in situ* "gross" tests (*After* Viana da Fonseca *et al*., 2003)

$E_0(CH)/N_{60}(SPT)$	$E_0(CH)/q_c(CPT)$	$E_0(CH)/q_d(DPL)$	$E_0(CH)/P_L(PMT)$
$\cong$ 10(MPa)	$\cong$30	$\cong$50	$\cong$8

CH, PLT – ibidem; N_{60}, q_c, q_d, p_L - resistance values

Frost, 1988). However, the specific evaluation of E/E_0 associated with this FS equal to 4 (E_{25}) was found to be 0.34.

The specific application of footing settlement prediction methods based on in situ tests

Viana da Fonseca (2001) adapted some solutions available in the literature that use SPT parameters for settlement evaluation, and the following conclusions were reached.

Methods based on SPT

Terzaghi and Peck (1967)
SPT is really a crude test developed from a method developed by the Raymond Piling Co. in 1912 to obtain samples of the soil at the base of their bored piles. A thick walled 5 cm diameter steel tube was hammered into the ground to obtain the sample, and it was realised that the energy required to cause penetration gave an indication of the strength of the ground. The test was very easy to do because little special apparatus was needed in addition to the heavy well boring equipment already being used on the site. Through the years very many tests were carried out, but research workers were somewhat unhappy about the non-scientific nature of the test, and were doing their best to have it replaced by a penetration test such as the Dutch cone test, when Terzaghi and Peck published their semi-empirical method for estimating settlement in granular materials. As it is recognised today, the predictions are very conservative and, in the present case, the observed settlement would have been predicted under a load of ¼ to ½ of that actually applied. As a result it will not be developed further here.

Parry (1978)
The method of Parry (1978) is based on the expression of the Theory of Elasticity for the calculation of settlements:

$$s = q \cdot B \cdot \frac{1 - \nu^2}{E_s} \cdot I_s \tag{8.1}$$

with the deformation modulus taken as a function of an average value of N_{60} determined in the depth 2B below the footing base ($\overline{N_P}$), where N_{60} is the SPT number of blows, allowing for the method of dropping the driving weight and assuming a 60% efficiency, and the suffix P refers to Parry.

$$E_s = \overline{N_P}/\alpha_P \tag{8.2}$$

In the study presented by Viana da Fonseca (2001), the parameter α_P for the best adjustment ranged from 0.2–0.3, although only for the lower stress levels, becoming strongly non-conservative for stress levels above the "elastic" threshold. Its limitation is mainly due to the fact that it does not consider the non-linearity of stiffness with depth of the influence zone in relation to the dimension of the loaded area, which is not in agreement with reality (Jardine *et al.*, 1986; Burland, 1989; Tatsuoka and Shibuya, 1992). There is a risk therefore, when extrapolating to larger loaded areas (which are usually the case), of overestimating the settlements by calculating them on the basis of an average value of N_{60} over the depth of $2 \cdot$ B, particularly in soils that exhibit increasing stiffness with depth.

Burland and Burbidge (1985)

This proposed method for settlement calculation uses an average value of N_{60}, determined over a depth below the footing base ($\overline{N_{BB}}$), through the following expression:

$$s = \alpha_{BB} \cdot \frac{B^{0.7}}{\overline{N_{BB}}^{1.4}} \cdot q_s \tag{8.3}$$

with α_{BB} varying between 0.93 and 3.09, and 1.71 being the most probable value. In the expression, B denotes footing width, q_s the average contact pressure, and the suffix BB stands for Burland and Burbidge.

When applied to residual soils in Porto, using $\alpha_{BB} = 1.71$, the method was found to be grossly conservative, giving rise, for average service stress conditions, to ratios of 2 to 3 between predicted values and those observed. With the purpose of best adapting the method to suit the experimental results, the values of α_p and α_{BB} were calculated to obtain convergence for the two, following typical values of settlements:

(i) s/B = 0.75%, a level corresponding to a certain "elastic" threshold;
(ii) s = 25 mm, the limit value in accordance with Terzaghi and Peck proposal.

It was then concluded that:

(i) the approach of limiting the settlement to 25 mm produces a reasonable consistency of values in the two cases. This is a consequence of assuming a factor of 0.7 for the minimum size of the loaded area B.
(ii) for the same approach, the method of Parry gives values with slight variations for α_P, resulting in much greater reduction of B (factors of 0.32–0.44) than the maximum proposed by the author (0.30);
(iii) the approach using the "elastic" threshold level ($s/B = 0.75\%$) which is considered more realistic, confirms the good results from the Parry method for loading

over relatively small areas; it being noticed, however, that there is an increasing value of α with increasing foundation size from the plate to the footing, indicating the beginning of a breakdown in the assumption of direct proportionality with B;

(iv) it should be noted that for this approach, the values obtained for α_{BB} were very low (0.63, for the footing, and 0.50 for the plate of 60 cm of diameter) compared with the initial proposals (0.93–3.09).

This last result shows that residual soils studied possess a more pronounced structural stiffness than those analysed by Burland and Burbidge, which did not include residual soils. From the work of Rocha Filho (1986), the application of the Burland and Burbidge proposals to the results of loading tests on shallow foundations and plates with diameters from 0.40 to 1.60 m, carried out on residual soils from gneiss in the university campus of PUC in Rio de Janeiro, resulted in ratios of calculated to observed settlements of between 1.5 and 2.5. The ratios obtained in this study are even larger (2.7–3.4).

Another reason for lack of agreement with the Burland and Burbidge method when applied to residual soils may lie in the fact that the influence zone considered should be smaller than that suggested, due to the higher rate of stiffness increase with depth caused by the simultaneous increase of confining stress as the degree of weathering decreases. It can be considered that the proposal of Burland and Burbidge (1985) will be applicable to larger foundations resting on residual soils (for example $B = 3$–4 m), readopting the average value of coefficient α_{BB}. For the case of $s/B = 0.75$, the following conservative value is suggested:

$$\alpha_{BB}\text{ (saprolitic soil from granite)} = \frac{\alpha_{BB}\text{ (original)}}{2} = \frac{1.71}{2} = 0.85 \tag{8.4}$$

Anagnastopoulos et al. (1991)

The authors processed statistically 150 cases of shallow foundations with several sizes and subjected to different load conditions, mainly on sandy soils (of different origins), and proposed the following expression:

$$s = f\frac{q^{n_q} \cdot B^{n_B}}{N^{n_N}} \tag{8.5}$$

The terms were obtained by multiple regression, with priority for the dependent variables as a function of the relative influence of each one. It should be noted that the expression of Burland and Burbidge (1985) constitutes a particular case of this more general one, with $f = 0.93 - 3.09$; $n_q = 1$; $n_B = 0.7$ and $n_N = 1.4$.

It is interesting to observe that the parameters proposed by Burland and Burbidge are reasonably similar to those indicated by Anagnastopoulos *et al.* (1991)as representative of all sets of studied cases.On the other hand, it is to be noted that there is a high dispersion of the parameters corresponding to the several classes of stiffness, and of the size of the loaded surface. In order to obtain the parameters that give the best agreement with the experimental results, Viana da Fonseca (2001) suggested that the proposals of Burland and Burbidge (1985) be used for the influence depth $z = B^{0.75}$

and for the factor n_N (=1.40). With these factors fixed, multiple regression analyses were carried out assuming the following variants:

(i) the n_q exponent was allowed to be greater than 1, which corresponds to considering the non-linearity of the solution, and the best fit of the curves was found for a bearing pressure $q_s = 400$ kPa;
(ii) a linear solution was assumed ($n_q = 1$) and the convergence for values of the settlement defined for $s/B = 0.75\%$.

Figure 8.14 shows a comparison between the curves obtained for those two hypotheses, illustrating the following: (i) excellent agreement between the theoretical and the experimental results when using the value $n_q = 1.23$. The resulting non linearity causes the value of the constant f to be reduced to 0.18, much lower than the value of 0.60 usually defined in linear elasticity; (ii) the imposition of a linear relationship, as shown by Figure 8.14(b), always implies a subjective approach; the values of the constant α_{BB} obtained for the hypotheses associated with the Burland and Burbidge (1985) proposal, are similar to the one now deduced ($f = 0.60$), depending on the value of B being equally large.

From this, it can be concluded that the sensitivity analysis, by applying exponents to the factors that influence the development of settlements of shallow foundations under service loads, seems to offer a good method for prediction. This, however, needs future confirmation by other experimental studies, in particular those including larger loaded areas. To summarise the results obtained with SPT based methods, it can be stated that:

(i) the depths over which the values of N_{SPT} should averaged, can be accepted in the same terms as stated by Burland and Burbidge (1985);
(ii) the non-linear exponents, in relation to the applied load (n_q) should be assumed to be greater than unity (the deduced resulting value was around 1.23), causing relatively low constants, e.g. for safety, $f = 0.20$;
(iii) although these comparative analyses of the test results indicate n_B values close to 1, smaller values should be adopted (for example, $n_B = 0.7$, as proposed by Burland and Burbidge, 1985) when designing shallow foundations with dimensions generally larger than 2 to 3 m. This method reflects the reducing dependence of settlements on increasing values of B (Bjerrum and Eggestad, 1963).

Methods based on CPT

Schmertmann et al. (1978)

The semi-empirical method of Schmertmann (1970), upgraded in Schmertmann *et al.* (1978), assumes a simplified distribution of the influence factor for the vertical strains under the footing, with these formulations:

$$s = \int_0^{2\cdot B(4\cdot B)} \varepsilon_z \, dz \cong \Delta p \cdot \int_0^{2\cdot B(4\cdot B)} \frac{I_z}{E_z} dz \cong C_1 \cdot C_2 \cdot \sum_{i=1}^{n(2\cdot B;4\cdot B)} \frac{I_{z_i}}{E_{z_i}} \cdot \Delta Z_i \qquad (8.6)$$

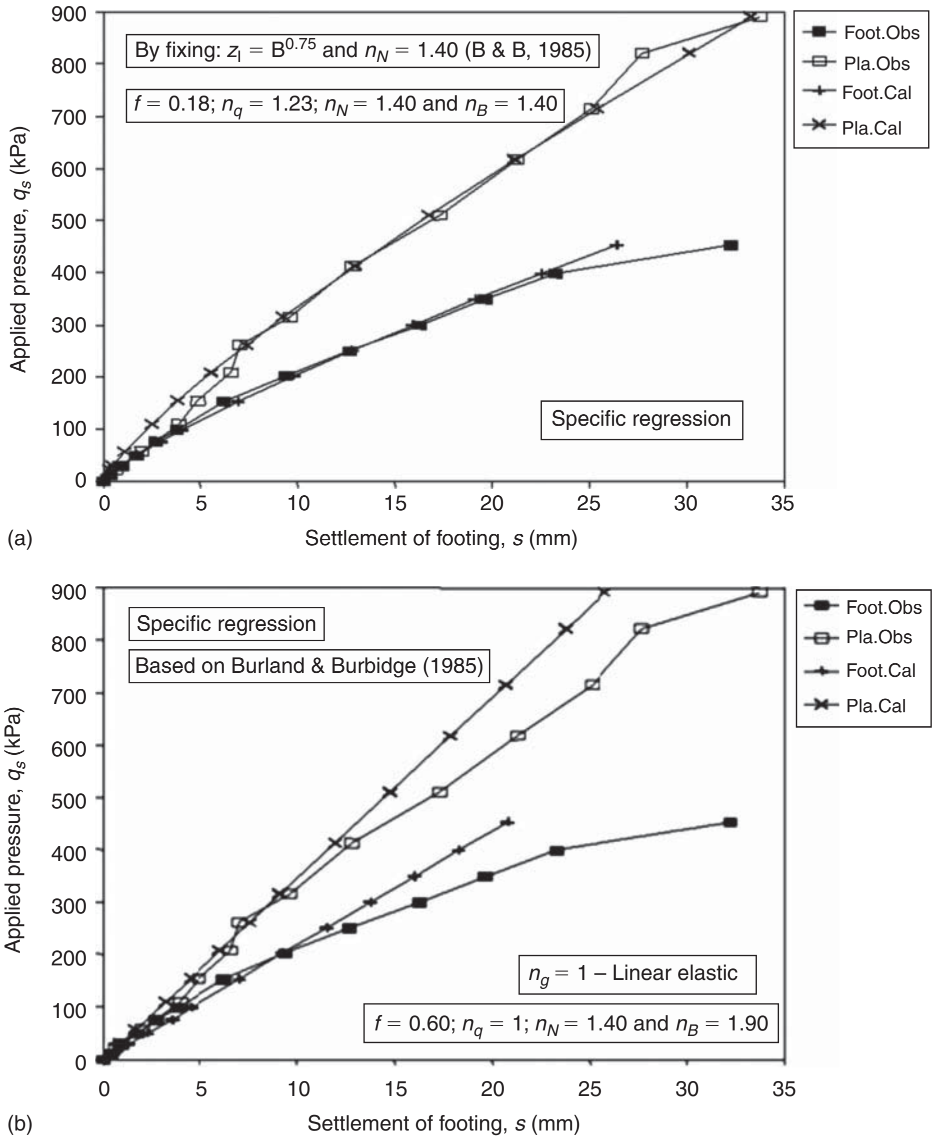

Figure 8.14 Determination of values for f, n_B and n_q that give best agreement with experimental results (a) for the non-linear relation $n_q < 1$ and (b) the linear relation $n_q = 1$ [n_g fixed at 1.40]

the values of which are computed on the basis of a deformation (secant) modulus variable with depth, which can be correlated with the CPT cone resistance:

$$E_{S(z)} = \alpha \cdot q_{c,CPT}(Z) \tag{8.7}$$

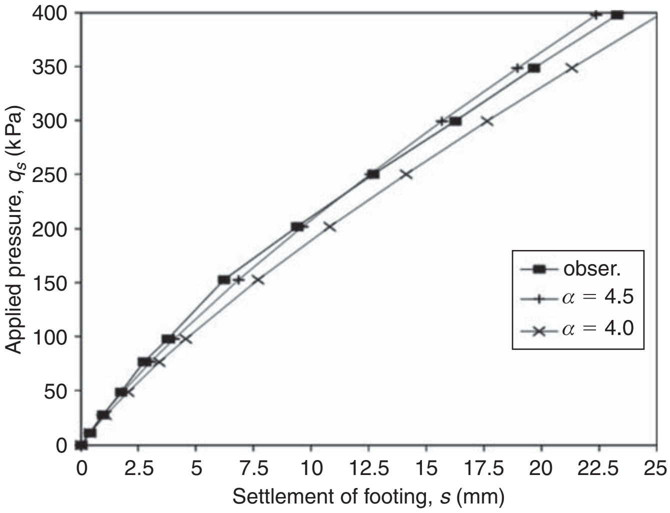

Figure 8.15 The effect of varying values for α (*After* Viana da Fonseca, 2001)

where, $E_{S(z)}$ represents Young's Modulus at depth z and q_c represents static cone resistance at the same depth. In granular soils, the values of the coefficient α are:

$\alpha = 2.5$ for axisymmetric loadings;
$\alpha = 3.5$ for plane loading conditions;

Robertson *et al.* (1988) have suggested that α should increase to:

$3.5 < \alpha < 6.0$ in aged soils;
$6.0 < \alpha < 10.0$ in overconsolidated soils.

This method was applied to the load test in residual soils by adjusting the α parameter in order to fit the observed curve (Viana da Fonseca, 2001). As shown in Figure 8.15, the best agreement was achieved with values of 4.0 to 4.5. These relatively high values should probably be attributed to the influence of the cemented structure of the saprolitic soil, being situated in the range referred to by Robertson *et al.* (1988) as applicable for aged sands.

Robertson method
This method is based on the results of CPT tests carried out under the area to be loaded, and it incorporates factors related to the degree of stress induced by the foundation and the effects of the stress-strain history (including the natural structure of the ground).

Figure 8.16 represents the normalised values of the shear modulus for very small strains, G_0, obtained from cross-hole testing, as a function of the normalised cone resistance, q_{c1}, defined by Robertson (1991).

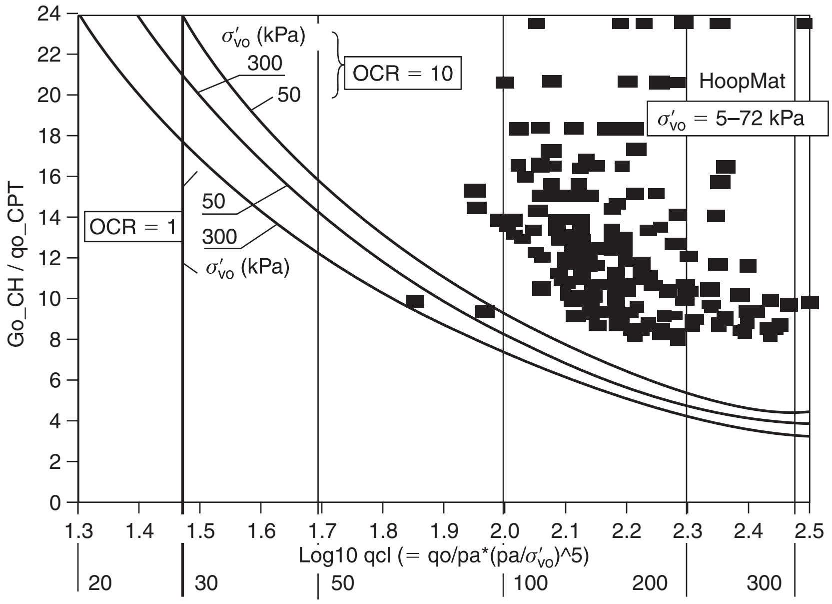

Figure 8.16 G_0/q_c versus q_{c1}; Comparison with Robertson (1991)

From an analytical interpretation of these plotted results, the following is obtained:

$$\left(\frac{G_0/q_c}{q_{c1}}\right)_{porto\ saprolitic\ soil} \cong 1.8 - 2.0 \left(\frac{G_0/q_c}{q_{c1}}\right)_{non\text{–}cemented\ sands} \tag{8.8}$$

revealing that the natural cemented structure of these residual soils generally induces higher values of the ratio between the elastic or "pseudo-elastic" stiffness and the strength, than those corresponding to transported soils, either normally or over-consolidated. This tendency is especially noticed at low confinement stress levels, revealing a relative independence of the shear modulus at low strain levels ($<10^{-6}$–10^{-4}) in relation to the at rest stress states (Tatsuoka and Shibuya, 1992). We should also note that the results obtained for the normalised cone resistance, q_{c1}, vary between the values of 100–300, the mode being about 150. This corresponds, in sedimentary soils, to dense sands. Figure 8.17 shows the relationship between E_s/q_c and load level, q_{ser}/q_{ult}, obtained from the results of the footing load test, together with curves indicated by Robertson (1991) for dense sands. Also shown, in the inset, are similar curves proposed by Stroud (1988) for over-consolidated (aged) sands. The curves for dense sand and those obtained from test results shown in the main Figure 8.17 and in the inset are the same, but to a different scale in order to permit a comparison with Stroud.

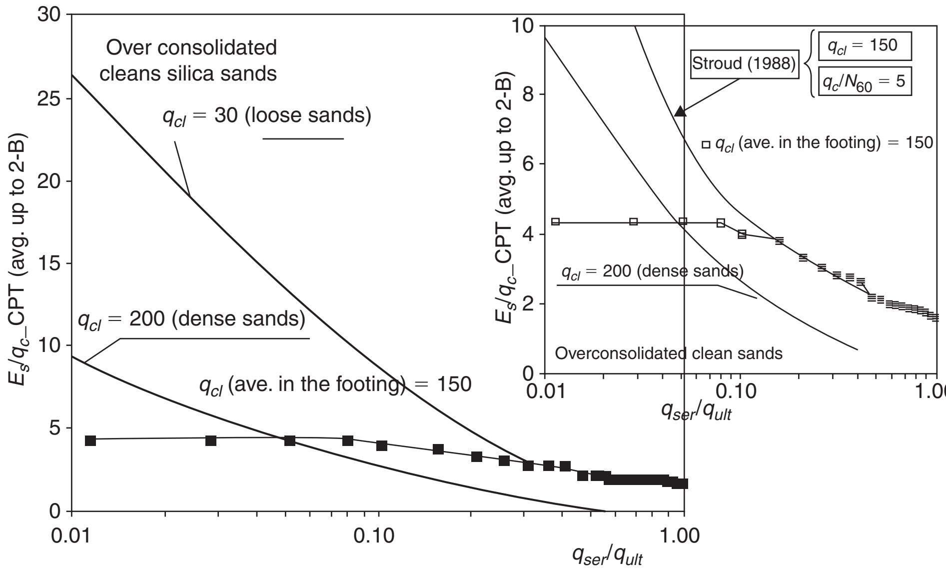

Figure 8.17 E_s/q_c versus q_{ser}/q_{ult} from the footing load test. Comparison with Robertson (1991)

From consideration of the three curves shown by Figure 8.17, it can be concluded that:

(i) for very low load levels, below around 10% of ultimate, the non-linearity of the relationship of E_s/q_c with q_{ser}/q_{ult} is much more accentuated for clean sands, even when over-consolidated (aged), than for the granitic saprolitic soil. This may be the consequence of a larger material stability in the saprolitic soil, due to the cemented structure between particles;

(ii) for higher load levels, there is a good agreement between the experimental curve for the saprolitic soil and the proposal of Stroud (1988) for over-consolidated sands.

It should be noticed however, that the values of the q_{c1} ($\cong$150) indicated by Stroud (1988) for the test results, are typical of the middle range for dense over-consolidated sands, with ageing.

With shallow foundations on saprolitic soils derived from granite, the dependence of the secant deformability modulus on the load level seems to represent, in a consistent way for the highest load levels, the proposal of Stroud, according to Robertson (1991), to use the value $q_c/N_{60} = 5$.

Methods based on PLT

Ghionna et al. (1991)

The Ghionna *et al.* (1991) method considers the dependence of the deformability modulus on the normalised stress-strain levels. It uses a hyperbolic relationship to model

Table 8.3 Hyperbolic *K* and *n* parameters for different triaxial testing results

Deformation Modulus	*K*	*n*
E_{el} (linear elastic)	35660	0.263
E_{ur} (unload-reload)	19637	0.250
$E_{ti,h}$ (hyperbolic, $q = 70$–95% of q_f)	2749	0.539
$E_{s25\%}$ (secant for $q = 25\%$ of q_f)	1804	0.588
$E_{s50\%}$ (secant for $q = 50\%$ of q_f)	1517	0.504

the behaviour of the soils (Duncan and Chang, 1970) and allows the extrapolation of the results of load tests on foundations of different sizes and shapes for the evaluation of the settlement of larger loaded areas and with different geometries, considering an equivalent homogeneous mean.

In the proposed expression for the evaluation of settlement:

$$s = \frac{1}{K_i} \cdot \frac{q_n \cdot B \cdot I \cdot (1 - \nu^2)}{\overline{\sigma'_{oct}}^{\,n} \left(q_n \cdot B \cdot I \cdot (1 - \nu^2)\right) \big/ \left(\overline{\sigma'_{oct}}^{\,1-n} \cdot C_f \cdot H_i\right)} \tag{8.9}$$

the parameters have the usual meaning, but the following ones require special mention:

1. $q_n = q_s - 2/3\sigma'_{v_0} = q_s$ because, in our foundation loading tests, σ'_{v_0} at the loaded surface, is zero;
2. H_i represents the depth of the load influence zone that, according to the authors, should be considered down to a depth of $2 \cdot B$ from the footing base;
3. n is a suitable hyperbolic exponent;
4. K_i, C_f represent hyperbolic parameters (the first, of stiffness, and the second, of strength) that will be determined from the load tests. There is a larger dispersion of the K_i values, due to the high stiffness sensitivity.

In the present case, the *n* parameter was determined from the common expression:

$$E = K \cdot (\sigma'_{oct_0})^n \tag{8.10}$$

produced from the similar analysis of different deformability moduli taken from anisotropically consolidated triaxial compression tests, referred to as CID and CAD tests (Viana da Fonseca, 1996, 2003), on samples taken from the zone of influence of the pilot load tests (see Table 8.3). Values for E_{el} were deduced from the initially linear reload branch of an intermediate unload-reload cycle; those for E_{ur} between vertices of that cycle; E_{ti} obtained from the initial tangent by hyperbolic modeling; and $E_{s25\%}$ and $E_{s50\%}$ from secant values for 25% and 50% of the failure load, respectively.

In the subsequent study, in order to analyse the influence of the parameter *n*, the following two values were taken:

1. $n_{el} = 0.263$ – corresponding to very low loads, within the elastic threshold;
2. $n_{25\%} = 0.588$ – corresponding to the mobilisation of medium stress levels.

Table 8.4 K_i and C_f values determined from the loading tests ($z_I = B/2$)

	Footing (D 120 cm)		*Plate (D 60 cm)*		*Average values*	
Exponents	K_i	C_f	K_i	C_f	K_i	C_f
$n = 0.263$ (E_{el})	46.3	1.87	45.6	1.95	46.0	1.91
$n = 0.588$ ($E_{s25\%}$)	14.6	1.83	15.6	1.88	14.9	1.86

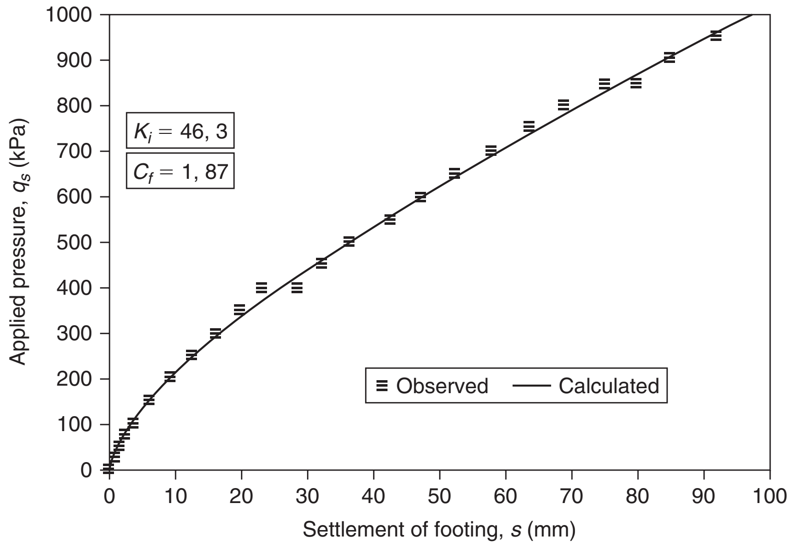

Figure 8.18 Comparison of predictions given by the Ghionna *et al.* (1991) method with observed values from the footing load test ($n = 0.263$)

Based on the results of the loading tests on the footing and the 60 cm diameter plate, the values obtained for K_i and C_f are given in Table 8.4. Depth to the settlement centre was taken as $z_I = B/2$, as assumed in the method of Ghionna *et al.* (1991).

The predicted results, using $n = 0.263$ with the corresponding values for K_j and C_f, are in very good agreement with the observed results from the footing load test, as shown by Figure 8.18.

The general application of this method requires a strict adoption of representative values of the ground in question. It is therefore necessary to use average values of n, K_i and C_f or, alternatively, those critically selected from the available values obtained from the individual analysis of each test. The results of a general analysis of the footing and plate tests, taking into account the average values for n proposed by Ghionna *et al.* (1991) are presented in Viana da Fonseca (2001). It was proved that a low value of n gives the best simulation for the low stress levels. Good agreement is lost for higher stress levels, giving rise to a non-conservative result for the larger footing sizes, which will limit extrapolation for larger size footings. It is clear that this tendency decreases its relevance as, in general, the parameters K_i and C_f refer to the test over the largest

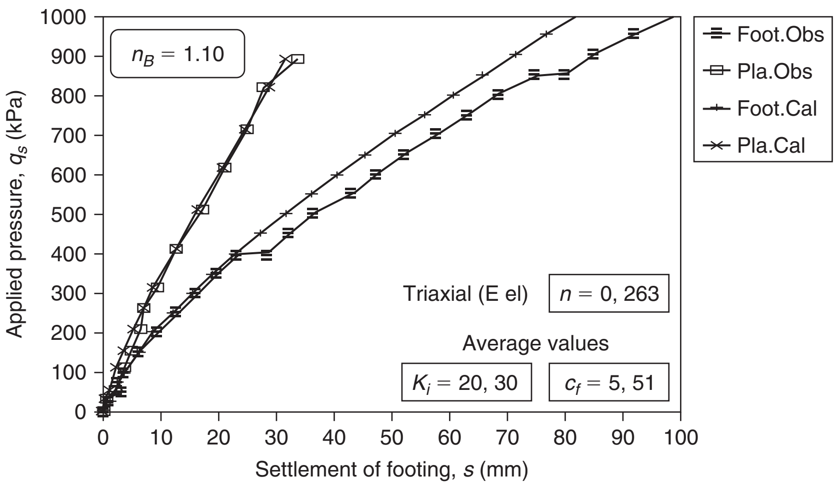

Figure 8.19 Application of Ghionna *et al.* (1991) method by considering a dimension factor, $n_B \neq 1$

size of loaded area. Although it is conservative for small footings, on the whole this approach seems to be acceptable.

To ameliorate the performance of the method, the following modifications to the original method of Ghionna *et al.* (1991) were considered by Viana da Fonseca (2001):

(i) depth of the point of maximum influence: $z_I = B$ instead of $B/2$;
(ii) exponential dependence of the footing breadth by a factor $n_B \neq 1$.

The results obtained from the first modification, taking average values of K_i and C_f, although considerably better, were not satisfactory. The second modification required alteration of the original formulation to produce the following equation:

$$s = \frac{1}{K_i} \cdot \frac{q_n \cdot B^{n_B} \cdot I \cdot (1 - \nu^2)}{(\sigma'_{oct})^n - (q_n \cdot B^{n_B} \cdot I \cdot (1 - \nu^2))/((\overline{\sigma'_{oct}})^{1-n} \cdot C_f \cdot H_i)} \tag{8.11}$$

A best fit of the curves was then possible by assuming average parameters of K_i and C_f, making $q_n = q_s$, and introducing n_B as a weighting factor related to the loading area. As seen in Figure 8.19, making $n = 0.263$ and considering the value $n_B = 1.10$ gives a good fit. This tendency for $n_B > 1$ is contrary to what was verified with the other methods under review, because it was considered convenient to maintain the proportionality in relation to B presented by the authors.

To conclude, the applicability of the Ghionna *et al.*'s (1991) method to residual soils can be inferred from:

(i) the model, which integrates results of both *in situ* load tests and laboratory tests, presenting a good approach for foundation settlement prediction; this should be applied exclusively for moderate load levels.

(ii) with regard to the geometric assumptions, it is reasonable to retain the direct proportionality in relation to the breadth of the loaded surfaces, while for the depth of the point of maximum influence, for evaluation of the "at rest" effective octahedral stress and that induced by the loading process, it seems better to adopt $z_I = B$, instead of $z_I = B/2$. This alternate proposal however, requires confirmation by a greater amount of experimental data, especially for large loaded areas (more common in practical foundations), where the relative depth of influence tends to decrease (Burland and Burbidge, 1985).

(iii) ground heterogeneity has significant consequences in the model, particularly in the parameter C_f;

(iv) the dependence of the deformability modulus in relation to the at rest effective octahedral stress should be evaluated for the lowest stress-strain levels, which could be achieved with triaxial tests on undisturbed samples plus local instrumentation or, alternatively, by the use of seismic refraction ("cross-hole" tests). If it proves impossible to obtain site specific values, it is suggested values for $n \leq 0.5$ should be adopted.

(v) in choosing values for K_i and C_f, the average values obtained in load tests with different loading areas should be used, provided that the variation between them is not high. When there is considerable variability of those parameters, the lowest values of K_i and, above all, of C_f should be chosen to ensurea conservative result.

Wahls and Gupta (1994)

The method of Wahls and Gupta (1994) accurately considers the non linear nature of the stress/strain relationships ($\sigma - \varepsilon$). Firstly, as a basic formulation taking account of the penetration testing parameters (N_{SPT} or q_c-CPT) and the resulting correlations with the low strain shear modulus ($G_0 = G_{\max}$) and, secondly, as a law of variation of the secant or tangent shear modulus with the distortion level proposed by other authors (such as Seed and Idriss, 1982). These laws apply only to the materials of the type from which they were developed. Alternatively, the method can be based on the back-analysis of one or more load tests on plates or experimental footings, preferably of different sizes to enable definition of the non-linearity, giving a variation law of Young's modulus with load level (q_{sj}) in relation to failure.

Adapting the Wahls and Gupta method for this last alternative, and assuming a given load step q_{sj}, applied to a foundation on a layer i, of thickness Δh_i and with deformability modulus E_{ij} (i and j translate the dependence in relation to the depth and to a certain load level, respectively), the vertical deformation can be calculated by:

$$\Delta s_{i_j} = \frac{I_{si}}{E_{i_j}} \cdot q_{sj} \tag{8.12}$$

and the corresponding settlement by:

$$s_j = \sum_{i=1}^{n} \Delta s_{ij} \cdot \Delta h_i = q_{sj} \cdot \sum_{i=1}^{n} \frac{I_{si} \Delta h_i}{E_{ij}} \tag{8.13}$$

where n is the number of sub-layers into which the ground is divided within the main settlement influence zone, which should extend to such a depth that the shear stress increment does not exceed the value of initial shear stress, with depths of around $2 \cdot B$ for $L/B \leq 3$, and of $4 \cdot B$, for $L/B > 3$. L and B are the dimensions of rectangular footings.

The greater the number of divisions used, the greater will be the accuracy. I_{si} is the load coefficient for the layer "i", dependent on the size of the loaded area and the value of Poisson's ratio.

The dependence of the deformability modulus on depth can be related to the at-rest octahedral effective stress at the centre of the layer, σ'_{mij}, by means of:

$$E_{ij} = E_{0j} \cdot (\sigma'_{mij})^{\overline{n}} \tag{8.14}$$

with $n = 0.5$, as suggested by the authors.

Dependence in relation to the vertical stress can be expressed by the following relationship:

$$E_{0j} = f\left(\frac{q_{s_j}}{q_{s_{ref}}}\right) \cdot E_{ref} \tag{8.15}$$

or, alternatively, by:

$$E_{0j} = f\left(\frac{(s/B)_j}{(s/B)_{ref}}\right) \cdot E_{ref} \tag{8.16}$$

where $q_{s_{ref}}$, s_{ref} and E_{ref} represent, respectively, the load, the settlement and the deformability modulus, corresponding to certain reference load steps (for example: $s/B = 0.1\%$) and q_{s_j} and s_j the load and the settlement for a generic load level.

Viana da Fonseca (2001) presented a back-analysis of the footing load test and for $s/B = 0.1\%$, a value of $q_{s_{ref}}$ (26 kPa) was obtained and the value of the reference modulus (for $n = 0.5$) deduced from:

$$E_{ref} = \frac{q_{s_{ref}}}{s_{ref}} \cdot \sum_{i=1}^{n} \frac{I_{s_i}}{\sqrt{\sigma'_{m_j}}} \cdot \Delta h_i \tag{8.17}$$

On the other hand, with the pair of values s_j and q_{s_j}, corresponding to each loading step and obtained from the experimental curve, the respective equivalent modulus can be calculated (for an increment from zero to q_{s_j}) from:

$$E_{0_j} = \frac{q_{s_j}}{s_j} \cdot \sum_{i=1}^{n} \frac{I_{s_i}}{\sqrt{\sigma'_{m_i}}} \cdot \Delta h_i \tag{8.18}$$

To define the relationship of non-linear dependence of E_{0j} with the strain level, defined as $(s/B_j)/(s/B_{ref})$, or with shear stress levels, defined by $q_{s_j}/q_{s_{ref}}$, a logarithmic scale was adopted. Two influence depths were considered: $z_I = 2 \cdot B$ and $z_I = 5 \cdot B$.

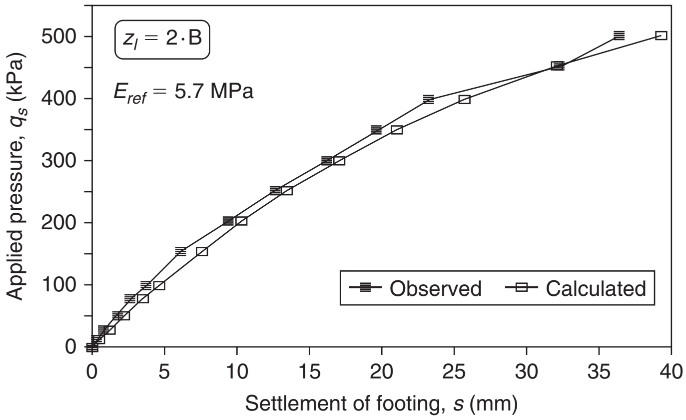

Figure 8.20 Comparison of the experimental curves and those simulated by Wahls and Gupta model for $z_I = 2 \cdot B$

In Figure 8.20, a comparison is made between the experimental and simulated curves, with parameters adjusted to give a good fit. For both influence depths the agreement is excellent, revealing the potentialities of the method to model the non-linearity of the load-settlement behaviour of the experimental footing.

Concerning definition of the reference modulus, there is obvious potential for this formulation in the design of shallow foundations, by means of a specific load test or by pre-loading an experimental footing, using $(s/B)_{ref} = 0.1\%$.

In the work reported before, Viana da Fonseca (2001) proved that the method proposed by Wahls and Gupta (1994) using the results of triaxial tests could be applied to determine the values of Young's modulus from the relevant depth and shear stress level in the soil. These parameters are subsequently used in a simplified nonlinear elastic analysis of the footing load test.

Methods based on DMT

The most widely used methods for the prediction of settlement of shallow foundations based on DMT test results are those due to Schmertmann (1986), and Leonards and Frost (1988). The first is a general method based on the Theory of Elasticity, using weighting factors variable with depth, similar to Schmertmann's CPT method described before, providing a nonlinear pressure-settlement curve, since the strains depend on the ratio between the incremental pressure and the initial effective vertical stress at foundation level.

The method has advantages in relation to the method originally proposed by Marchetti (1980), since the total settlements of common foundations seldom have conditions of lateral confinement (situation represented by the constrained modulus, M_D), so it is more consistent to use a deformation modulus, with analogies to triaxial compression tests. The methods are reasonably adjusted to real situations of isolated footings, in which the stiffness may vary randomly with depth. The groundwater conditions are also integrated in the values of the modulus and the formulation includes the geometric factors of the foundation (shape and embedment in depth).

Table 8.5 Deformation modulus from DMT versustriaxial tests in recent silica sands (*After* Berardi *et al.*, 1991)

OCR	$E_s(0,1\%)/E_{D,DMT} \pm$ *variation*
1	0.99 ± 0.19
1.4–8.8	3.25 ± 0.71

The formulation proposed by Leonards and Frost (1988) is a generalisation of Schmertmann's (1986) proposal, with the following expression:

$$s_j = C_1 \cdot C_2 \cdot q_{effect_j} \left(\sum_0^{H_i} I_{Z_{i_j}} \cdot \Delta Z_i \cdot \left[\frac{R_z(OC)_i}{E_z(OC)_i} + \frac{R_z(NC)_i}{E_z(NC)_i} \right] \right)_j \tag{8.19}$$

where:

C_1: correction for embedment (=1, shallow [surface] foundations);

C_2: correction for time (=1, short term analysis);

q_{effect_j}: effective stress transmitted to the base of foundation;

H_i: depth of influence, similar to the proposal of Schmertmann (1978);

$I_{z_{i_j}}$: influence factor for deformations (Schmertmann, 1978);

Δz_i: depth of sub-layers (20 cm – coinciding with the intervals in DMT);

$R_z(OC)_{ij}$: ratio of stress increment for the overconsolidated portion (OC);

$R_z(NC)_{ij}$: ratio of stress increment for the normally consolidated portion (NC); being expressed by:

$$R_z(OC) = \left(\frac{\sigma'_p - \sigma'_{v0}}{\sigma'_f - \sigma'_{v0}} \right); \quad R_z(NC) = \left(\frac{\sigma'_f - \sigma'_p}{\sigma'_f - \sigma'_{v0}} \right)$$

where: $\sigma'_f =$ the vertical effective stress after consideration of final load q_{effect_j},

and: $q_{effect_j} = \sigma'_{v0} + \Delta\sigma'_v$, calculated by the Theory of Elasticity;

E_{ziD}(OC); E_{ziD}(NC): appropriate values of deformation modulus corresponding to the over-consolidated and normally consolidated portions, respectively, for the increment of stress in the layer i for the load q_{effect_j}, and deduced from the correlations between $E_s(n\%)$ and $E_{D,DMT}$.

In Table 8.5, a summary of the correlations obtained in calibration chambers are presented (Berardi *et al.*, 1991).

These formulations have been applied to the case study reported by Viana da Fonseca (2001) taking account of the results of an extensive site characterisation campaign (Viana da Fonseca, 2003), and testing the application of the Leonards and Frost (1988) method. The variation of the Dilatometer modulus with at rest vertical effective stress was expressed by:

$$E_D = 5.54 + 430\sigma'_{v0} \tag{8.20}$$

The resulting pattern of variation is shown in the curves plotted in Figure 8.21.

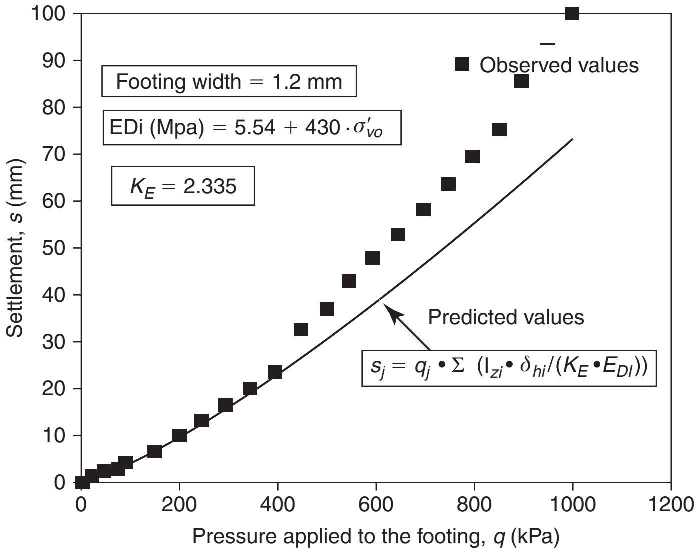

Figure 8.21 Comparison of the measured settlement of the footing (*After* Viana da Fonseca, 2001) with the prediction based on DMT using Leonards and Frost (1988) method

A value of $K_E = 2.34$ was found by fitting a curve through the early pressure-settlement curve, suggesting that:

a) correlations with E_D modulus to be adopted in residual soils, such as these silty saprolites from granite, may be inbetween the proposals due to Berardi *et al.* (1991) for recent sandy soils ($OCR = 1$, $K_E = 0.99 \pm 0.19$) and overconsolidated/aged soils ($OCR = 1.4$–8.8, $K_E = 3.25 \pm 0.75$); these trends are similar to those derived for *CPT* and *SPT* methods presented above; in fact these saprolitic soils may be situated in class 2 of Berardi *et al.* (1991) proposal for the ratio of stiffness to strength (the class 1 for $OCR = 1$ and class 3 for high values of OCR).
b) this value of K_E only applies for moderate values of applied pressure, $q < 35\% q_{ult}$, which is in agreement with the perception of the high level of non-linearity for these young residual soils.

Methods based on pre-bored Pressuremeter (PMT) or Ménard's pressuremeter (MPM)

Many kinds of pressuremeter probes are currently in use (Briaud, 1992; Clarke and Smith, 1993). Their differences are mostly related to the way they are inserted into the ground, such as predrilled hole (PMT), self-bored (SBPT), or pushed-in (CPMT). Since the PMT causes an unavoidable stress relief, and the CPMT causes an unavoidable stress increase, it is obvious that the SBPT is the one that causes the least soil disturbance. Consequently, the SBPT is the only one that allows the measurement of the geostatic total horizontal stress σ_{h0}. It also offers a better interpretation of test results from small to large strain levels. Jamiolkowski and Manassero (1995) summarised the different geotechnical parameters that can be obtained by the three types

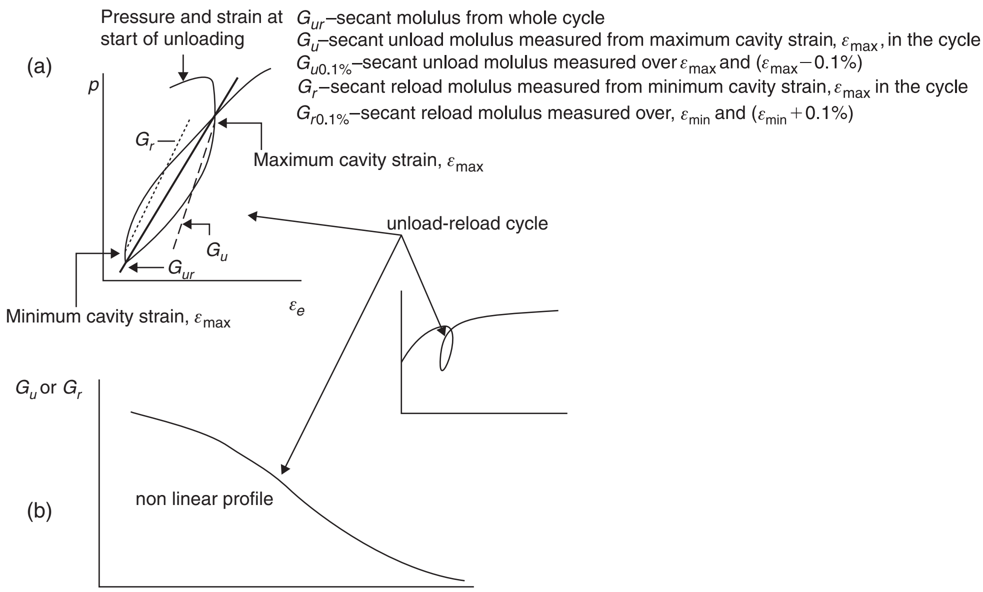

Figure 8.22 Selection of shear moduli (*After* Clarke, 1995)

of pressuremeters. The different moduli that can be obtained by the SBPT are shown in Figure 8.22.

Theoretically, the initial slope of an SBPT pressure/strain curve yields the G_0 value. However, in practice there is still some disturbance (Wroth, 1982) and the modulus must be taken from an unload-reload cycle (G_{ur}). For heavily over-consolidated soils and cemented geomaterials, it could be assumed that $G_{ur} = G_0$ if the strain of one cycle is less than 0.01%.

There are two approaches to the use of G_{ur} in practice:

- To link G_{ur} to G_0 using a determined stress-strain relationship (Bellotti *et al.*, 1994; Ghionna *et al.*, 1991);
- To compare G_{ur} values to the degradation modulus (G/G_0) versus shear strain (γ) curve from the laboratory, taking into account the average values of shear strain and mean plane effective stress associated with the soil around the expanded cavity (Bellotti *et al.*, 1994).

It is not appropriate to obtain G_0 directly from the PMT because of the unavoidable disturbance during predrilling.

By careful testing, with a simple and expeditious methodology, the PMT can be adapted to determine different levels of stiffness and strength in difficult materials such as the highly heterogeneous conditions found in residual profiles.

The routine analysis of PMT tests follows the method originally developed by Ménard (1955). It gives design parameters directly obtained from the pressuremeter

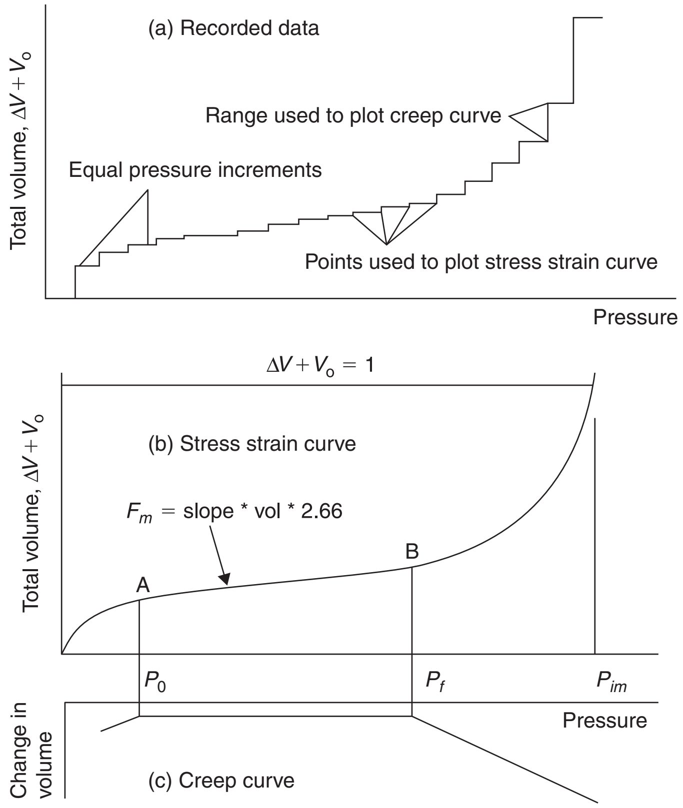

Figure 8.23 Interpretation of PMT according to the ASTM standard (*After* Clarke and Gambin, 1998)

test curve (ASTM, 2004). Figure 8.23 shows the interpretation of the curve and Figure 8.24 shows the procedure to obtain the pressuremeter modulus (E_m), based on the present ASTM (2004) standard.

The interpretation of the results is solely based on the analysis of two curves: the pressuremeter curve (v_i *versus* p_i, recorded at the end of each minute) as shown in Figure 8.24a and the yield curve (the difference between the volumes at 30 sec and 1 min versus pressures) as shown in Figure 8.24b. From these tests, the following parameters are deduced:

- the ***pressure meter modulus*** (E_m):

$$E_m = 2 \cdot (1 + v) \cdot V_m \frac{\Delta p}{\Delta v} \qquad (8.21)$$

  where V_M is the volume of the cylindrical cavity in the beginning of the linear behaviour (the pseudo-elastic range), observed between stress and strain, Δp and Δv;
- the ***limit pressure*** (p_L): the pressure necessary to double the initial volume of the original excavated cavity; or the *differential limit pressure* ($p_L^* = p_L - p_0$),

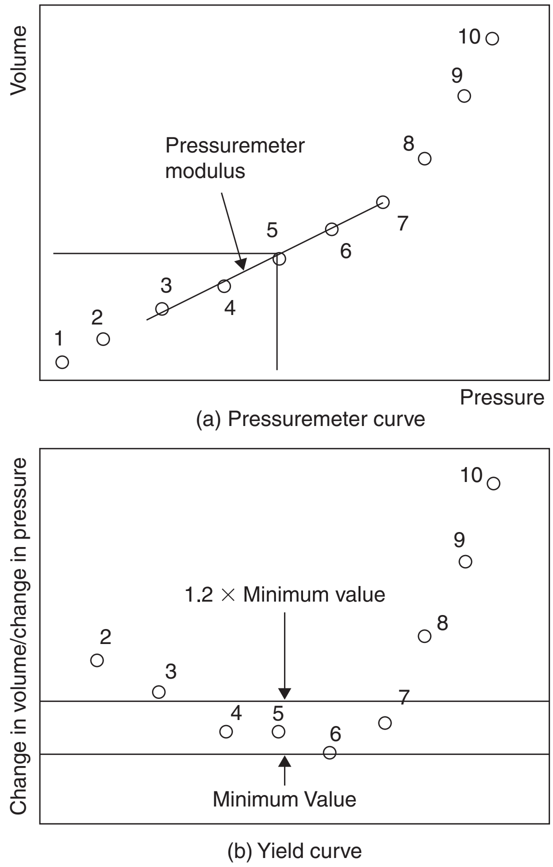

Figure 8.24 Selection of the pressure range to calculate E_m according to the ASTM standard (*After* Clarke and Gambin, 1998)

which is less sensitive to drilling damage or imperfections of the initial shape of cavity;

- a ***yield pressure*** (p_f): the end of the linear range in the curve, corresponding to the value with a clear increase in the change in volume between 30 sec and 1 min.

It must be pointed out that this modulus is related to the average stiffness of the ground associated with a particular strain level. Consequently the use of this value must only be applied in settlement formulae developed by Ménard (Ménard, 1963, 1965), as is done in the French Code for foundation design Fascicule No 62 (Gambin and Frank, 2009). Consequently the PMT modulus must be considered as a test-specific design parameter (Gomes Correia *et al.*, 2004).

For the evaluation of deformability characteristics, Ménard and Rousseau (1962), using the equations of the elasticity, proposed a transformation of the pressuremeter modulus to Young's modulus by using a rheological factor:

$$E = \frac{E_{pm}}{\alpha} \tag{8.22}$$

where α is dependent on the type of soil and the proper ratios defined by the parameters deduced in the tests, which are a sign of the class of the material (E_m/p_L^*). Others authors (Kahle, 1983; Konstantinidis *et al.*, 1986; Rocha Filho, 1986) have suggested the use of the unload-reload modulus in the elastic equations for settlement evaluation.

This pressuremeter test is especially suitable for heterogeneous soils and IGM (Intermediate Geo-materials) where the penetrability of other more common tests, such as CPT, DMT, or even SPT, are difficult (or impossible) and, most importantly, where the validity of correlations developed for transported soils are dubious (Viana da Fonseca and Coutinho, 2008). Nevertheless, the application of this test to design in residual soils, which is definitely a versatile technique with great potential, has to be done using specific regional correlations, made for typical residual materials.

Experimental *in situ* work, described by Viana da Fonseca (2003), showed that the stiffnesses determined from reload-unload cycles of PMT (E_{pmur}) and SBPT tests in saprolitic granite soils were, apparently, very different. For the PMT it was found that $E_{pmur}/E_{pm} \cong 2$ and $E_0/E_{pm} \cong 18$–20, with E_0 determined from seismic survey (G_0-CH), while for the SBPT $G_0/G_{ru} \cong 2.6 - 3.0$. It must be noticed that these last values are substantially lower than the ratio ($\cong$10), reported by Tatsuoka and Shibuya (1992) on Japanese residual soils from granite. The non-linearity model of Akino, cited by the previous authors, developed for a high range of soil types, including residual soils, is expressed simply by:

$$E_{sec} - E_0 \ (\varepsilon \leq 10^{-4}) \tag{8.23}$$

$$E_{sec} = E_0 \cdot \left(\frac{\varepsilon}{10^{-4}}\right)^{-0.55} (\varepsilon > 10^{-4}) \tag{8.24}$$

It should be noted however, that pressuremeter data has been used in France (and elsewhere where PMT is common practice) for settlement evaluation, following a specific formulation (known as the "French method") that will be explained below.

EN 1997-2: 2007 (E): Method to calculate the settlements for spread foundations

There is a preference to use results from the PMT (MPM, meaning Ménard Pressuremeter Tests) directly to calculate the settlement, s, of spread foundations using a semi-empirical method developed using influence factors. This is expressed by the following equation:

$$s = (q - \sigma_{v0}) \times \left[\frac{2B_0}{9E_d} \times \left(\frac{\lambda_d B}{B_0}\right)^a + \frac{\alpha\lambda_c B}{9E_c}\right] \tag{8.25}$$

Table 8.6 The shape factors, λ_c, λ_d, for settlement of spread foundations

L/B	*Circle*	*Square*	*2*	*3*	*5*	*20*
λ_d	1	1.12	1.53	1.78	2.14	2.65
λ_c	1	1.1	1.2	1.3	1.4	1.5

Table 8.7 Rheological factor α for settlement of spread foundations

Type of ground	*Description*	E_M/p_{LM}	α
Peat			1.0
Clay	Over-consolidated	<16	1.0
	Normally consolidated	9–16	0.67
	Remoulded	7–9	0.50
Silt	Over-consolidated	>14	0.67
	Normally consolidated	5–14	0.50
Sand		>12	0.50
		5–12	0.33
Sand and gravel		>10	0.33
		6–10	0.25
Rock	Extensively fractured		0.33
	Unaltered		0.50
	Weathered		0.67

where:

B_0 is a reference width of 0.6 m;
B is the width of the foundation (m);
λ_d, λ_c are shape factors given in Table 8.6;
α is a rheological factor given in Table 8.7;
E_c is the weighted value of E_M immediately below the foundation;
E_d is the harmonic mean of E_M in all layers up to $8B$ below the foundation;
σ_{v0} is the total (initial) vertical stress at the level of the foundation base;
q is the design normal pressure applied on the foundation.

In residual soils the values of the rheological factor should be adapted for each situation. Viana da Fonseca (1996) studied thoroughly the application of the elastic formulation:

$$s = \frac{p \cdot B \cdot I}{E_{M/\alpha}} \tag{8.26}$$

By taking representative values for the centre of settlement (as defined by Burland and Burbidge, 1985; or Schmertamn *et al.*, 1970, 1978) and applying them to the footing prototype and large plate load tests, a very clear trend to the rheological coefficient was found, with $\alpha = 0.5$ for service loads, decreasing to $\alpha = 0.33$ for higher loads. These materials have typical values of E_M/p_{LM} in the range of 10–12, agreeing well with the silty materials group in Table 8.7.

It is also interesting to complement the trend of this parameter with the observation that has been made of the applicability of the unload-reload modulus from the PMT (E_{MR}) for the settlement estimation of shallow foundations.

Typical ratios of E_{MR}/E_M of 1.4–2.0 have been found for these soils (Viana da Fonseca and Coutinho, 2008) which, for $\alpha = 0.5$, converts the previous simple elastic formulation to:

$$s = \frac{p \cdot B \cdot I}{E_{MR}} \tag{8.27}$$

The determination of this modulus has been accepted as good practice and defended by the French rules and elsewhere, since it provides a way to solve some of the problems associated with soil disturbance in pre-bores, which affect the "virgin" curve and consequently the E_M.

Conclusion on the methods for prediction of settlement of footings in residual soils

In summary, one can point out the following trends:

- Terzaghi and Peck proposal led to settlements 2 to 4 times higher than observed;
- Parry's (1978) proposal, taking $\alpha = 0.3$, has given reasonable results for the very early load levels (up to 20% of failure, before yield, defined in Viana da Fonseca *et al.*, 1997), but is strongly non-conservative for higher load levels;
- Burland and Burbidge (1985) proposal (average $\alpha = 1.71$) is roughly conservative, with values of predicted settlements 2 to 3 times higher than the observed ones (for loads up to serviceability limits, $s/B = 0.75\%$); a lower value for $\alpha = 0.855$, is in accordance with similar trends in Brazilian residual soils (Rocha Filho, 1986).
- From the CPT based semi-empirical solutions for settlement evaluation, Schmertmann *et al.*'s (1978) method was tested with fine layer discretisation for the most representative PLT ($D = 0.60$ m and 1.20 m). An excellent reproduction of the observed curves was obtained (even in non-linearity terms) when the values of $E/q_c = \alpha$ were modified to 4.0 to 4.5, higher than those proposed by the authors for sandy soils.
- Ménard's rheological factors ($\alpha = E/E_{pm}$) for correction of PMT modulus in order to get the best convergence between observed settlements in PLT tests (at serviceability load levels) and calculated by means of the classical elastic solution taking into account the concept of settlement centre (Viana da Fonseca, 1996), were found to be typical of silty soils ($\alpha = 1/2$), corresponding to the actual grain size distribution of this saprolitic soil. The use of PMT unload-reload modulus happens to give the direct values of the Young's modulus to be taken in the same solutions. On the other hand, the values of SBPT unload-reload moduli reproduce the behaviour of intermediate cycles in PLT tests.
- Finally, a load-settlement analysis of the most significant PLT, similar to CPT interpretation but using DMT Modulus (E_D) was made. The non-linear methods from Leonards and Frost (1988), based on Schmertmann's influence diagrams, and Robertson (1991) were used and the best fit with the experimental results was obtained for a factor of $E/E_D = 2.34$, which is an intermediate value between that for NC and OC sandy deposits (Berardi *et al.*, 1991). The non-linearity of both PLT curves ($D = 0.60$ m and 1.20 m) was also reproduced.

Table 8.8 Secant deformability modulus back-calculated from the footing load test

Load criteria	$s/B = 0.75\%$	$F_s = 10$	$F_s = 5$	$F_s = 2$
E_s (MPa)	17.3	20.7	17.5	11.0

A more detailed analysis of some approaches based on the Theory of Elasticity was developed in another paper (Viana da Fonseca, 2001), comparing semi-empirical methodologies using the results of SPT, CPT, PLT and triaxial tests on high quality samples, with the results from instrumented field tests. Some of the well-established methods (Parry, Burland and Burbidge, Anagnastopoulos *et al.*, Schmertmann *et al.*, Robertson, Ghionna *et al.*, and Wahls and Gupta) were tested and some modifications to the parameters and methods were suggested to give a best fit to the observed behaviour.

- An analysis of the results of the footing test was conducted by reference to the serviceability limit state criteria referred to above (Décourt, 1992). From this load value, which corresponds to a settlement of 0.75% of the loading area diameter, and the loads corresponding to different global safety factors towards bearing capacity failure, it is possible to calculate the secant modulus by elasticity theory (see Table 8.8).
- Accepting that the design modulus E is proportional to q_c ($\alpha = E/q_c$);
- Considering the increase of q_c from CPT with depth (see Figure 11a), a convergence analysis was made, based on an elastic solution, by accepting the settlement centre concept. The procedure was based on the proposal of Burland and Burbidge (1985) for evaluation of the depth of influence as a function of the degree of non-homogeneity, E_0/kD.
- The degree of inhomogeneity, E_0/kD, enabled the determination the position of the settlement centre from Burland and Burbidge's chart. Associating the value of q_c for that depth with the secant deformability modulus back-analysed from the footing load test, the value of α becomes equal to 3 for global safety factor of around 5, and 4 for global safety factor of around 10. The lower value ($\alpha = 3$) is consistent with the serviceability limit criteria, although it can involve significant plastification in the ground. This has been confirmed by numerical elasto-plastic analysis (Viana da Fonseca *et al.*, 1998; Viana da Fonseca and Almeida e Sousa, 2002).
- The method of Schmertmann *et al.* (1978) for settlement evaluation was considered, combining the proposed strain influence factor diagrams with the variation of E over depth. It has to be noted that this approach introduces a non-linearity in stiffness, in spite of being based on a unique equation for E. This formulation was applied to the footing load test results, considering moderate stress levels ($Fs \cong 2.4$, $q_s = 400$ kPa), and revealed excellent agreement between calculated and experimental load-settlement curves for α equal to 4.5, with the non-linear response very well modelled (Figure 8.25).

  The value of α is somewhat higher than that commonly considered for normally consolidated sandy transported soils, due to natural structural factors, associated

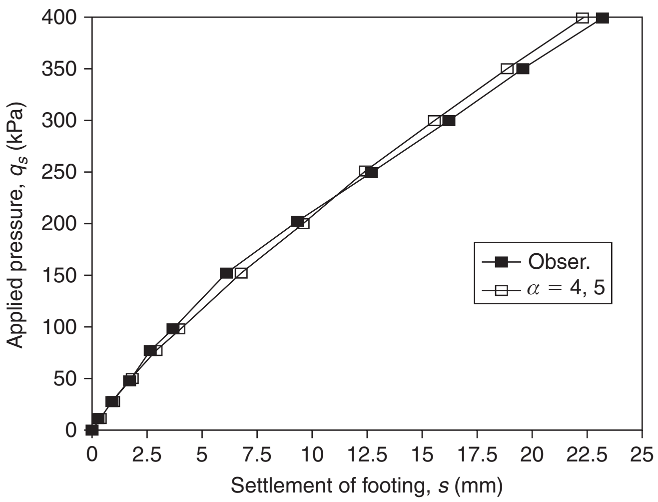

Figure 8.25 Comparison between observed settlement of the footing load test and that calculated using CPT results and adopting Schmertmann *et al.* (1978) coefficients

with the relict interparticle cementation and fabric of residual soils. Robertson *et al.* (1988) had already stated that α values could be as high as 3.5 to 6.0, or 6.0 to 10.0, for aged normally consolidated and highly overconsolidated sandy soils, respectively. The coefficients to be applied to these solutions for settlement evaluation in Brazilian residual soils are in strict accordance with these. Rocha Filho (1986) applied the Robertson *et al.* proposals to the results of loading tests on shallow foundations and plates with diameters from 0.40 to 1.60 m, carried out on residual soils from gneiss in the university campus of PUC, Rio de Janeiro, resulting in ratios of calculated to observed settlements of between 1.5 and 2.5. The ratios obtained in this study are even larger (2.7–3.4).

Note on the strength for ultimate capacity evaluation in residual soils

With regard to strength evaluation, theoretically a peak and a post-peak resistance can be obtained by pressuremeter tests (Gomes Correia *et al.*, 2004). However, because of the influence of disturbance during installation, the peak resistance is usually ignored for PMT. The undrained shear strength can be obtained from the Ménard limit pressure, p_{lm} (Amar *et al.*, 1994):

$$s_u = \frac{(p_{lm} - \sigma_h)}{5.5} \quad \text{for } (p_{lm} - \sigma_h) < 300\,\text{kPa} \tag{8.28}$$

$$s_u = 25 + \frac{(p_{lm} - \sigma_h)}{10} \quad \text{for } (p_{lm} - \sigma_h) > 300\,\text{kPa} \tag{8.29}$$

where p_{lm} is the applied pressure required to double the cavity diameter and σ_h is the estimated *in situ* horizontal stress.

For granular residual soils, Cassan's (1978) assumption that the behaviour of a granular material is a function of the average effective stress $[(\sigma'_r + \sigma'_\theta)/2]$ and that the volume change will follow a curve that has two plastic components (one under constant volume and other variables, allowing relationships between the volume and strain to be formulated), together with the plastic criteria, allows the determination of the Mohr-Coulomb strength parameters ϕ' and c':

$$p_L = (1 + \sec\phi') \cdot (p_0 + c' \cdot \cot\phi') \cdot \left[\frac{E_{pm}}{A \cdot (p_0 \cdot \sec\phi' + c' \cdot \cos\phi')}\right]^{(\sec\phi'/1+\sec\phi')} - c' \cdot \cot\phi' \quad (8.30)$$

This method requires more than a single test in a specific horizon, and ideally a multiple regression analysis. In materials where the dilatancy is significant, however, it may have errors of up to 30%.

Method to calculate the bearing resistance of spread foundations

A semi-empirical method to calculate the bearing resistance of spread foundations using the results of an MPM test is as follows:

$$\frac{R}{A'} = \sigma_{v0} + k(p_{LM} - p_0) \quad (8.31)$$

where

R is the resistance of the foundation against normal loads;
A' is the effective base area as defined in EN 1997-1;
σ_{v0} is the total (initial) vertical stress at the level of the foundation base;
p_{LM} is the representative value of the Ménard limit pressures at the base of the spread foundation;
$p_0 = [K_0(\sigma_{v0} - u) + u]$ with K_0 conventionally equal to 0.5, σ_{v0} is the total (initial) vertical stress at the test level and u is the pore pressure at the test level;
k is a bearing resistance factor given in Table 8.9;
B is the width of the foundation;
L is the length of the foundation;
D_e is the equivalent depth of foundation.

Ultimate Limit State defined by excessive deformations – numerical modelling

An FEM numerical analysis of a load test on a carefully instrumented concrete footing, resting on a residual soil from Porto granite, is described in Viana da Fonseca and Almeida e Sousa (2002). The hyperbolic soil model was adopted in order to examine the ideal range of stress-strain level data for parametrical evaluation, when the purpose is to simulate foundation pressure-settlement relations in service conditions. The importance of accurately defining the volume for the overall simulation of such a test, taken up to failure, was emphasised.

A large number of triaxial tests (43) wereperformed with different specimen sizes, consolidation stress conditions and stress-paths. These specimens were obtained by driving thin wall steel tubes (with dimensions equal to those of the specimens to be

Table 8.9 Correlations for deriving the bearing resistance factor, *k*, for spread footings

Soil category	p_{LM} *category*	p_{LM} *(MPa)*	K
Clay and silt	A	<0.7	$0.8[1 + 0.25(0.6 + 0.4\,B/L) \times D_e/B]$
	B	1.2–2.0	$0.8[1 + 0.35(0.6 + 0.4\,B/L) \times D_e/B]$
	C	>2.5	$0.8[1 + 0.50(0.6 + 0.4\,B/L) \times D_e/B]$
Sand and gravel	A	<0.5	$[1 + 0.35(0.6 + 0.4\,B/L) \times D_e/B]$
	B	1.0–2.0	$[1 + 0.50(0.6 + 0.4\,B/L) \times D_e/B]$
	C	>2.5	$[1 + 0.80(0.6 + 0.4\,B/L) \times D_e/B]$
Chalk			$1.3[1 + 0.27(0.6 + 0.4\,B/L) \times D_e/B]$
Marl and weathered rock			$[1 + 0.27(0.6 + 0.4\,B/L) \times D_e/B]$

Note: This example was published in *Fascicule* No 62-V (1993).

used in the triaxial cell) into blocks extracted from a depth of 0.5–1.0 m below the level of the footing base (Viana da Fonseca and Almeida e Sousa, 2002). All the sampling and handling procedures were undertaken with the utmost care in order to preserve, as much as possible, the natural structure of the soil.

The curves resulting from these tests exhibit substantial brittleness for the lowest effective consolidation stress, while for the others the brittle behaviour tends to disappear, probably due to the development of volumetric (collapsible) plastic strains prior to shearing. Thus, for consolidation stresses much higher than those at rest stress state, the stress-strain response tends to be typical of de-structured materials. For the lower consolidation stresses (10 and 20 kPa) peak values of deviator stress are mobilised before the highest value of the dilatancy ratio is reached. This indicates that mechanical behaviour of the saprolitic soil is controlled by cementation between particles rather than by dilatancy phenomena related to particle interlocking. This latter type of behaviour, which is typical of dense granular transported soils, is not compatible with the fabric of saprolitic soil that exhibits a low to medium density ($e = 0.60$–0.85) for an essentially sandy soil.

Figure 8.26a presents stress-strain curves from one of the tests obtained by classical (external LVDT) and local strain measurement systems (Viana da Fonseca, 1996). The former technique leads to rather unrealistic values of stiffness. The curve for the local instrumentation results was assumed as representative and plotted in the modified axis in order to derive the hyperbolic parameters (Figure 8.26b).

As is clear in Figure 8.26b, the Young's modulus deduced from testing results using a hyperbolic trend will depend strongly on the strain range where the model is applied. To best understand this pattern of behaviour, Figure 8.26b may be seen as a good model of what should be expressed as a multiphase solution. The mechanical performance seems to be marked by different trends in three ranges of values that could be associated with three pre-yield zones. Three different initial tangent Young's moduli can then be derived, one for each of these zones, from a classical hyperbolic approach of the stress-stain curve: designated by $E_{ti,0}$, $E_{ti,i}$ and $E_{ti,h}$, these moduli have taken into account, respectively, the lowest shear stress values (where the natural bonding between particles is mostly preserved inside the elastic yield locus), the intermediate states (representative of the metastable condition, where progressive de-structuring

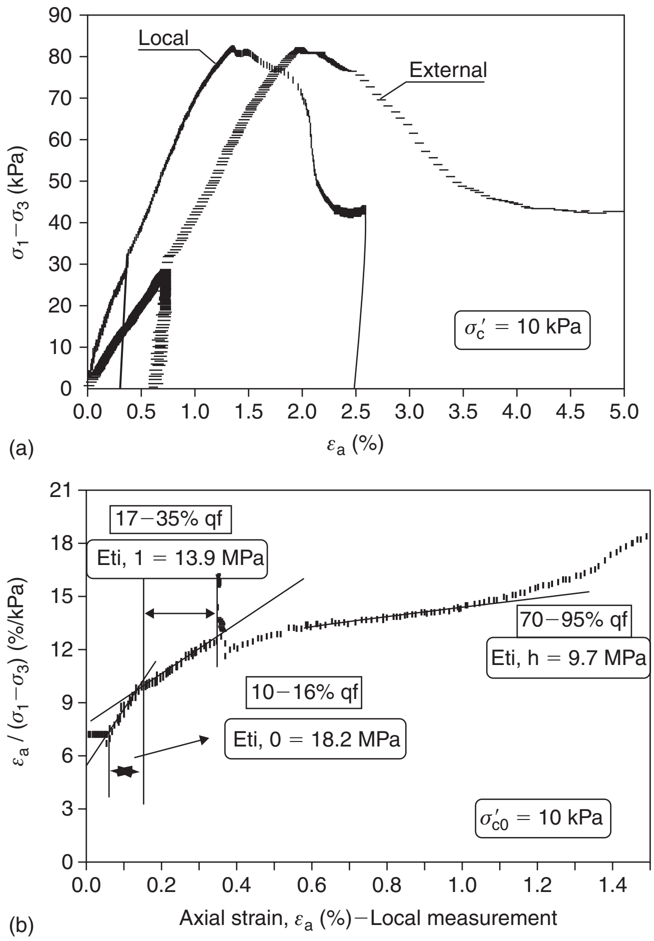

Figure 8.26 CID triaxial test. (a) Stress-strain relations with local and external instrumentation; (b) Hyperbolic tangent Young modulus for different stress ranges: $E_{ti,0}$, $E_{ti,i}$ and $E_{ti,h}$

is observed), and finally the values of shear stress between 70 and 95% of failure and where the behaviour is significantly of a granular type. Figure 8.27 illustrates these different trends and adopted options (Viana da Fonseca and Almeida e Sousa, 2002). The first parameters reflect the lowest stress levels where interparticle structure is more preserved and elasticity seems to prevail. The second value, ranging over the intermediate stress levels, can be associated with the beginning of plastic yielding and progressive breaking down of micro-structure (phenomena that will dominate major zones of the ground below the footing, since an at-rest stress state, characterised by low values of K_0, ~[0.35–0.59] is expected – Viana da Fonseca and Almeida e Sousa, 2001). Finally, the highest stress levels, at the stable classically assumed ranges of 70–95% of failure (Duncan and Chang, 1970) that will be associated with strongly de-structured matrices.

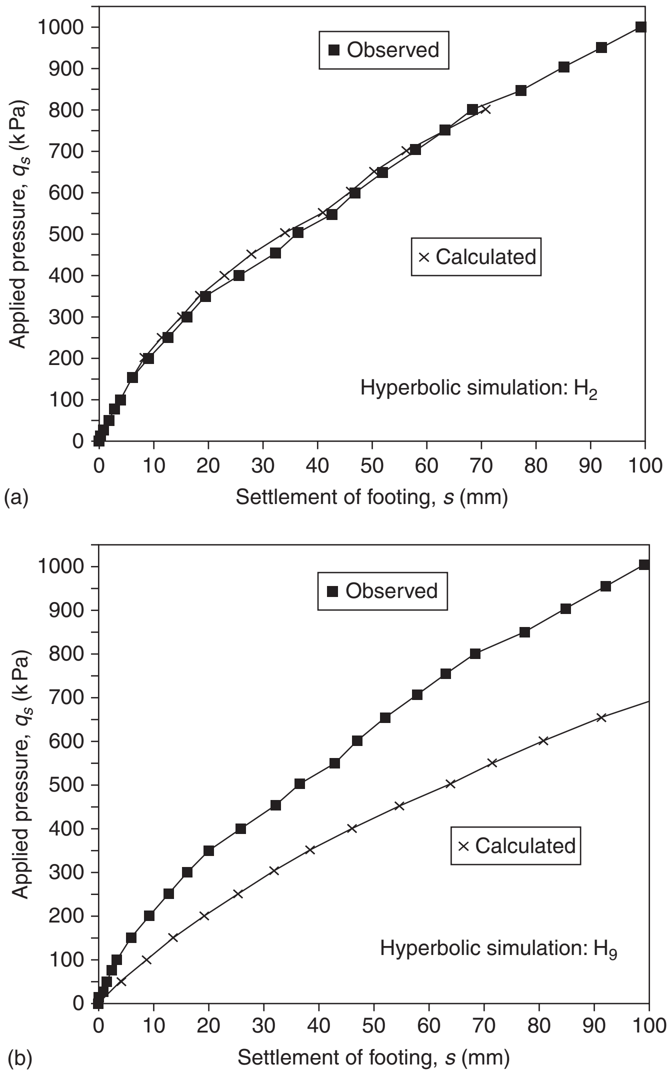

Figure 8.27 Numerical simulation of the footing load test using the hyperbolic model parameters from triaxial tests for the two extreme modelling assumptions: (a) low strain level, and (b) high strain level

The definition of the overall set of hyperbolic parameters for these distinct levels of stress-strain is presented in Viana da Fonseca and Almeida e Sousa (2002), together with a modelling of all significant triaxial tests executed for this study.

From the observation of these curves, it has been found that:

(i) the hyperbolic modelling of the tests with a single set of parameters does not reproduce the overall behaviour of the stress-strain curves;

(ii) modelling the curves from parameters based on $E_{ti,0}$ reproduces with great accuracy the low stress-strain levels but is very conservative on the whole curve;
(iii) on the other hand, the curves modelled from $E_{ti,h}$ values fit very well the later part of the curves, showing important differences when compared to the low to medium levels; the use of intermediate parameters ($E_{ti,i}$) will be a compromise.

Additional studies have been carried out on the importance of the stressed volume on the behaviour of this soil, as it was expected that the ground below the footing would be subjected to increasing average stresses.

The numerical analysis of the concrete footing load test was intended to determine the best parameters for the modelling and prediction of the behaviour of such a foundation. It was presented in the paper by Viana da Fonseca and Almeida e Sousa (2002). Two of the figures presented are combined in Figures 8.27a and b, allowing a comparison between the curves of the applied pressure versus the settlement of the footing obtained experimentally and resulting from the numerical simulation using the hyperbolic model.

There is a clear benefit in showing the sensitivity of the parameters to different levels of stress-strain. A brief summary of the results of the analysis by Viana da Fonseca and Almeida e Sousa is as follows:

(i) only the analyses based on the initial tangent Young's modulus, defined from the low strain ranges of triaxial tests on undisturbed samples ($E_{ti,0}$), represent the footing test reasonably throughout the loading steps;
(ii) the value of $Rf = 0.9$ seems to help the model to fit the data well, particularly in the global definition of the observed curve, while the option for $Rf = 0.7$ shows a poorer fit when considering the deformability parameters for "small" strain ranges, and also in the vicinity of failure;
(iii) analyses that are based on the initial tangent modulus for ranges of "medium" and "large" deformations in the triaxial tests ($E_{ti,i}$ and $E_{ti,i}$) significantly overpredict the observed settlements in the footing load test;
(iv) it is essential to consider the variation of Poisson's ratio along several loading steps, up to values very close to the ultimate load ($q = 950$ kPa), with clear benefit in the definition of the solution of the settlement of the footing base.

It is pertinent to reiterate the reasons why the calculation, based on the parameters deduced from initial tangent modulus for very low stress-strain ranges ($E_{ti,0}$) of triaxial tests, seems to simulate the behaviour of the load test very well. In fact, the parameters deduced from triaxial tests taking higher levels of stress-strain modulus, already include the effect of plastic deformations related to progressive failure of the soil structure, and therefore they represent less satisfactorily the behaviour of the soil in natural conditions. The consequence of this, as was illustrated in Figure 8.9 where modelling parameters were defined from the classic ranges of 70–95% of failure stress, is to significantly overestimate the observed settlements. For these elevated levels of deviatoric stresses the material behaves as a non-structured soil, and the parameters deduced cannot represent foundation behaviour under service conditions.

The influence of different model parameters, in accordance with distinct stress-path zones in the ground, was analysed. This can be relevant in some marginal zones, where stress-paths are rather different from classical compression paths. It was shown that, up to moderate load levels, that is to say, to stress-strain levels not dominated by significant plastic behaviour, this stress-path factor is not important in the simulation of the settlements of the footing base. The influence of the anisotropy of the stiffness characteristics is, however, relevant in the prediction of the settlement of external points to the loaded area, where the stress-paths are significantly different from classic compression.

In tropical residual soils, most shallow foundations will involve dealing with unsaturated soils, and two common problems which flow from this relate to collapsible soils and expansive soils.

8.3 FOUNDATIONS ON UNSATURATED SOILS

According to Fredlund and Rahardjo (1993), matric suction dramatically increases the bearing capacity of the soil, and this is shown in Figure 8.28 which illustrates the effect of various matric suction values on the bearing capacity of shallow foundations. When attempting to arrive at a suitable design value for matric suction, it is useful to construct a plot similar to this figure.

Since shallow footings are normally placed well above the ground water table, if adequate surface and subsurface drainage is provided around the structure, it may be reasonable to assume that negative pore-water pressures will be maintained immediately below a footing. It should also be realised that there may be a fluctuation in the groundwater table as a direct result of building the structure. In some cases, the

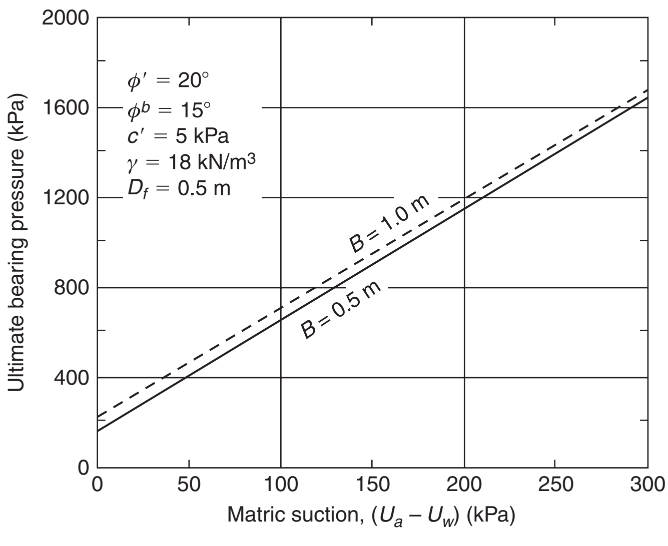

Figure 8.28 Bearing capacity of a strip footing for various matric suction values (*After* Fredlund and Rahardjo, 1993)

groundwater table may be lowered but, more commonly, the water table will rise due to excessive watering of the vegetation surrounding the building.

There are many situations where the groundwater table is far below the ground surface and a hydrostatic profile is not reasonable for design purposes. In these cases, measurements of the *in situ* suction below the footings of existing structures in the vicinity can prove to be of value. These suctions can be relied upon to contribute to the shear strength of the soil, but the decision regarding what value of suction to use in design becomes dependent upon local experience and the microclimate in a particular region.

Design considerations for shallow foundations

The following soil-structure interaction issues should be considered in foundation design. First, soil-structure interaction implies, by definition, that the response of the soil and the structure are interdependent; i.e., the reaction of the soil to the structure affects the performance of the structure, and the reaction of the structure to the soil affects the behaviour of the soil. One of the two following approaches is needed to solve this problem (Houston, 1996).

Method 1: Employ a finite element code which models all components including the structure and the soil in contact with it. However the commercially available codes, being the ones in common use, tend to be either written for structural analysis and hence model structures well (and soils less so), or written for geotechnical analysis and hence model soils well (and structures less so). Ideally, the model for the soil would account for non-linearity in the stress-strain-time constitutive law, including water flow and the strains induced by changes in soil water content. By this method, all responses to load and water would be totally coupled.

Method 2: The response of the soil and structure are decoupled, and then recombined to ensure compatibility via iteration.

Houston (1996) showed an example of this approach with details, and concluded that simplified, and often greatly simplified, versions of this procedure are used in design practice, with corresponding approximations and errors. In most cases, the factors of safety are adequate to accommodate these approximations and errors.

8.3.1 Shallow foundations on collapsible soils

In the case of collapsible unsaturated soils, foundations can behave satisfactorily for some time, and then suddenly suffer significant additional settlement, due to the accidental appearance of a water source that starts to flood through the soil (see Coutinho *et al.*, 2004b).

The amount of volume decrease experienced by a collapsible soil upon wetting under load depends on several factors, including the soil type, the initial water content and dry density, the degree of wetting, and the stress state and boundary conditions.

According to Houston (1996), difficulties associated with estimating collapse settlement include the typical variations in cementation and gradation causing soil properties to change over distances of only a few centimeters both laterally and vertically, and also lack of knowledge of sources of water. The greatest uncertainty in estimating collapse settlement is linked to the uncertainty of the lateral extent and

Table 8.10 Comparison between r_{cpred} from PMT data and r_{cmeas} (*After* Dourado and Coutinho, 2007)

		Settlement predicted (mm)		
Test	σ_{soaked} *(kPa)*	*Before wetting*	*After wetting*	*Collapse (mm)* ($r_c = r_{P\ soaked} - r_{P\ nat}$)
PC 01	100	0.56	15.06	**14.5**
PC 02	60	0.34	8.84	**8.5**
		Settlement predicted (mm)		
Test	σ_{soaked} *(kPa)*	*Before wetting*	*After wetting*	*Collapse (mm)* ($r_m = r_{m\ soaked} - r_{m\ nat}$)
PC 01	100	1.24	46.24	**45.0**
PC 02	60	0.56	21.06	**20.5**

degree of wetting. The degree of saturation achieved during the conduct of conventional laboratory response to wetting tests is quite high, typically 85 to 95%. Estimated collapse settlements based on full-wetting collapse potential may not be realised in-situ.

The most likely explanation for why the actual field collapse settlement is less than the estimated settlement is that, when a soil is only partially wetted, only a portion of the full collapse potential is realised. In practice, there are many field situations for which only partial wetting occurs. However, not all field wetting conditions result in low degrees of saturation. If the water source is due to a rising groundwater table, or perhaps from long-term, steady state wetting by ponded water, the degree of wetting achieved *in situ* may be adequate to result in essentially full-wetting collapse. In these cases, however, the lateral extent of wetting may still be quite difficult to estimate (Houston, 1996).

Dourado and Coutinho (2007) predicted collapse settlements using PMT results and considering the traditional methodology of Briaud (1992) for footing settlement on sand. The settlements were calculated at both natural water content and fully saturated conditions and the difference in these two conditions was considered as the collapse settlement (rc) of the soil (see Table 8.10).

$$s = \frac{2}{9E_d} \cdot \sigma'_{v0} \cdot B' \cdot \left(\lambda_d \cdot \frac{B}{B'}\right)^{\alpha} + \frac{\alpha}{9E_c} \cdot \sigma'_{v0} \cdot \lambda_c \cdot B \tag{8.32}$$

where

s = footing settlement (final);
E_d = pressuremeter modulus within the zone of influence of the deviatoric tensor;
E_c = pressuremeter modulus within the zone of influence of the spherical tensor;
σ'_{vo} = footing net bearing pressure;
B' = reference width of 0.6 m;
B = width or diameter of the footing ($B > B'$);
α = rheological factor;
λ_d = shape factor for deviatoric term and
λ_c = shape factor for spherical term.

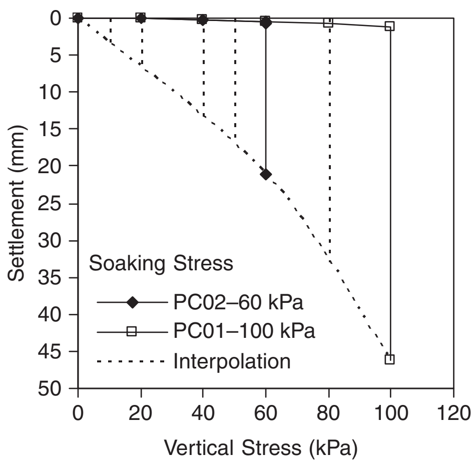

Figure 8.29 Interpolation of the settlement-stress relationship from *in situ* collapse tests (*After* Dourado & Coutinho, 2007)

Table 8.11 Comparison between $r_{c\,int}$ obtained by interpolation and r_c predicted (*After* Dourado & Coutinho, 2007)

Stress (kPa)	$r_{c\,int}$ *(mm)*	$r_{c\,pred}$ *(mm)*	*Factor of increase* ($F_m \cdot r_{c\,pred} = r_{c\,int}$)
100	45.0	14.5	3.1
80	31.6	11.4	2.8
60	20.5	8.5	2.4
40	12.5	5.7	2.2
20	6.3	2.8	2.3

Table 8.10 shows that the predicted settlements in the natural condition (0.56 and 0.34 mm) were about 50% of the measured settlements (1.24 and 0.56 mm). It is also seen that the predicted collapse settlements $r_{c\,pred}$ (14.5 and 8.5 mm) were between about 33 and 50% of the measured settlements $r_{c\,meas}$ (45 and 20.5 mm).

An increase in settlement is also seen with an increase in soaking stress. Thusthe influence of the soaking stress in the $r_{c\,pred}$ was evaluated. The data is summarised in Figure 8.29 and Table 8.11.

Dourado and Coutinho (2007) concluded that for any stress, predictions based on PMT data underestimated the r_c measured in the plate load test. The use of a factor of increase (F_m) of 2.5 in predicted collapse settlement $r_{c\,pred}$ ($F_m \cdot r_{c\,pred} = r_{c\,int}$) by the PMT, would lead to a better approach to the prediction of r_c for the *in situ* collapse tests. However, the authors cautioned that this factor applied only to the soil studied.

8.3.2 Deep foundations on collapsible soils

Typically, the calculation of load capacity of piles seeks a balance between the applied loads (Q) and the available resistance, made up of Shaft Resistance (R_s) and Toe

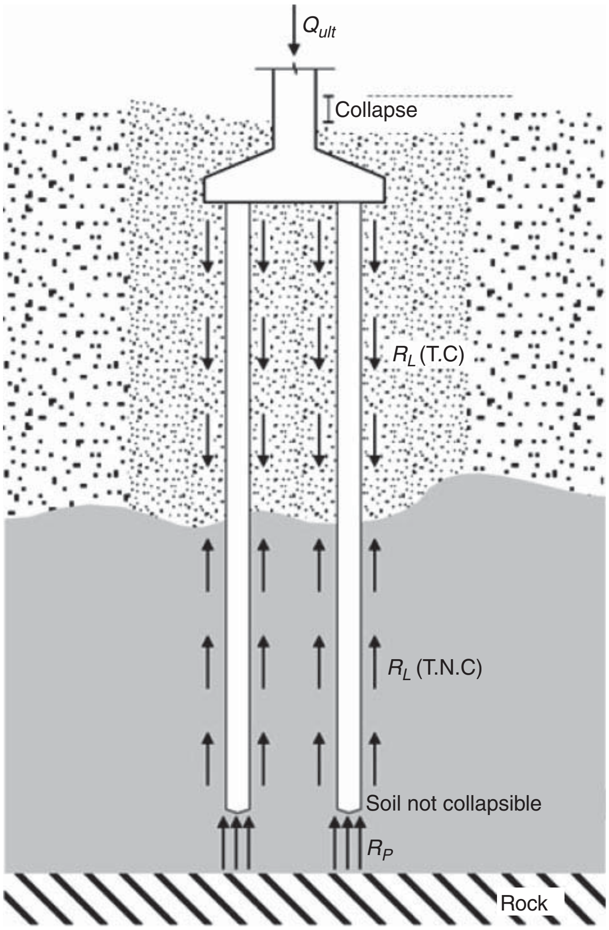

Figure 8.30 Considering the effect of the collapse load capacity of piles

Resistance (R_p) (Figure 8.30). In the presence of collapsible soil, we must consider the additional applied load due to the collapse, in the form of negative shaft friction. This is difficult to determine because of the complexity of the relative movements along the shaft. As a simplified solution, we can calculate the shaft resistance of the collapsible segment and apply this as a distributed load along the shaft. In general we have the following equation:

$$Q_{ult} + R_s(TC) = R_p + R_s(TNC) \tag{8.33}$$

where

Q_{ult} = Maximum applied load acting on the pile;
R_s (TC) = Applied load due to negative shaft friction on the collapsible length;
R_p = Toe resistance;
R_s (TNC) = Shaft resistance of non-collapsible length.

In some standards, such as AS 2159 in Australia, negative shaft friction (NSF) is assumed not to affect the Ultimate Limit State, since the deflections associated with the ULS are generally much greater than those required to fully reverse any NSF. However, NSF can have a significant effect on settlements at working load and hence on the Serviceability Limit State (SLS). Checks on the SLS with full NSF applied are therefore required. The same may well be true with regard to collapse settlements and R_s (TC), but the magnitude of the collapse settlement will need to be checked against the magnitude of the settlement at ULS.

Both shallow and deep foundations in collapsible soil can behave satisfactorily for some time, and then suddenly incur additional settlement of considerable magnitude, due to the accidental appearance of water that starts to flood through the soil.

A geotechnical profile and water content from Eunápolis City was described by Coutinho *et al.* (2010). This site experienced damage during the execution of the deep foundations, and the presence of collapsible soil was considered to be one of the causes. The objective of this study was to identify and characterise the soil and investigate the possibility of influence on the pile foundation.

For this purpose, two static compression pile load tests were performed; one with the soil in natural condition and the other after a flooding process. A system of soaking was used for the flooded load test, through a pit built with soil drains. The pit was subjected to a constant water head, using a water reservoir connected to a car. The total time of soaking was 72 hours, after which the flooded load test was started. Further information is given in Coutinho *et al.* (2010).

Comparing the natural and flooded moisture content profiles, it was seen that flooding was effective to a depth of 10 m, showing that all the length of the pile shaft was flooded. However, due to the higher N_{SPT}, of the order of 50 blows, in the layer at the tip of the piles, the soaking did not reduce the toe resistance.

Analysis of load/settlement curves

Figure 8.31 shows a comparison between the results of the two load tests. Some points of the curve were used to help in the interpretation and comments:

1 At the vertical axial working load of 40 tf (400 kN), there is no significant difference in performance between the piles;
2 Differences in the behaviour of the two piles are observed above an applied load of 51 tf (510 kN);
3 In relation to the settlements, there was a significant increase for the flooded soil; for example, at the load of 64 tf (640 kN), it increased from 10 mm to15 mm;
4 At a load of 72 tf (720 kN), the settlement in the natural soil was 15 mm and in the flooded soil 20 mm. It might have been expected that the difference would be larger, however at this point, the pile toe starts to work for the flooded pile because of the high N_{SPT}.

The blue dotted line shows an extrapolation of the curve for flooded soil without the influence of the strong toe. Considering the pile response in natural soil, the maximum load of 80 tf (800 kN) corresponds to a settlement of 27.1 mm. For this value of settlement to occur, according to the blue dotted line, the applied load would be

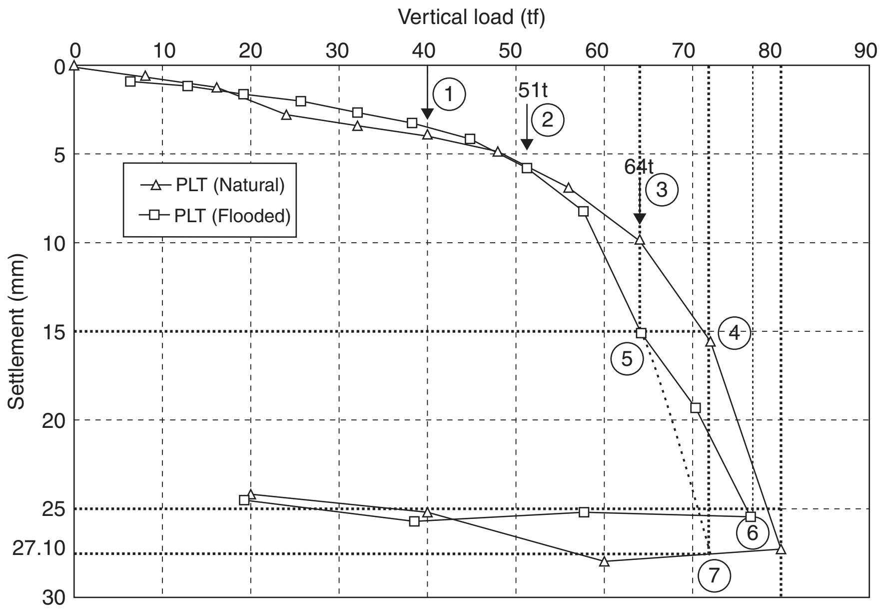

Figure 8.31 Pile load test curves and settlement data for the piles in natural soil and in flooded soil

only 72 tf (720 kN). This represents a reduction in the rupture load of 80 kN, or in the order of 10%.

Load capacity

a) Natural load test (PC – Natural)

Décourt and Quaresma (1978), and Décourt (1996) considered a layered soil profile. The shaft resistance (R_s) was calculated using the average value of N_{SPT} for each layer. For the toe resistance, an undrained shear strength of $s_u = 250$ kPa was used.

In lateritic soils, the shaft resistance of piles can be 2 to 3 times the resistance calculated by conventional prediction methods (Décourt, 2002). The R_s in the layer with iron concretions (between 7.0 and 8.0 m) was calculated separately using a factor of increase of 2.5.

A total shaft resistance (R_s) of 475.4 kN and a tip resistance (R_p) of 227 kN were calculated, making a total ultimate capacity (Q_f) of 702.4 kN (see Table 8.12).

b) Flooded load test (PC – Flooded)

For the flooded soil, a total shaft resistance (R_s) of 291.5 kN and a tip resistance (R_p) of 340 kN were calculated, making a total ultimate capacity (Q_f) of 631.5 kN. The results of both load tests are presented in Table 8.12.

Thus, using the Décourt and Quaresma (1978) method, it can be seen that the predicted shaft resistance reduces from 475.4 to 291.5 kN, or 38%, due to the flooding. The value of the flooded toe resistance (340 kN) was greater than in the natural soil

Table 8.12 Summary of the results

	Décourt and Quaresma (1978) – results (kN)		
Load test	*Shaft resistance (R_s)*	*Toe resistance (R_p)*	*Ultimate capacity (Q_f)*
Natural	475.4	227.0	702.4
Flooded	291.5	340.0	631.5

Table 8.13 Estimates of Q_f obtained and measured

	Rupture Load (Q_r) (kN)			
Load test	*Décourt (1996)*	*Van Der Veen (1953)*	*Décourt and Quaresma (1978)*	*Dynamic load test*
Natural	812 RL = 504 kN	809	702.4	770
Flooded	–	836	631.5	–

because of the differences between the soil profiles. However, a reduction in the flooded failure capacity of 10% (702.4 to 631.5 kN) was observed.

The Van Der Veen (1953) method was also used to estimate the ultimate capacity. It gave a good estimate for both curves, with values of $Q_f = 809$ kN (natural) and $Q_f = 836$ kN (flooded).

Van Der Veen method was also applied for the hypothetical case of the corrected flooded curve, the blue dotted line in Figure 8.31. The results showed a Q_f in the order of 700 kN, confirming the conclusion above (reduction of $809 \rightarrow 700 = 13.5\%$).

Table 8.13 presents the ultimate capacities obtained through the three methods utilised in this work (Van Der Veen, 1953; Décourt and Quaresma, 1978; Décourt, 1996). The result obtained by a dynamic load test on the same pile while in a natural condition is also shown.

It can be seen that the values obtained for the failure load were all around 800 kN. The exception was the prediction by the Décourt and Quaresma (1978) method for the flooded pile.

Effect on the ultimate capacity

For the total failure load, the difference is relatively small (10%) because the reduced shaft capacity was replaced by increased toe resistance as a result of the differences between the soil profiles.

The values obtained in the static load tests (Figure 8.31) were of the same order of magnitude. However, if the very resistant layer below of the toe of the flooded pile did not exist, an influence in the order of 10%, after flooding was expected. A similar result is seen in the prediction by the Décourt and Quaresma (1978) method.

Some cases reported in Brazilian literature show a reduction in the results of the total failure load due to the flooding process in the order of 20%. For most well designed foundations, a reduction in ultimate capacity of 10 to 20% would probably not be critical. However, as noted previously, the effect on the Serviceability Limit State could be very important, as suggested by the increase in settlement in the test pile at 640 kN.

8.3.3 Mitigation measures

Several mitigation alternatives are available for dealing with collapse phenomena. Mitigation measures which have been used in the past can generally be fitted into one of the categories below. Often a combination of mitigation measures is used (Houston, 1996):

- Removal of a volume of moisture-sensitive soil;
- Removal and replacement or compaction;
- Avoidance of wetting;
- Chemical stabilisation or grouting;
- Prewetting;
- Controlled wetting;
- Dynamic compaction;
- Pile or pier foundations;
- Differential settlement resistant foundations.

More details of mitigation measures can be seen in Houston (1996).

The following measures for minimising wetting represent good practice. If the wetting is anticipated to occur from surface or near surface infiltration, consider:

1 restricted irrigation watering (e.g. desert landscaping);
2 restricted landscape vegetation adjacent to structures, unless placed in planters;
3 paved surfaces around the structure to the maximum extent practical;
4 use of watertight water and sewer lines in double pipes or troughs, and;
5 replacement or removal and compaction of near surface layers to form a low permeability barrier to water. The barrier to water should be composed of moisture-insensitive soils.

As the probability of wetting is reduced, the risks associated with the collapse phenomena are reduced. In the final analysis, the total costs, including the consequence of estimated collapse settlements, over the lifetime of the structure must be considered and compared for various alternatives.

8.3.4 Recent research and developments for dealing with collapsible soils

The importance of effects of wetting on unsaturated soil response is very well documented. The potential for wetting-induced volume change of all unsaturated soils is becoming widely recognised in the geotechnical profession. Most of the early literature on volume moisture-sensitive soils dealt with naturally-occurring deposits, and widespread recognition of wetting-induced compression and swell of compacted soils is relatively more recent. The importance of coarse aggregate to the swell/compression response of soil upon wetting under load has begun to receive attention. *In situ* methods used in the past, and those presently under development, appear promising for studying the response to wetting of gravelly and other difficult-to-sample unsaturated soils. Lateral movements associated with collapse settlement have been considered in some current and recently completed studies. Lateral strains due to wetting are of particular importance for embankments and slopes, whether made of naturally-occurring or compacted unsaturated soils (Houston, 1996).

Studies of collapsible soils currently in progress and planned for the near future include: (1) the response of collapsible soils to earthquake loading, before and after wetting, (2) strength of collapsible soils after wetting, and (3) constitutive soil model development, considering the role of cementation, including soil suction. Constitutive models incorporating stress state, soil suction, and strain, coupled with unsaturated flow models are desirable. Improved methods for estimating the degree and lateral extent of wetting are needed. Additionally, considerations of risk and integration of risk assessment and total life cycle cost estimates into the mitigation and foundation design selection process are very important to the success of future efforts.

8.3.5 Shallow foundations on expansive soils

Expansive soils, which increase in volume when water is available, but shrink if water is removed, are a continuing source of problems in the design, construction, and maintenance of buildings, buried pipes, roads and airfields, canals, and retaining structures. Wray (1995) reported that a soil is commonly considered to have limited expansive tendencies when its plasticity index (PI) is less than 20. If the plasticity index is greater than 20 but less than 40, the soil is considered to have moderate expansive properties. The soil is considered to be highly expansive if the PI is between 40 and 60. Soils with PI's greater than 60 are considered to be very expansive. Another method often used to classify the expansive potential of soil is the expansion index (EI). The EI is determined from a special laboratory test that is performed in a specified standard manner. A soil with an EI of 50 or less is considered to have low expansion potential. A soil of 91 or greater indicates a soil with high or very high expansion potential.

The properties associated with expansive clays such as heave and swell pressure are dependent on three factors: (i) natural soil properties such as moisture content, dry density, plasticity index and compaction, (ii) environmental conditions including temperature and humidity, and (iii) vertical stresses such as overburden pressure and foundation loading conditions. The following sections explain the influence of some of the above factors on the swell properties of expansive soils.

Many unsaturated soils are also expansive. Environmental conditions such as temperature and humidity influence swell potentials by changing suction in unsaturated expansive soils. The engineering behaviour of unsaturated soils can be interpreted in terms of two key stress state variables, namely: net normal stress and suction (Fredlund and Rahardjo, 1993). The suction changes associated with the movement of water in the liquid and vapour phases are called matric suction and osmotic suction, respectively. The total suction is equal to the sum of matric and osmotic suction. More recently, the focus of research has been directed towards understanding the effects of different types of suctions and their influence on swell characteristics in unsaturated expansive soils.

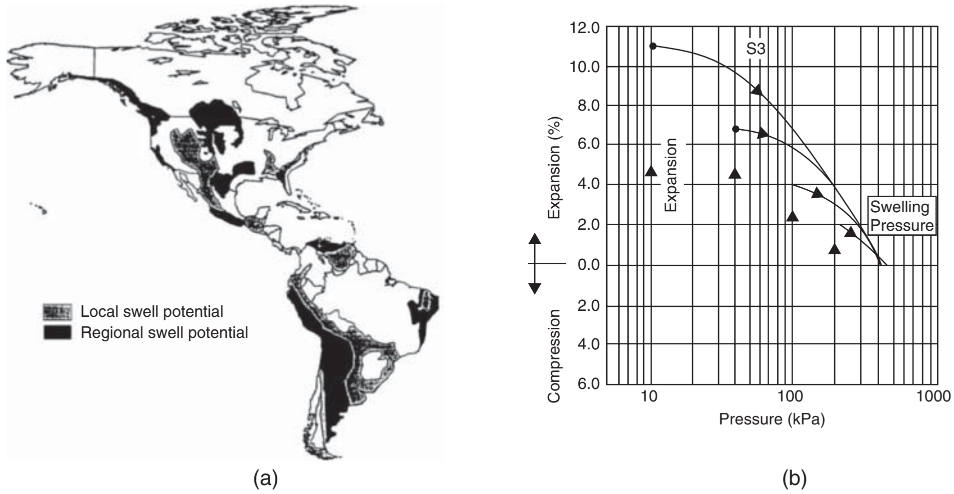

Figure 8.32 (a) Generalised map showing expansive soil distribution in the Americas; (b) Typical results for oedometer tests on samples of an expansive residual soil from Pernambuco, Brazil (*After* Mitchell and Coutinho, 1991)

The final factor that has a major influence on swelling in soils is the effect of overburden pressure on the foundation material at a site. It is well known that the magnitude of swell under confined loading conditions is less than that in unconfined conditions. However, in conventional engineering practice, the majority of laboratory swell tests are conducted either in unconfined conditions with low seating pressures, or in rigid apparatus with unknown lateral confining pressures.

Formation and distribution of expansive soils

Expansive soils are commonly found in arid and semi-arid regions in the world such as Australia, Canada, China, India, Israel, Iran, South Africa, UK and USA. In these areas, the rainfall is moderate, precipitation is seasonal and there are high evaporation rates. Drainage must be sufficiently restricted to permit pore-water salts to remain and become concentrated by evaporation. The topography may be flat, as in bentonite/marine shale deposits, or the grade may be steep, as in volcanic or orogenic settings, where slope stability can be a geotechnical hazard.

Mitchell and Coutinho (1991) included a generalised map showing the distribution of expansive soil in the Americas, compiled on the basis of climate, geology, and engineering experience (Figure 8.32). The distribution in the United States is fairly accurate, since most of the areas are defined from engineering experience. The distributions shown for Canada, Central and South America are less precise, as they rely on climate and geology to a greater degree. Regions of swell (RS) show areas where expansive soils are likely to occur. They do not indicate swelling soils over the entire area. Local areas of swell (LS) represent a more localised potential for expansive behaviour.

Indications of swelling potential may appear from the results of routine tests such as grain size analysis, Atterberg limits, and *in situ* moisture content and dry density.

Table 8.14 Characterisations based on Direct Measurements (from Pupalla *et al.*, 2004)

References	*Test Details*	*Expansion Index*[1]	*Swell Strain, %*	*Characterisation*
Holtz and Gibbs (1956); USBR Method	Oedometer, Zero Lateral Strain; Seating Pressure −7 kPa	—	>30	Very High
			20–30	High
			10–20	Medium
			<10	Low
FHA/HUD classification (1960)[2]	Oedometer, Surcharge of 7 kPa	>130	>12	Expansive
		90–130	7–12	Highly expansive
		50–90	4.7	Moderate expansive
		<50	2.4	Marginal
Ladd and Lambe (1961) (FHA)	Oedometer Setup (Seating Pressures are not known)	—	>6	Very Critical
			4–6	Critical
			2–4	Marginal
			<2	Non-Critical
Chen (1965)	Oedometer, Seating Pressure 48 kPa		>10	Very High
			3–10	High
			1–5	Medium
			<1	Low

[1]Specified by Southern California Local Codes
[2]Federal Housing Administration/Housing and Urban Development

The activity (the ratio of plasticity index to percentage finer than 2 μm) provides a useful measure of expansion potential. Several correlations, based on the above parameters, have been proposed for preliminary estimation of expansive deformations (Snethen, 1984; Chen, 1988). Any expansive soil has a lower and upper limit of moisture content between which swelling and shrinkage can take place. Therefore, if movement is to occur, moisture changes must occur within this critical range.

8.3.6 Characterisation by swell strains

Puppala *et al.* (2004) described two approaches that are commonly used for the characterisation of expansive soils, based on swell strains. The first one is a direct approach using oedometer and/or other test methods to measure volumetric or vertical swell strains in soils. The second is an indirect approach based on soil index parameters or suction based measurements to evaluate the swell strain percentages, and then to address the problematic nature of these soils.

Direct approach

In the direct approach, swell strains are measured using conventional oedometers or other equipment such as confined swell test apparatus and three dimensional free swell test setups. In 3D setups, both lateral and vertical swelling can be measured. The volumetric swell strain information can be calculated from the measurements of lateral and vertical swelling. Table 8.14 presents a few of the characterisation methods available in the literature for classifying expansive soils based on swell strain measurements. Holtz and Gibbs (1956) developed an oedometer test based characterisation method in which a seating pressure of 6.95 kPa was used. Based on this method, a vertical

Table 8.15 Characterisations Based on Suction Measurements (from Pupalla *et al.*, 2004)

Reference	*Soil Suction at Natural Moisture Content, kPa*	*Related Swell Strain (%)*	*Characterisation*
Snethen *et al.*	>400	>1.5	High
(1977)	150–400	0.5–1.5	Marginal
	<150	<0.5	Low

Table 8.16 Characterisations Based on Total Suction Measurements (from Pupalla *et al.*, 2004)

Reference	*Total Suction – Water Content Index (Suction in pf/Water Content in %)*	*Characterisation*
McKeen (1992)	> -6	Very High
	-6 to -10	High
	-10 to -13	Moderate
	-13 to -20	Low
	< -20	Non-expansive

swell strain of 30% or above indicates a very highly problematic soil and a swell strain of less than 10% represents a non-problematic soil.

Chen (1965) applied higher seating pressure of ∼48 kPa, for the characterisation of expansive soils. In this approach, soils with swell strains of 10% or above were classified as very highly problematic soils. The soils with swell strains less than 1% were regarded as non-problematic soils. The above two methods can be used in characterising expansive soils for designing both lightly and heavily loaded foundations. The characterisation used for lightly loaded structures can be extended to transportation infrastructure including pavements and runways.

Indirect approach

Several characterisations based on properties from indirect tests are available in the literature. These characterisations are based on soil index parameters and suction measurements. Table 8.15 presents a characterisation based on *in situ* suction using both total and matric suction potentials. This approach requires suction properties to be measured on soil samples using different methods. Instruments such as tensiometers, thermal conductivity sensors or filter paper methods can be used for measuring matric suction. The psychrometer or filter paper method can be used to measure total suction in soils. Table 8.15 can be used to characterise expansive subgrades based on suction potentials. McKeen (1992) developed another procedure based on total suction and water content of soils (Table 8.16) to estimate the swelling potentials.

Fredlund and Rahardjo (1993) provide an approach to calculate swell strain, $\Delta h_i/h_i$ in expansive soils:

$$\frac{\Delta h_i}{h_i} = \frac{C_S}{1 + e_{oi}} \log \frac{P_{fi}}{P_{oi}} \tag{8.34}$$

where

e_{oi} = initial void ratio of the soil layer,

Table 8.17 Characterisations Based on Soil Index Parameters (from Pupalla *et al.,* 2004)

Reference	*Test Type*	*Plasticity Index, PI*	*Characterisation*
Raman (1967)	Atterberg Limits	>32	Very High
		23–32	High
		12–23	Medium
		<12	Low
Chen (1988)	Atterberg Limits	35 and above	Very High
		20–55	High
		10–35	Medium
		0–15	Low

h_i = thickness of the soil layer,
P_{fi} = final stress state in the soil layer,
P_{oi} = initial stress state in the soil layer,
C_S is the swelling index and
Δ_{hi} is swell in the expansive soil layer.

Another indirect characterisation approach is based on soil index parameters, primarily using Atterberg limits or plasticity characteristics. This is the most frequently used method in geotechnical practice since these tests are simple to perform and inexpensive. In a study carried out on San Antonio and Corpus Christi expansive clays, swell characterisation based on Atterberg limit values was used (King *et al*., 2001). A large scatter was observed, and practitioners should be careful when characterising expansive subgrades using only Atterberg limits. The same study recommends the use of liquidity index and consistency index parameters to aid in the characterisation of expansive soils, and provides a wide range of indices to differentiate between lean, fat and other clays that exhibit swelling behaviour. Table 8.17 presents characterisations based on soil index parameters.

The Potential Vertical Rise (PVR) method also estimates the swell potentials of expansive soils in length units based on Atterberg limits, overburden pressure and loading conditions of various layers. This method has been used in the characterisation of subgrades and design of pavements. The Texas Department of Transportation (TxDOT) is currently involved in the development of new or alternative methods to characterise expansive soils, which may replace the PVR method. Further details on this method can be found in TxDOT testing manual (see TxDOT website).

In addition to the above characterisations, there are a few more empirical relationships available in the literature to predict swell strains, which use soil plasticity index, compaction moisture content and the activity parameter of the soil (Table 8.18). Once the swell strain percentages are determined, they can be used along with Table 8.14 to estimate the severity of the natural expansive subgrade.

8.3.7 Types of foundation that are used in expansive soils

The majority of foundations used on expansive soil sites are one of the following:

- Slab-on-grade
- Slab-on-grade with piles

Table 8.18 Empirical Relations for Percent Swell (S) from soil properties (from Pupalla *et al.*, 2004)

No.	*Description*	*Reference*
1	$S = 0.00216 \times PI^{2.44}$	Seed *et al.* (1962)
2	$S = [(0.00229 \times PI)(1.45 \times C)/w_o] + 6.38$	Nayak *et al.* (1974)
3	$\text{Log } S = 0.9 \times (PI/w_o) - 1.19$	Schneider *et al.* (1974)
4	$S = 83 \times (2 \times A\text{-}1)$	El-sohby (Unknown)
5	$\text{Log } S = 0.08 \times (0.44 \times LL - w_o + 5.5)$	Vijayvergiya *et al.* (1973)

PI = Plasticity Index; C = Clay percent; w_o = Initial water content; A = Activity

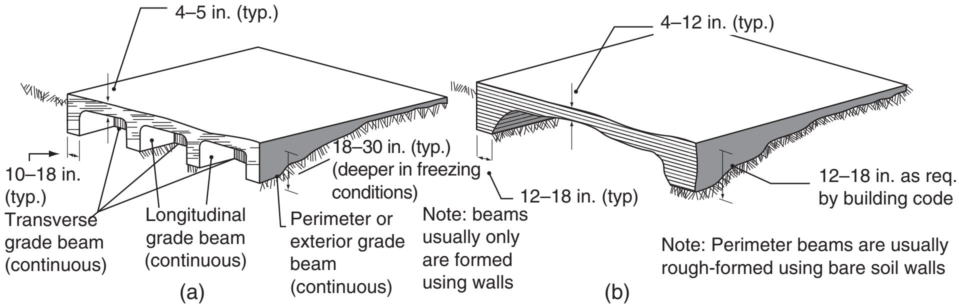

Figure 8.33 Cut-away sketch of a typical stiffened slab-on-grade foundation: (a) thin slab; (b) slab with thickened edges or perimeter beams (*After* Wray, 1995)

- Pile-and-beam
- Basement with wall footings and slab floor
- Basement with wall piles and slab floor
- Structurally suspended floor slab on piles.

Slab-on-grade foundations are usually constructed with either welded wire fabric reinforcement, mild steel bar[1] or deformed bar reinforcement, or with post-tensioning as the reinforcement. Welded wire fabric reinforced slabs are constructed with wire mesh placed in the forms before the concrete is poured over it. Steel bar reinforced slabs are constructed with the rebars fixed and placed inside the concrete forms, and then the concrete is poured and compacted. Post-tensioned slabs are constructed with steel cables covered with a plastic sheathing instead of using steel bars. The cables extend through the sides of the forms and, after the concrete is poured over the cables and has reached its initial strength, the steel cables are tensioned and fixed (see Figure 8.33).

Welded wire fabric-reinforced slabs often do not perform well in expansive soils. Both steel bar and post-tensioned types of slabs can work equally well, but each type has a different technical objective. A structural engineer, working with a geotechnical engineer, should have the principal responsibility for choosing the foundation system.

[1]In some countries mild steel reinforcement is no longer available.

8.3.8 Mitigation and preventive measures

Methods for mitigating the damaging effects of expansive soils include (Chen, 1988):

1. Excavation with or without replacement of the soil by a compacted non-expansive soil;
2. Flooding the in-place soil to achieve swelling prior to construction;
3. Control of compaction water content and density;
4. Mixing the soil with lime or cement before compaction;
5. Using footings or piers that extend below the depth of seasonal moisture change;
6. Using a bearing pressure that is high enough to balance the swell pressure;
7. Use of procedures to minimise changes in the soil water content, including adequate drainage systems and waterproofing of adjacent surface areas;
8. Use of structural mats and slabs that are resistant to differential movements;
9. Use of deep foundations down to non-expansive material;
10. Treatment or replacement of the upper 1–3 m with non-expansive soil (usually granular material) in embankment construction.

There is a "best time" to construct foundations in expansive soils. This is when the soil is neither at its wettest nor at its driest condition, i.e., when the soil is near "equilibrium". However, it is usually impractical to wait for this optimum time to start building. Thus, it is important that a foundation be designed and built so that it will perform adequately under all of the normally expected conditions that the building will experience during its usable lifetime.

Excavation and backfill

If the building is to have a shallow foundation, one solution that has been used successfully is to remove the expansive soil down to a specified depth and replace it with a non-expansive soil. Sometimes the terrain lends itself to constructing an elevated pad of foundation soil beneath the foundation without causing a significant increase in foundation cost. In replacing the expansive soil already existing at the building site, a "non-expansive soil" should be used. A non-expansive soil is usually considered to be a soil that has a plasticity index less than 20 and preferably less than 10. Sandy or coarse silty soils meet this criterion but, because of their relatively high permeability or hydraulic conductivity, if water should ever be introduced into this type of soil, it could travel throughout the soil mass, wet the underlying expansive soil, and cause the heaving that the non-expansive soil was meant to prevent.

If the building has a basement, the backfill soil ideally should be a non-expansive clayey soil, not a sandy soil. Steps should be taken to prevent water from entering the backfill regardless of whether or not the soil is expansive or non-expansive. If the backfill is expansive, then unwanted lateral swelling pressures will be imposed on the basement wall. If the backfill soil is non-expansive and if a considerable amount of water collects in the backfill, the water will impose a hydrostatic pressure against the wall. Water collecting behind the wall can cause damage because basement walls are seldom designed for hydrostatic pressure unless the basement extends below the groundwater table.

"Ponding" the foundation soil before construction

The principle behind the idea of "ponding" is to flood the foundation site and keep it flooded for several weeks so that the water percolates down into the expansive soil and causes it to "pre-heave". Although it is a good idea in principle, it has never been shown to have been successfully applied. If the ponding operation is applied for several weeks, the result will be that the soil near the surface will be very wet. The foundations will then have to bear at a depth below this very wet soil because it is likely to have a low bearing capacity and be highly compressible. In addition, should the ponded soil ever dry out, the foundation will be subjected to shrinkage, which can be just as damaging as the distortion that results from heaving soil. Thus, this method is not recommended.

Soil treated with a stabilisation method

Chemical stabilisation has been used effectively to stabilise highways, airport pavements, and large industrial sites. It has also been used successfully on smaller projects, such as single lot residences and other small buildings, but it is more expensive on a per unit basis than for the larger projects, because of the cost of mobilisation of the necessary plant.

There are two methods commonly employed in chemically treating expansive soils on small lots. One method is to treat the top 12 to 24 inches by mixing lime, cement, or flyash into the soil and then recompacting the mixed soil. This mixing operation requires special equipment which is difficult to operate and manoeuvre on small lots; hand methods of mixing do not do as good a job as the mechanised mixing methods. This method also requires laboratory testing to determine the appropriate amount of chemical to mix with the soil to produce the desired effect. However, these chemicals, when used in the proper proportions, properly mixed, and properly applied to the soil, are known to effectively reduce the amount of shrinkage and heave which the soil might experience if not treated.

The second commonly used method of chemically treating expansive soils is to inject pressurised slurry of water and lime, cement, or flyash to depths of a few metres below the ground. The concept is that the pressure will make the slurry flow through cracks in the expansive soil and effectively seal the soil to the required depth from subsequent penetration of water. The slurry is also expected to interact with the clay particles and reduce the affinity for attracting free water in the same manner as the surface mixing method does. Pressure injected slurry applications have been found to be quite successful in many instances; however, there have also been many instances when the injected slurry seemed to have had no effect on the resulting soil movement.

"Moisture barrier"

A moisture barrier is a structure or material that prevents or retards moisture from moving into or out of the soil. Moisture barriers are used to either prevent moisture from migrating from outside the foundation to a location under the foundation or to prevent moisture from migrating from under the foundation to outside the foundation. Barriers can also be used to prevent roots from trees or bushes from penetrating beneath foundations.

Moisture barriers may be vertical, horizontal, or a combination of horizontal and vertical. The principle behind a vertical moisture barrier is that, if it is attached to a foundation, the distance that water must travel to either get beneath a foundation from the outside or to get out from under the foundation is greatly increased. Because the soil permeability or hydraulic conductivity is so small, it is hoped that the increased distance, which means an increased travel time, will not permit the soil water content to change appreciably from one season to the next and the magnitude of shrinkage or heave correspondingly becomes only a nominal amount.

A similar principle applies to the horizontal moisture barrier, except that only a very wide horizontal barrier will produce the same "time of travel effect" that the vertical moisture barrier produces. The principal advantage of the horizontal moisture barrier is that it effectively moves the edge moisture variation distance out from under the structure to where it is acting under the horizontal moisture barrier, and where there is less concern if the soil heaves and shrinks.

The combination vertical and horizontal barrier might be employed if it is difficult to excavate deep enough to place a deep vertical moisture barrier, or if there are lateral constraints that prevent a full horizontal barrier from being used. One application of the combination barrier is adjacent to a structure but beneath a flower bed or decorative bushes, where the vertical barrier is taken deep enough to allow the plants to grow and then the horizontal barrier is placed beneath the bushes or flower bed which tends to prevent any overwatering from being transported to beneath the foundation.

Other things that can be done to avoid or mitigate any damage

Many things can be done in the design and construction of new buildings that can prove to be beneficial to the long-term acceptable performance of the structure. One of the first things that must be decided is, how much movement, and what effects of that movement, can be tolerated? A stiffer or stronger foundation, particularly with respect to slab foundations, will permit less deflection or distortion in the superstructure of the building which, in turn, will lead to fewer cracks.

Large shrubs, and especially trees, should not be planted close the building. Smaller bushes or flowerbeds adjacent to the house or building should not be watered by "ponding" water in the bed where the bushes or flowers are growing. Trees should be planted so that the drip line of the tree at maturity is still several feet from the edge of the building. If the location of the mature tree's drip line cannot be determined in advance, then a rule of thumb that seems to work well is to plant the tree a distance from the building equal to the mature height of the tree.

Downspouts should discharge at least 1.5 m away from the edge of the structure. Downspouts must also carry water over, and discharge some metres beyond the edge of, any backfilled excavation adjacent to the building, such as for a basement. Porches, steps, sidewalks, patios, and driveways should not be physically connected to the building. These minor structures will move differentially with respect to the house and this can result in damage. Make sure that water cannot pond or pool adjacent to or near the foundation. If a swale was constructed across a property to carry surface runoff water from lots at higher elevations to a storm water sewer or channel, do not alter or change it. Ensure that the gutters and downspouts on the buildings are clean and clear of debris. Make sure that debris or other material has not accumulated in any swales

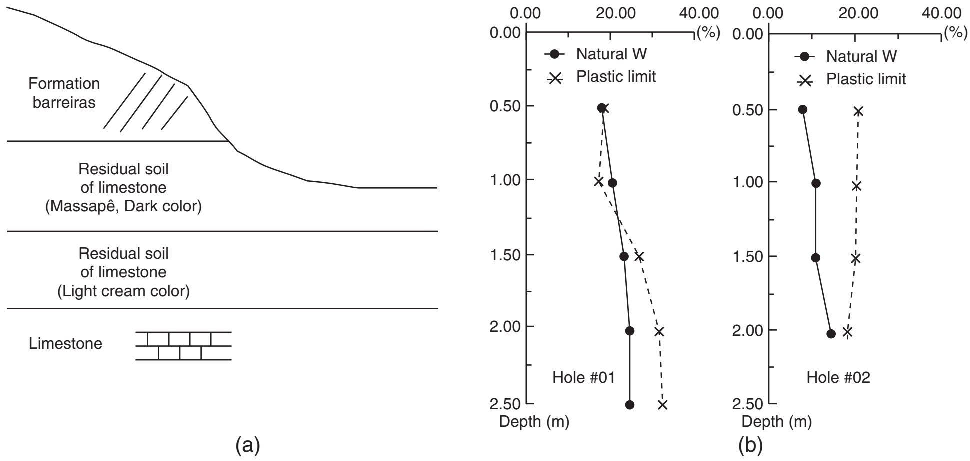

Figure 8.34 (a) Geological section; (b) Estimation of action zone (*After* Gusmão Filho *et al.*, 2002)

that cross the property. Maintaining relatively constant soil water content is a very important task in mitigating or reducing soil shrinkage and heave. This means watering more during hot, dry periods, but it also means continuing to water during cooler ones.

8.3.9 Case histories

Gusmão Filho *et al.* (2002) described two cases which occurred in school buildings, called CAICs (Centers of Integral Education of Children), in the Northeast region of Brazil. The CAICs were similar, with one floor and column loads of approximately 100 kN. They are located in small villages inland to assist the low income population. In this region, seasons produce significant differences in rainfall, so climates vary from super-humid to semi-arid classifications. In this region there are many examples of collapsible and swelling unsaturated soils.

Case history 1

This was where the CAIC/Laranjeiras was constructed, in the Sergipe, Brazil. The geological profile is shown in Figure 8.34:

- *Bedrock of limestone*, with some degree of weathering and fracturing;
- *Residual soil of limestone* shows the typical horizons. A transition from horizon C to B is typical of saprolitic soil. The rock appears much altered and can easily be broken by hand. The B horizon has very fine texture and fracturing when it is exposed. Its surface in cuts shows undulation due to the action of water on the clay material. The A horizon is the superficial residual soil, being clayey with contraction fissures up to 1 cm across, dark colour and roots. This indicates a highly expansive material;
- *Formation Barreiras* was deposited over the residual soil and comprises sediments of varied textures. The tops of the hills are made of clay sedimentary deposits; they

have a red colour with many pebbles. A layer of quartz pebbles can be observed at the contact with the residual soil. The terrain shows a much altered residual soil of limestone with cream colour. Several cracks are observed in the ground alongside and parallel to the slopes. On the limestone in the hill, deposits of clay sediments with many quartz pebbles caneasily be seen.

Twelve borings were made in the area of the CAIC buildings. They show an initial layer of clay, locally called "massapê", which is dark in colour, with a consistency increasing with depth and thickness around 2 m. This is underlain by a 3 m thick layer of light yellow medium to stiff silty clay with fine sand, beneath which is the highly decomposed limestone rock.

The terrain is a plateau with higher ground around, so the buildings will be founded in residual limestone soil with a high probability that the soil will be expansive. The investigation programme was planned as follows:

- *Two holes* ($\phi = 10$ cm) to collect samples from depths of 0.5, 1.0, 1.5, 2.0 and 2.5 m;
- *Natural moisture content test* in all samples collected from the two holes (see Figure 8.34b;
- *Wet particle size distribution and index tests* to define the clay fraction and limits W_L, W_p and W_s in the samples collected at depth 0.5 m (dark "massapê"), 1.5 m ("massapê") and 2.5 m (light yellow silty clay);
- *Compaction test*, *CBR and expansion test* in samples from the Formation Barreiras, in a given section at two different depths.

Special expansion tests in the "massapê" clay were not requested since they take a long time. The results of index tests and field evidence allow the swell potential of the soil to be estimated and suggest solutions for foundations, pavements, buried pipes, etc.

The results for both holes are presented in Table 8.19, and these data allow the swell potential of the soil to be estimated. According to Holtz and Gibbs (1954), the swell potential can be taken as medium to high based on the Ip and high based on the grain size (percentage of fines). Seed *et al.* (1962) considered the Activity, so the soil is medium to a depth of 1 m and high at greater depths.

Predictions of swelling are all subject to errors (O'Neill and Poormoayed, 1980). The method of Vijayvergiya and Ghazzaly (1973) yields percentage swell of a clay sample in a consolidometer, under a 10 kPa surcharge, as a function of moisture content and liquid limit, in the form of a graph, giving the free swell percentage "s1". The method of Seed *et al.* (1962) gives percentage swell of a clay sample, compacted at near optimum moisture content, under 1 kPa surcharge in anoedometer, giving a free swell percentage "s2". The results are shown in Table 8.19.

In the Vijayvergiya and Ghazzaly method (1973), the values in hole #01 are similar, giving an average of 1.8%. However, in hole #02, the values are quite different, from >10% to 3%, with an average around 6%.

In the method of Seed *et al.* (1962), the values for hole #01 range between 2.7% and 6.8%, with an average of about 4%. In hole #02, the two values are more

Table 8.19 Results from holes #01 and #02 – Case history 1 (*after* Gusmão Filho *et al.*, 2002)

Hole	Depth (m)	I_P (%)	% < 1 μm	Activity*	W_{nat} (%)	W_L (%)	Swell (%) s1**	Swell (%) s2**
01	0.0–0.5	20	30	0.83	18.5	39	1.8	2.7
	0.5–1.0	20	35	0.74	21.3	38	1.3	2.9
	1.0–1.5	29	30	1.16	24.2	57	2.2	6.8
	1.5–2.0	24	–	–	26.3	57	2.0	–
	2.0–2.5	23	35	0.77	26.6	57	1.5	4.2
02	0.0–0.5	19	32	0.79	8.1	40	>10	2.4
	0.5–1.0	17	41	0.52	11.3	38	6	–
	1.0–1.5	17	–	–	11.7	38	6	2.1
	1.5–2.0	19	–	–	15.1	38	3	–

*Activity $= I_P - [\% < 2\,\mu m - 10\%]$
**s1 = free swell percentage (Vijayvergiya and Ghazzaly 1973), $s2 = 3.60 \times 10^{-5} \times D^{2.44} \times C^{3.44}$ (Seed *et al.*, 1962), where $C = \% < 2\,\mu m$ and $D = I_P/[C - 5\%]$.

consistent and the average is around 2.25%. The depth of the active zone can be assumed where the moisture content does not vary with the seasons.

In summary, various methods have been used to determine the swell potential of the material. The results showed a soil having medium to high swell potential.

From the natural moisture content it is estimated that the active layer is about 2.5 m thick, within which the natural moisture content is lower than the plastic limit, explaining why the surface has tile cracks. This layer of soil is susceptible to volume change due to seasonal variation of moisture content. A suitable remedial measure is to excavate the expansive soil and replace it with an inert soil in order to ensure the safety of foundations, pavements, and buried pipes.

Case history 2

The second case was recorded in Nossa Senhora do Socorro/Sergipe where another CAIC structure was built. The terrain has a very uneven topography, with 8 m difference in level between the children's school and the platform below where the rest of buildings are located (Figure 8.35).

The exposed slopes allowed the Formation Barreiras to be identified in the area. The surface soil is a cream colour with 1 m thickness, having a pebble horizon separating it from the lower layer. This is a red lateritic clay and silt matrix. It shows the presence of gravel, included in the laterite, indicating the f1uvial origin of the soils.

At the middle of the cut slope, there is a change to a "massapê" clay, which is a type of soil very different from the other soils found in Formation Barreiras.

On the platform, at a depth of 8 m, cracks were observed and some slopes also were fissured indicating their instability. Fifteen borings were made in the area of CAIC buildings. Only two of them were located in the high part of the terrain, including the Formation Barreiras. The other borings were made at platform level. Underlying the Formation Barreiras is a silty clay of variable consistency, around 1–2 m thick, followed by the "massapê" clay which also varies in consistency.

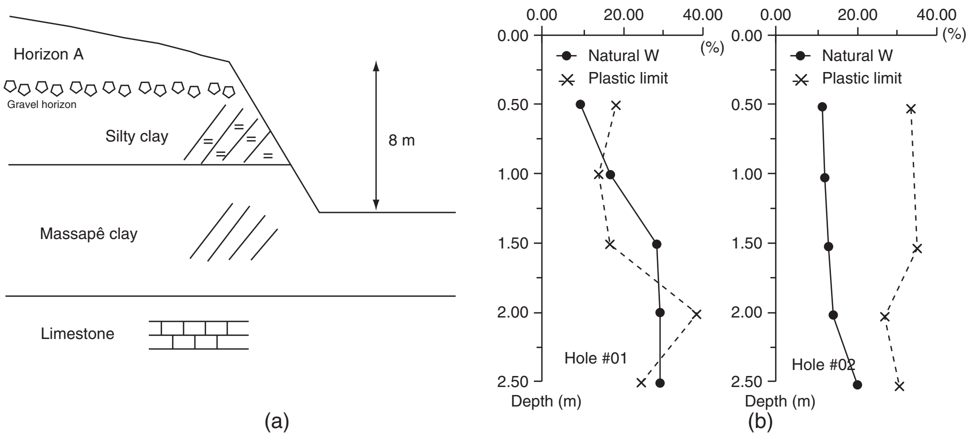

Figure 8.35 Case Number 2: (a) Geological section (b) Estimation of action zone (*After* Gusmão Filho *et al.*, 2002)

The following investigation programme was established in the location of buildings:

- *Two holes* ($\phi' = 10$ cm) to collect samples at depth of 0.5, 1.0, 1.5, 2.0 and 2.5 m;
- *Natural moisture content test* on all samples collected from the two holes;
- *Wet particle size distribution and index tests* to define the clay fraction and limits W_L, W_p and W_s in the samples collected at depth of 0.5, 1.5 and 2.5 m.

As for Case history 1, special expansion tests were not requested since they take a long time. The results of index tests and field evidence allow the swell potential of the soil to be estimated and suggest solutions for foundations, pavements, buried pipes, etc. The results for each hole are presented in Table 8.20, and thesedata allow the swell potential of the soil to be estimated.

According to Holtz and Gibbs (1954), if the I_p of the soil is used as the basis of classification, the swell potential of hole #01 can be taken to be medium to high, and the swell potential of hole #02 is low. Using the activity to classify the swell potential (Seed *et al.*, 1962), in hole #01 it varies from low to high as the depth increases, whereas in hole #02, the swell potential is low at all depths. Figure 8.35b shows the moisture content and plastic limit versus depth, from which the active zone is estimated to reach 2.5 m depth in hole #02.

The swell can be predicted, but not with a great deal of confidence, as was shown before. Table 8.20 shows the free swell percentage according to the method of Vijayvergiya and Ghazzaly (1973), and Seed *el al.* (1962). Both of them show wide scatter in the final results.

Using the Vijayvergiya and Ghazzaly (1973) method, the values for hole #01 vary by a factor of 10, giving an "average" of 3.2%. In hole #02, the numbers are higher, between 6% and 10% with an average of 7.3%.

Table 8.20 Results from holes #01 and #02 – Case history 2 (*After* Gusmão Filho *et al.*, 2002)

Hole	Depth (m)	IP (%)	% < 2 μm	Activity*	W_{nat}(%)	W_L(%)	Swell (%) s1**	Swell (%) s2**
01	0.0–0.5	14	36	0.39	9.30	32	4.5	0.8
	0.5–1.0	19	–	–	16.9	33	–	–
	1.0–1.5	24	34	0.71	28.6	41	0.4	2.9
	1.5–2.0	30	–	–	29.7	69	–	–
	2.0–2.5	39	58	0.67	29.9	64	1.5	15.8
02	0.0–0.5	12	43	0.28	5.70	29	10	0.67
	0.5–1.0	NP	–	–	6.10	NL	–	–
	1.0–1.5	9	35	0.26	6.70	27	6	0.27
	1.5–2.0	13	–	–	7.40	27	–	–
	2.0-2.5	13	24	0.68	10.30	36	6	0.78

*Activity = I_P − [% < 2 μm − 10%].
**s1 = free swell percentage (Vijayvergiya and Ghazzaly 1973), s2 = $3.60 \times 10^{-5} \times D^{2.44} \times C^{3.44}$ (Seed *et al.*, 1962), where C = % < 2 μm and $D = I_P/[C - 5\%]$.

In the method of Seed *et al.* (1962), the values are quite different in hole #01, ranging between 0.8 and 15.8, while in hole #02 they are more consistent. Taking the active zone as 2.5 m deep, the total surface swell is less than 0.5 cm using the Seed *et al.* method in hole #02.

The site for the CAIC building had evidence of being expansive soil. Many methods were used to show the special character of the soil, although the soil was not extreme, having a low swell potential. A suitable remedial measure is to excavate the expansive soil and replace it with an inert soil in order to ensure the safety of foundations, pavements, and buried pipes.

8.4 INDIRECT (DEEP) FOUNDATIONS

8.4.1 General concepts

All types of piles which are used in sedimentary soils and weak rocks can be used in residual soils. The main differences are in the design parameters required to calculate a bearing capacity for the pile. As discussed elsewhere, many of the standard relationships which apply to sedimentary soils do not apply to residual soils because of their history. For example, the conventional relationships between vertical and horizontal stress will not apply where a rock, with high built-in stresses due to tectonic action, weathers to a residual soil. This will in turn affect the shaft friction which can be mobilised on the outside of a pile.

It should also be noted that, in many parts of the world where there are no tropical residual soils, extensive soil investigation, laboratory testing and research over many decades have produced a wealth of knowledge on the fundamental properties of soils. This applies to such soils as the London Clay, Boston Blue Clay, many Scandinavian soils and others. The sampling and testing has been of high quality, and has been supplemented by *in situ* tests, many with sophisticated instrumentation. It will also be shown later that some European countries have built up significant databases using advanced *in situ* testing such as the Cone Penetrometer Test (CPT) or the pressuremeter test (PMT), tied to results of static pile load tests. By comparison, many of the countries where tropical residual soils are prevalent have less well developed geotechnical databases, and this often starts with the basic soil investigation. For example, whereas in stiff clays in Europe it is standard to take undisturbed samples and carry out triaxial testing in the laboratory, in Asia it is more common to rely upon the Standard Penetration Test, often carried out with poor quality equipment. This means that design methods for piles rely in turn on empirical methods and relationships, because fundamental relationships cannot be determined without the parameters on which to base them.

Even this is not as easy as it might be. The Standard Penetration Test itself was developed for the testing of granular soils, and it is normal to stop the test once a soil layer has been proved to be very dense, which is equivalent to a total of 50 blows for a penetration of less than 300 mm. It has since been extended to test cohesive soils, and empirical relationships between blow count N and consistency have been derived and published. It is also widely used in weak rocks, and the work of Stroud (1974, 1988) has established widely accepted correlations. But is there any reason why the same correlations should apply to residual soils? The way in which the soils are produced, by decomposition of a massive rock rather than by deposition and consolidation, would suggest that there may be differences. It should also be noted that the processes at work turning sedimentary soils into rocks are ones which produce an increase in density, while the weathering process will often produce a reduction in density as chemicals are leached out. As a result the standard definitions of dense and very dense will not apply to residual soils, and in some areas it is common to continue the Standard Penetration Test, and to get meaningful results, with blow counts of up to 200. Nevertheless this leads to very heavy wear on the equipment, and certainly the risk that counting may not be too accurate.

Gradually local correlations are being built up based on experience in tropical residual soils, but often this cannot be linked to conventional strength testing because of a lack of comparative data. It is really up to each country to develop their own empirical correlations based on local geology, to publish these within local networks such as conferences and seminars, and to work with neighbours to find common ground in their correlations. Some work was done in the 1980s to establish relationships between shaft friction and pile/soil displacement, often called *t-z* curves, for soils and weak rocks including tropical residual soils in Singapore, and to relate these to ranges of SPT N values. Much of the work in Hong Kong has been reviewed in the two editions of the piling guide, Foundation Design and Construction (GEO 1/2006).

For historical reasons, much of the pile design work in tropical residual soils is based on the concept of undrained shear strength, correlated with shaft friction through a coefficient α, hence these methods are often called the α methods. The SPT N value is then converted empirically to undrained shear strength, and this to shaft friction by multiplying by an appropriate value of α. This concept was initiated by Skempton based on work in London Clay, but has been extended by others and has been shown that α decreases with increasing shear strength. Unfortunately there is no valid reason why the values derived by Skempton for London Clay, and others for sedimented soils, should apply equally well to tropical residual soils, bearing in mind their very different mode of formation and structure.

In fact, the other group of methods, often called the β methods, based on effective stresses, is more likely to be suitable for tropical residual soils, where the weathering process has contributed to the permeability which allows relatively fast drainage of excess pore pressures caused during pile installation.

Displacement piles

All types of displacement piles are used in tropical residual soils, including concrete, cast *in situ* and precast, and both reinforced and prestressed, steel in a variety of shapes including H- or I-sections and pipes, and timber. Steel sections have special design problems, such as how to calculate the end bearing component of an I-section or a pipe, which depends on the balance between the maximum shaft friction available against the surface of the pile and the end bearing of a larger area, such as the whole square for an I-section or the whole circle for a pipe. This determination is further complicated by the differences between static and dynamic behaviours, such that a pipe pile may be plugged statically at a certain length, where the internal shaft friction is enough to overcome the end-bearing over the whole area, and yet the plug continues to rise up under driving because the dynamic action reduces the shaft friction.

Driven piles are often noted to be affected by “set up” or “soil freeze”, in which the capacity in both shaft friction and end bearing is reduced by the excess pore pressures mobilised during driving. As these dissipate, the capacities are noted to increase. At the site of the Bishan Depot for the Singapore MRT, a large number of square section precast concrete piles had been driven into the weakly cemented sand called the Old Alluvium. When dynamic pile testing was attempted a few days later, most of the pile heads broke before any measurable pile movement could be achieved, because of the set up which had gripped the outside of the pile.

At another site in the Gulf of Thailand, steel pipe piles were being driven with a hydraulic hammer from flying leads for a mooring dolphin at a fuel unloading facility, but the piles, which were being continuously monitored by dynamic pile testing, failed to reach the required capacity. Driving was stopped when the instruments, near the top of the pile, were about to become submerged in sea water. The piles were already 45 m long, to pass through sea water and mud before reaching firm founding strata, and were extended by welding on another 12 m length over the following day. By the time driving started again, some 36 hours from when it had stopped, it was not possible to drive the pile any further and the dynamic pile testing showed that the pile had more than reached the required capacity.

Dynamic pile testing has given us a unique opportunity to investigate this phenomenon practically in the field, since we can now make good estimates of pile capacity at any instant of time, from the end of initial driving till as long as we want to wait and carry out a restrike. This is an invaluable tool in finding the optimum length and driving conditions for any pile, since the pile design is always for the long term value and we do not need to be concerned if the capacity at the end of initial driving is lower. However the problem will always occur, both for land piles and in marine applications, that it becomes extremely difficult to get the driving plant, be it a crane or a barge, back onto the previously driven pile. It therefore becomes necessary to carry out local calibrations, on as many piles as possible and with varying lengths of delay, to find the capacity at end of initial drive which will lead to the required final capacity after

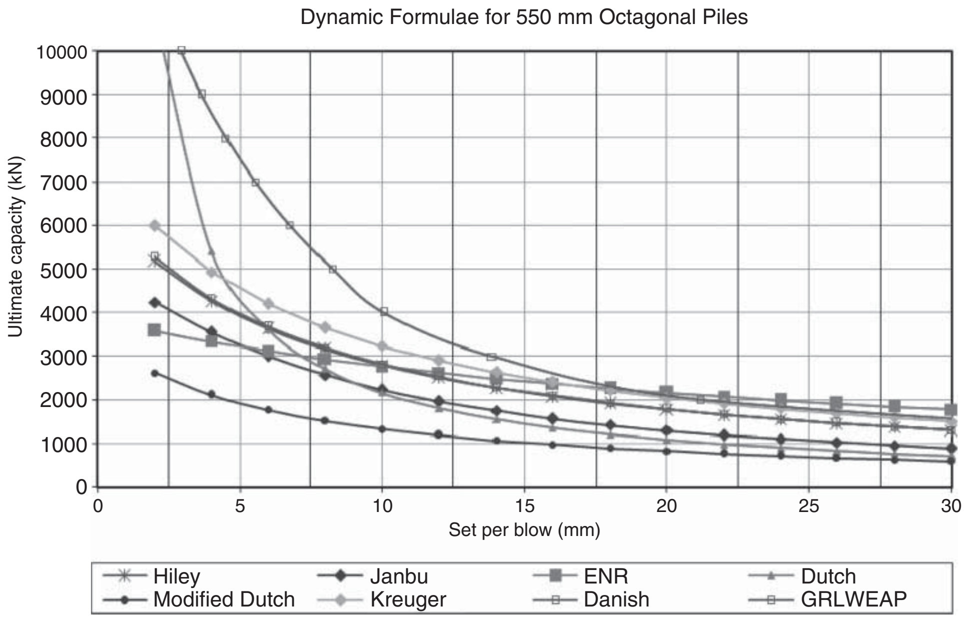

Figure 8.36 Relationship between set per blow and ultimate pile capacity by dynamic formulae

a period of time. This sort of data can very usefully be built up locally, and shared through local publications, conferences and seminars.

It has been noted that, of the many dynamic formulae available, there is a very strong tendency throughout South East Asia, and further a field, to favour the Hiley formula over all the others. Figure 8.36 shows the relationship between set per blow and ultimate pile capacity for a selection of 7 well known dynamic formulae. It is to be expected that each formula has, for at least one set of conditions related to hammer type, pile type and soil type, given acceptable results, since all are essentially empirical. It is equally to be expected that no single formula will work with equal accuracy for all types of hammer and all types of pile material in all types of soil. It is recommended that dynamic pile testing is used to give a more reliable indication of capacity, and that a suitable calibration is then obtained for a dynamic formula which gives the best agreement.

Replacement piles

One of the major problems with replacement piles in tropical residual soils, in this case often bored piles, has been the presence of corestones or boulders within the weathered rock profile. This led historically to the use of techniques such as the hand dug caisson, in which a man excavated the soil and weathered rock about 1 metre vertically at a time, from the top downwards. The spoil would be shovelled into a small skip, hauled to the surface and tipped by his partner, often his wife. As he went, he would build a support with *in situ* concrete, formed behind a tapered shutter. Next morning, as he continued the excavation, the formwork would drop away from the taper and was stored for later reuse. Any boulders encountered in the sides of the hole would be broken away by percussive drilling and chiselling, until hard rock was encountered over the whole base. Even then it was necessary to prove that the base was not another isolated boulder in a soil matrix, and this was done by drilling a small rotary percussive hole through the base for about 3 to 5 metres. If soft ground was found, the hole was excavated until hard rock was again encountered over the whole of the base, and the proving process repeated.

Now occupational health and safety issues have taken over, and the practice of sending a man down a deep shaft is virtually outlawed except under very stringent safety precautions. It is certainly impractical to excavate shafts in that way. At the same time, mechanical plant has been greatly improved, and the technology which allows us to bore tunnels through hard rock has been employed on the picks of drilling buckets. Nevertheless problems still remain, such as the difficulty of drilling through hard rock when it is held in a matrix of weaker material, and also of proving hard rock beneath the base. For a man standing at the bottom of a pile shaft on a layer of hard rock 30 m below ground level and holding a rotary percussive drill, the process was quite simple, but try to do the same thing from the surface and it becomes much more complicated. The best solution is probably to drill from the ground surface at every pile location in advance of the pile boring, and this was done for each of the forty-eight piles, separated into two piers, of the Gateway Upgrade Project in Brisbane (Day *et al.*, 2009). However, in practice, it will prove difficult in many real situations to persuade the project owner to invest this amount of money in ground investigation, and it will generally involve a two stage process which absorbs crucial amounts of time. It is necessary to make a preliminary investigation which will allow the best type and size of pile to be determined, and to make an estimate of the depth based on available information. This will then provide the locations for the piles, and the estimated depth can be used to decide the level at which the boreholes can be terminated. Getting the required amounts of time and money into a project budget is a major challenge.

8.4.2 Pile design

At this time, with the increased importance of the Serviceability Limit State, understanding the performance of a pile under load is probably more important than ever. According to Baguelin *et al.* (1978), the *in situ* testing equipment which helps the most to visualise the way soil behaves around a pile is probably the Ménard pressuremeter (MPM). Although this statement was made primarily in respect of sedimented soils, it is even more applicable when we deal with more complex materials such as naturally structured soils, like weathered rocks and residual soils, which are sensitive to penetration processes (for SPT or CPT) or sampling methodologies. The possibility of reaching most ground horizons by pre-boring in the case of the PMT (or MPM) prior to the insertion of a testing probe and executing the expansion test, allows very reliable and valuable information to be obtained, expressed as a pressure-displacement curve, which is very much better than any "simple" correlation with SPT or CPT.

There are criticisms of this test, bearing in mind that it may be a complex and time consuming process, for some materials. When dealing with extreme geomaterials, such as soft clayey soils or loose sands where penetration tests are possible, on the one hand, and rocks where rock coring and UCS tests for classification purposes are readily carried out, the PMT may be of less benefit. However, in IGM (Interface Geomaterials) or weathering profiles, the criticisms are unfair, or even erroneous. The feasibility of testing at all in such a heterogeneous environment, and with materials behaving under particular levels of cementation, and micro- and macro-structures and fabric, makes this test very valuable.

Piles in residual soils: Effects of installation process

The design of piles in residual soil is usually based on empirical correlations, mostly using the results of the standard penetration test, regardless of the construction method of the bored pile (Chen and Hiew, 2006). The use of "rational" (classical) methods or empirical solutions for residual soils, adapted from those for sedimented sandy or clayey soils, may overestimate the shaft friction, particularly with wet construction processes, and make the evaluation of base resistance very unreliable, dependent particularly on the cleaning of the pile base before concreting. The empirical correlations of the unit shaft friction (f_s) and base resistance (q_b) with SPT-N values, are commonly used loosely, regardless of the construction method, as follows:

$$f_s = K_s \cdot N \tag{8.35}$$

$$q_b = K_b \cdot N \tag{8.36}$$

K_s and K_b are the empirical factors for shaft friction and base resistance, respectively, in kPa. The K_s values generally vary from 2.0 to 3.0, but need to be treated with extreme caution. They are genuinely empirical, based on field tests, and therefore strictly relate only to similar piles, especially in terms of soil type and construction method. Although it may happen that similar K_s values will apply to residual soils in Singapore, Malaysia and Hong Kong, for example, there is no guarantee that this is the case. Local tests will always be required in confirmation but, if that confirmation is achieved, then the wider database of results may be able to be used. It also needs to be noted that some authors report the results of tests, where the K_s values refer to what was measured, whereas others refer to recommended design values, where more conservative values are used.

Lei and Ng (2007) describe the practice in Hong Kong, where excavated rectangular barrettes and large diameter bored piles have been commonly adopted, in the last two decades, as the foundations for tall buildings and heavy infrastructure projects. There is generally the aim of embedding the tip in sound rocks, because current design procedures assume a heavy reliance on end bearing for the Ultimate Limit State. When this is not possible, for technical or economic reasons, piles are designed relying on shaft resistance in the overlying deep-seated thick saprolites.

For private building works in Hong Kong, shaft resistance in excess of 10 kPa is not normally permitted by the local regulations, without performing a load test on site. While some studies into the behaviour of large diameter bored piles in saprolitic soils are reported in Ng *et al.* (2001a & 2001b) and Lei and Ng (2007), there is a re-evaluation of the behaviour in terms of fully mobilised or substantially mobilised shaft resistance in these local saprolites for rectangular barrettes under bentonite and circular bored piles, comparing it with other soils elsewhere. In these studies, instead of relating the shaft friction to the SPT-N value, by K_b, it is related to the effective vertical stress by β. The conclusions are as follows:

a. for the barrettes and bored piles in saprolites in Hong Kong, a moderately conservative local displacement for the mobilisation of the ultimate shaft resistance is found to be approximately 20 mm, which is larger than that found elsewhere;
b. the average K_s and β values for barrettes are 1.28 and 0.27, and for bored piles 1.2 and 0.30, respectively;
c. compared with barrettes and bored piles in Old Alluvium, residual soils and weathered granites in Singapore, and bored piles in residual soils in Malaysia, the K_s values for barrettes and bored piles in saprolites in Hong Kong are generally low. The range of β values for barrettes and bored piles in Hong Kong is comparable only to the β values recommended for the design of bored piles in loose sand elsewhere;
d. compared with non-grouted barrettes and bored piles, shaft-grouted barrettes and bored piles show a relatively stiffer unit shaft resistance response to local displacement and a higher ultimate unit shaft resistance.

From a loading test on a barrette in a residual soil named Guadalupe Tuff in the Philippines, a relatively low value of β of about 0.2 was back-calculated by Fellenius *et al.* (1999). For the design of bored piles in loose sand, Davies and Chan (1981) recommend β values of 0.15–0.3, and for the design of cast-in-place piles in loose sand, while others recommend β values of 0.2–0.4.

There are several cases reported in the bibliography that indicate a very clear dependence on construction methods, for the results of pile load tests when founded in residual soils (Chen and Hiew, 2006; Fellenius *et al.*, 2007; Viana da Fonseca *et al.*, 2007). The installation of piles by pushing or driving pre-cast units, by using bored cast-in-place methods with temporary steel casing or with bentonite or polymer as the stabilising fluid, or by using Continuous Flight Auger (CFA) methods, will lead to very different soil-pile interaction behaviours.

A series of published papers based on work in South East Asia started from testing associated with the Singapore MRT in the early 1980s. These included Buttling (1986), Buttling and Robinson (1987), Buttling and Lam (1988), Toh *et al.* (1989), Buttling (1990), Chang and Broms (1991), Phienwej *et al.* (1994), and Chen and Hiew (2006). Toh *et al.* (1989) reported K_s values for the Kenny Hill Formation in Malaysia of about 2.5–2.7 for SPT-N values less than 120 based on nine fully instrumented tested piles. A study by Chang and Broms (1991) on Singapore residual soil, suggested a design value of $K_s = 2$ for SPT-N values of less than 150. Phienwej *et al.* (1994) carried out a further study based on 14 fully instrumented bored piles constructed using both dry and wet methods, and reported a measured value of $K_s = 2.3$ for SPT-N values below 120. Tan *et al.* (1998) studied 13 bored piles constructed using both dry and wet methods, also suggested adopting $K_s = 2$ for design purposes, while limiting the maximum unit shaft friction to 150 kPa.

Note that the Chang and Broms suggestion refers to SPT-N values of 150, while that of Tan *et al.* (1998) implies SPT-N values of 75. Both are well above the standard limit of 50 blows and need to be treated with caution. Whereas in Europe, it is normal practice to stop the SPT when the blow count reaches 50, in other places, notably

Hong Kong, it has been the practice to carry on to blow counts as high as 200. One of the reasons for this is that the SPT was developed for testing sedimented granular soils, where a blow count of 50 shows a very dense soil and further driving will achieve very little. In a tropically weathered profile, it may be argued that the way in which the soil behaves is very different, and that useful information with regard to soil strength is gained up to higher blow counts. However, great care is needed with the higher numbers, as there is a great difference between a measured SPT-N value of 175, and one which has been extrapolated from 50 blows over a penetration of less than 300 mm. This has become common practice in some areas, but is highly questionable. Unless the 50 blows were achieving a similar penetration for each blow, then there is clearly no justification for extrapolation. If, for example, blow counts are recorded every 75 mm, and they show 19, 21, 10 for 30 mm, then some sort of extrapolation may be justified. However, if they are recorded every 150 mm, and show 6, 44 for 40 mm, they paint a very different picture. To turn the latter numbers into 50 blows for 190 mm, and therefore 79 blows for 300 mm, and use this to calculate a shaft friction could be very misleading.

It is also to be noted that there is widespread concern about the effect of support fluids, especially bentonite, on the shaft friction achieved. Bentonite is a slippery fluid if you place your hand in it, and we know that it forms a filter cake on the sides of a hole in permeable soils, where the water within the fluid flows out into the soil and leaves the bentonite behind, forming a very low permeability skin which enhances stability. Both of these factors make designers worry that shaft friction will be reduced. The major question which remains is "reduced with respect to what?" Since bentonite is normally used where other methods, such as boring in the dry, are not applicable, it is very difficult to obtain two numbers which can reasonably be compared. Equally, it is not of much help to know that a higher shaft friction could be used by boring in the dry, if boring in the dry is not practicable. This is also strength of empirical relationships, because any effects of using bentonite are built into the factors produced by back analysis of appropriate test results.

This is reinforced by Touma and Reese (1972), who performed load tests on drilled shafts constructed in sands with the use of slurry. They inferred from the results that there was no clear reduction of the shaft friction due to use of slurry in construction.

Fleming and Sliwinski (1977) studied 21 pile load tests in clays, 9 pile tests in sands, and three pile tests in chalk. In clays, the piles were constructed using both dry and wet methods, and in sands they were constructed using the wet method, and using temporary casing. Where used, the temporary casings were driven without pre-excavation with slurry. Fleming and Sliwinski (1977) concluded that in sands, a thin membrane, or filter cake, is formed at the soil/pile interface. The test results indicated that shaft friction at high displacements could be reduced about 10 to 30 percent compared with that developed using a temporary casing; however, they could not determine if that was because of the bentonite slurry, or because of some other factors, such as the larger diameter hole left behind when the temporary casing is removed.

CIRIA Report 77 (Fearenside and Cooke 1978) studied seven piles formed in London clay specifically to check the effects of bentonite on pile capacity; three were constructed using bentonite and four under dry conditions. There was no evidence that the use of bentonite adversely affected skin friction. In fact, piles constructed with slurry had higher capacities than those with the same diameter and length constructed

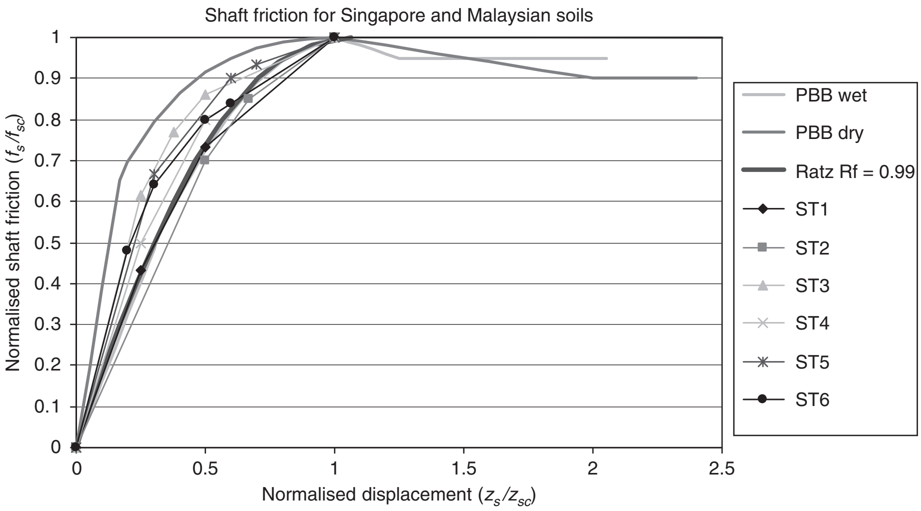

Figure 8.37 Variation of shaft friction with displacement

dry. However, it was suggested that this was due to the difference in sidewall roughness in shafts constructed with slurry using a drilling bucket, compared with shafts drilled dry using an auger.

As noted above, Phienwej *et al.* (1994) reported on 14 instrumented test piles formed in the Kenny Hill Formation in Kuala Lumpur. They summarised the data onto a plot of normalised shaft friction against normalised displacement, and this is reproduced as Figure 8.37. Although there is some scatter, it is small considering that the results from several layers in at least 10 piles on six different sites are included. It also appears to show a significant difference between the piles constructed wet and dry, with the dry piles showing a much stiffer response.

Also shown in Figure 8.37 is the shaft friction/displacement relationship, often referred to as a *t-z* curve, used in the program RATZ, which performs the same function as the load transfer relationships referred to by several of the authors listed above (Buttling, 1990; Chang and Broms, 1991; Phienwej *et al.*, 1994). It can just be made out that the shaft friction used by RATZ, with an Rf value of 0.99, agrees very well with the field data for wet piles, marked as PBB wet. In addition, a number of other curves have been plotted, based on instrumented pile tests on piles formed under bentonite in Singapore residual soils, taken from load transfer curves in Buttling (1987). These are seen to lie between the two extremes of the dry and wet curves, with a tendency to be nearer the wet curve. These curves are all normalised, such that actual shaft friction values can only be determined if the peak value of shaft friction is known, and this is where the importance of the K_s value lies. It is very interesting to note that, while Phienwej *et al.* (1994) show that the performance of the shaft is much stiffer for piles constructed in the dry, the data to support the relationship between peak shaft friction (f_{sc}) and SPT-N value appears to be independent of the process.

Table 8.21 K_s values for bored piles

Depth range (m)	*Empirical factor K_s*
Piles bored under bentonite	
12–18	0.87
18–21	0.45
21–24	1.18
24–26	0.69
Piles bored in the dry	
12–20	1.18
20–27.6	3.56
27.6–35.4	0.49

Chen and Hiew (2006) compared the results of static pile load tests on two fully instrumented bored piles in residual soil, also of the Kenny Hill Formation, using different methods for temporary support. The residual soil was mostly loose to medium dense silty sand, with SPT-N varying from 4 to 13. A very hard silt layer with SPT-N of more than 50 was found at 12 m below the ground surface.

The first was a test pile to failure, 1000 mm in diameter and 27 m long. It was started with a temporary casing 6 m long and, after the soil inside the casing was removed by auger, the bore was filled with bentonite slurry. Drilling was completed with a bucket, and the loose materials at the base were removed using a mechanical cleaning bucket. Concrete was placed using the tremie method.

The second was a working pile, 1200 mm in diameter and 36 m long. Because of a deep cut off, a temporary outer casing was installed to debond the upper part of the pile from the soil. The soil inside this casing was removed, and a concrete was formed inside this casing about 1 m thick. A smaller diameter casing was then installed and the boring work continued to the design depth in the dry. Concrete was placed using the tremie method after the base had been cleaned.

The results of the static load tests were analysed and compared, and it was found that the shaft friction was higher for the bored pile constructed using the dry method. The K_s values for different depth ranges in the two piles are presented in Table 8.21.

Chen and Hiew concluded that the K_s values for the dry pile may suggest that a value greater than 2 could be used, noting that this pile was not tested to failure so peak shaft frictions were not mobilised. However, it is hard to justify the value of 3, which they recommend for general use, on the basis of only this evidence. They also conclude that a lower value should be used for piles bored under bentonite, and suggest a K_s value of 2. While this is in keeping with the proposals of other authors referred to, as noted above, it cannot be justified on the basis of their test results. Noting that the piles were only 5 m apart, and that the larger diameter pile was bored in the dry, it is not at all clear why bentonite was used in the smaller test pile loaded to failure. Its relevance to the general design of piles bored under bentonite in residual soil is therefore questioned.

As pile diameters become larger, the relative importance of the end bearing capacity also increases. This is a point of major concern to designers for a number of reasons:

1 The contribution of the base resistance to the ultimate geotechnical capacity of the pile can be very significant;

2 This peak base resistance will usually occur at a significant displacement, which is often assumed to be about 10% of the pile diameter;
3 This displacement is often an order of magnitude greater than the displacement required to reach peak shaft friction, and this leads to a potential anomaly when simply adding peak shaft friction capacity to peak end bearing capacity and dividing by a simple factor, since the two peak values very rarely coexist;
4 The end bearing resistance which is available in practice is highly subject to quality of workmanship;
5 One of the common factors, which has been widely written about, is the cleanliness of the pile base at the time of placing the concrete via a tremie pipe;
6 Another factor, which has received much less attention, is the potential for loosening of material at the base of the pile by stress relief.

There is significant practical experience to show that, if the base of a pile is not properly cleaned prior to concreting, then the resulting layer of debris, usually comprising silt, sand and perhaps lumps of clay, in a loose state, will lead to sudden unacceptable pile head settlement once the shaft friction has been fully mobilised. The means of preventing this are not complicated, but require attention to detail, and an understanding of the processes involved.

Where bentonite is used as the drilling fluid, this has two main purposes. One is to maintain stability of the bore in cohesionless soil layers by applying an excess internal fluid pressure to the inside of the filter cake. The other is to hold soil particles in suspension through the combined effects of fluid density and viscosity. With the particles in suspension, they can be removed from the hole by exchanging the bentonite column. Thus the larger particles will fall under gravity and be removed by a mechanical cleaning bucket, while the smaller particles are distributed vertically throughout the bentonite column, as a result of the removal and reinsertion of the drilling tool. The viscosity of the bentonite means that it will take an unacceptably long time for particles of sand and silt near the surface to settle to the bottom to be removed mechanically. The correct process is therefore to remove the heavier, dirty, contaminated bentonite from the base of the pile, clean it in a desanding plant and hydrocyclone, and replace it with cleaned bentonite at the surface. The removal can be achieved by use of a submerged pump, but the air lift is generally more popular. Even this simple piece of plant is not widely understood in practice by the field operatives required to use it, and there can be a tendency to use too much air. The principle is based on simple fluid mechanics, which requires that, if a steel tube (the air lift pipe) contains a fluid with air bubbles, and the fluid outside the tube (in the pile shaft) does not contain air bubbles, then the difference in density between the two fluids will cause the lighter fluid to rise in the tube and be replaced at the base by the heavier fluid. For this reason very small air flows will work, and allow the base to be cleaned without applying high velocities or suctions. On the other hand, since the clean drilling fluid is lighter than the contaminated fluid, it cannot be displaced from above, and all the attempts to pump clean bentonite down from the surface, even through trumpet-shaped end pieces, will be to no avail. The table lamps containing different coloured oils, with the warmer, lighter one rising through the heavier one, are a good demonstration of what will happen when this is tried in the field.

Alternatively, increasing use is being made these days of polymer-based drilling fluids. These are made from long chain polymers, which can have the ability to behave quite unlike normal fluids. It is clear that polymers which, like bentonite, had their origins in the oilfield drilling industry, also, like bentonite, help to improve the stability of pile bores, especially in cohesionless soils below the water table. What is not quite so clear is exactly how they do this, because it is certainly not through the development of a filter cake and the creation of an internal excess fluid pressure. It seems likely that there is some way in which the long chains of the polymer are forced out into the interstitial voids of the cohesionless soil, and thereby create a form of soil reinforcement. If this is the case, it also explains why they perform well in circular holes, but not so well when it comes to rectangular holes such as diaphragm walls, where bentonite still seems to be the preferred fluid. It is also clear that we tend to use the same tests to check on the qualities of a drilling fluid, even though the way in which it works is completely different.

For example, as stated previously, we rely on the viscosity, and the shear strength, of a bentonite to support soil particles, and we generally measure the "apparent viscosity" based on the time it takes for a known volume of bentonite to pass through a small hole, as in a Marsh Cone. However the polymer-based drilling fluids do not have an increased viscosity, indeed particles are not held in suspension and settle out faster than in water, yet the long chains still slow the progress of the fluid through the small hole of the Marsh Cone, giving another "apparent viscosity", though for a different reason and in a different range from that expected of bentonite.

Where polymers are used, air lifts or submerged pumps are generally not required, since the particles will settle to the base very quickly. Instead a mechanical cleaning bucket can be positioned at the base of the hole to trap debris as it settles, and rotated gently to pick up the last few lumps before being slowly raised to the surface. There is not the tendency of the whole column of drilling fluid to become contaminated with debris, as there is with bentonite, so the cleaning process can be much quicker. Other benefits include a much smaller requirement for plant and storage, compared with bentonite silos, recirculating tanks, and desanding equipment, and also an easier disposal problem at the end of the project, since most polymer drilling fluids are biodegradable.

Even with the best cleaning techniques, it is not possible to counter the effects of stress relief. If the soil at the base of the pile is a very dense cohesionless material, at a depth of, say, 50 m, it is likely to be under a vertical effective stress of 400 to 500 kPa. If it is overconsolidated, and that applies to residual soils just as much as to sedimented soils, then it could be a higher value. By the time a hole has been bored and filled with drilling fluid with a density of about 1.03 g/cc, the vertical effective stress is only about 10 to 15 kPa, and this can cause the soil to swell, and to take in drilling fluid, whether it be bentonite or polymer, as it does so. This has been noted particularly in sedimented soils, such as piles in London taken down to the Thanet Sands, and piles in Bangkok where a series of pile tests on many sites for the Second Stage Expressway System, undertaken in about 1990, showed base stiffnesses in the range of 25 to 40 kPa/mm, for bases in very dense sands. It can reasonably be assumed that the same process will occur in residual soils, where there is limited cohesive material present to hold the material together. Since, if it occurs, this is a localised effect at the base, it may be corrected by base grouting after pile installation. On the other hand, with the use of limit state design, it may be unnecessary. As long as the ultimate geotechnical capacity is still present, even if at a large displacement, the serviceability limit state is still satisfied, which will probably be dependent on the shaft friction and then the piles will still work satisfactorily. It must also be remembered that in practice, where piles operate in groups of significant size, the overall behaviour is the result of the application of stress to a much larger zone than the base of the piles, and performance at working stress may not be affected by base stiffness.

Having said all that, the base resistance for a bored pile is difficult to estimate, because the resistance is very dependent on workmanship. Unlike the small variation in the K_s values, the K_b values vary significantly. The K_b values as reported by Toh *et al.* (1989), based on two test piles that were taken to failure, are between 27 and 60. They also suggested that, unless there is confidence in the cleaning of the base, bored pile design should consider shaft friction only. Chang and Broms (1991) had suggested K_b of 30–45 for the design of bored piles. However, Tan *et al.* (1998) found that the K_b values can be as low as 7–10, possibly as a result of poor cleaning. Chen and Hiew recommended a K_b value of 10 for preliminary design. They suggested a higher K_b value of 30 could be adopted if cleaning of the pile base before concreting could be carried out effectively.

A series of axial load tests on drilled shafts in a Piedmont residual soil are reported by Brown (2002). Several construction techniques were used to install the shafts in an attempt to identify the significance of installation technique on performance under axial load. These included:

(i) slurry shafts constructed using a truck-mounted drilling rig with a conventional soil auger. A casing was used in the upper 1 to 2 m and extended approximately 1 m above ground to facilitate testing. The bottom of each shaft was cleaned successively using a clean-out bucket and an air-lift. The slurry varied from high grade commercial bentonite to a polymer in dry pellet form;
(ii) four of the shafts were constructed using temporary casing advanced ahead of the excavation; and,
(iii) one CFA pile, constructed by screwing the hollow stem augers into the ground and filling the void with concrete during withdrawal.

Excavation and visual inspection of the concrete/soil interface provided additional insight into the effects of installation technique on side shear resistance. The following conclusions were drawn (Brown, 2002), and might be applied to soil conditions similar to this site:

- In these Piedmont fine-grained silty soils, the shafts installed using bentonite slurry had a reduced capacity compared to other installation techniques. This effect appears to be largely related to the presence of a thin film of bentonite left at the concrete/soil interface as a result of filter cake formation during drilling. This observation seems consistent with several other limited studies in granular soils, but the surprising finding at this site was that the effect seemed to be pronounced even for shafts with very limited exposure times. This effect may not extend to soils of lower hydraulic conductivity, which may reduce the tendency for filter cake formation.

Table 8.22 Measured and Computed Unit Load Transfer Values

Method	*Unit side shear (kPa)*	*Unit end bearing (kPa)*
Measured average (excluding bentonite)	55	850
FHWA 1999 guidelines, cohesive soils	51	830
FHWA 1999 guidelines, cohesionless soils	82	800

- The polymer slurry materials appeared to promote an excellent bond between the concrete and soil. There was a distinct tendency for shafts constructed using these materials to exhibit strain softening behaviour, although the mechanism for this effect is unclear. The strain softening may be related to dilatant behaviour of the relatively undisturbed Piedmont residual soil in the near field around the shaft during shear.
- The use of casing advanced ahead of the shaft excavation resulted in axial shaft capacity which was comparable to that of the polymer shafts, but without the strain softening tendency. The rotation of the casing during installation was observed to remould and distort the soil in the near field around the shaft and the casing produced a smooth concrete/soil interface. However, the twisting of the casing during extraction and the cutting teeth on the bottom of the casing left a rough macro-texture on the sidewall. The surface texture left by the cutting teeth appeared to be beneficial; a smooth steel casing which might be extracted by a vibrohammer could produce less desirable side shear capacity, particularly in cohesive soils (Camp *et al.*, 2002).
- The occurrence of soil inclusions with cross-sectional area of up to 20% of the shaft cross-section had no effect on the short-term performance under axial load. It should be noted, however, that the average compressive stress was only around 4.3 MPa, and so structural failure of the shaft column was not an issue.

Brown (2002) presents comparisons with recommendations used for routine design of drilled shafts in residual soil. Since Piedmont silty soils are intermediate between clay and sand, in practice design may include both a total stress and effective stress analysis.

For piles or drilled shafts in cohesive soil, the current FHWA guidelines suggest a unit shaft friction of $f_{\max} = \alpha \cdot s_u$, where $\alpha = 0.55$ and $s_u =$ average undrained shear strength, $= 92$ kPa in this case. Computed unit end bearing for cohesive soils is taken as $9 \cdot s_u$ kPa. For cohesionless soil, the current FHWA guidelines suggest a unit shaft friction of $f_{\max} = \beta \cdot \sigma'_v$, where $\beta = 1.5 - 0.245[z]^{1/2}$, $z =$ depth in metres to middle of cohesive layer, and $\sigma'_v =$ effective vertical stress at depth z. Computed unit end bearing for cohesionless soils is taken as $57.5 \cdot N_{SPT}$ kPa, where N_{SPT} is the standard penetration test resistance within two diameters below the base (around 14 in this case). These guidelines are based on the computed unit end bearing mobilised at a displacement of approximately 5% of the base diameter. The computed values of axial unit shaft friction and end bearing using the Federal Highway Administration (FHWA) guidelines (O'Neill and Reese, 1999) are provided in Table 8.22.

Figure 8.38 Installation of the bored piles with temporary casing

ISC'2 Pile Prediction Event in residual soil in FEUP, Porto

Scope and steps of the programme

In the Fall of 2003, the Faculty of Engineering of the University of Porto (FEUP) and the High Technical Institute of the Technical University of Lisbon (ISTUTL) invited the international geotechnical community to participate in a Class A prediction event on pile capacity and pile response to an applied loading sequence for Bored, CFA and Driven Piles. An extensive site investigation had been carried out, in which several *in situ* testing techniques were used. Undisturbed samples were recovered and an extensive laboratory-testing programme was carried out.

Two each of three different kinds of piles were installed. 600 mm diameter bored piles (E0 and E9) installed using a temporary casing, 600 mm diameter CFA piles (T1 and T2), and 350 mm square, driven, precast concrete piles (C1 and C2). Of these, 3 piles were tested dynamically (E0, T2 and C2), and 3 were loaded axially up to failure (piles E9, T1 and C1).

Piles E0 and E9 were constructed in August 2003 by first using a rotary drilling rig to install a temporary casing that was cleaned out using a 500 mm cleaning bucket (Figure 8.38). The external diameter of the cutting teeth at the bottom of the temporary casing was 620 mm. Concrete, with slump 180 mm, was placed by tremie. The casing was withdrawn on completion of the concreting and "overconsumption" was below 10%.

Piles T1 and T2 were constructed in August 2003 using a rotary drilling rig and a 600 mm continuous flight auger (see Figure 8.39). Concrete grout was ejected with a pressure of 6000 kPa at the beginning of the grout line and the flow rate was steady at 700 l/min. Concrete slump was 190 mm and "overconsumption" was less than 6%.

The C-piles, were driven on September 17, 2003 with a 40 kN drop hammer (Figure 8.40).

The piles were exhumed after testing, and Figure 8.41 shows the outside appearance of each pile type.

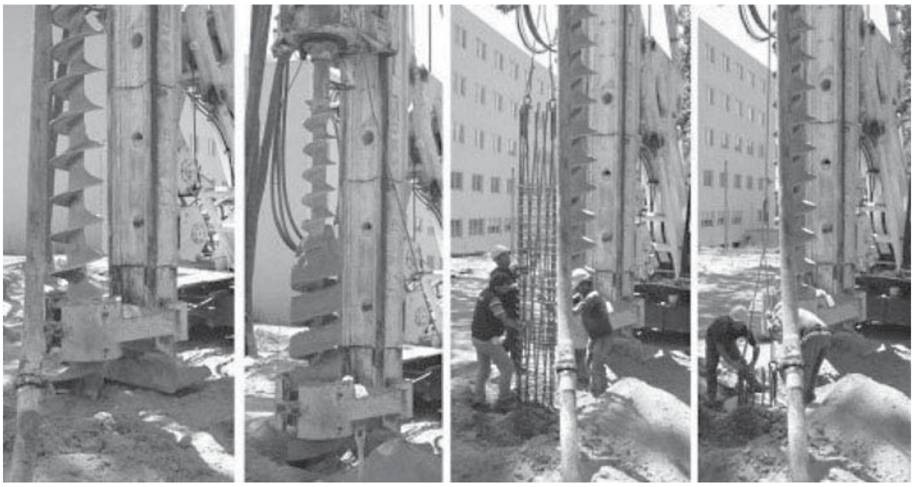

Figure 8.39 Installation of CFA pile

Figure 8.40 Installation of precast concrete driven pile

The predictions

For the Pile Prediction Event, the participants were provided with information on pile geometry, soil profile, equipment and high strain dynamic test results. They were challenged to predict the performance of the piles under static load by submitting a table of load vs. settlement at the pile head, and also:

(i) parameters and models used;
(ii) calculation methodology;
(iii) pile base resistance and shaft resistance, separately if applied;

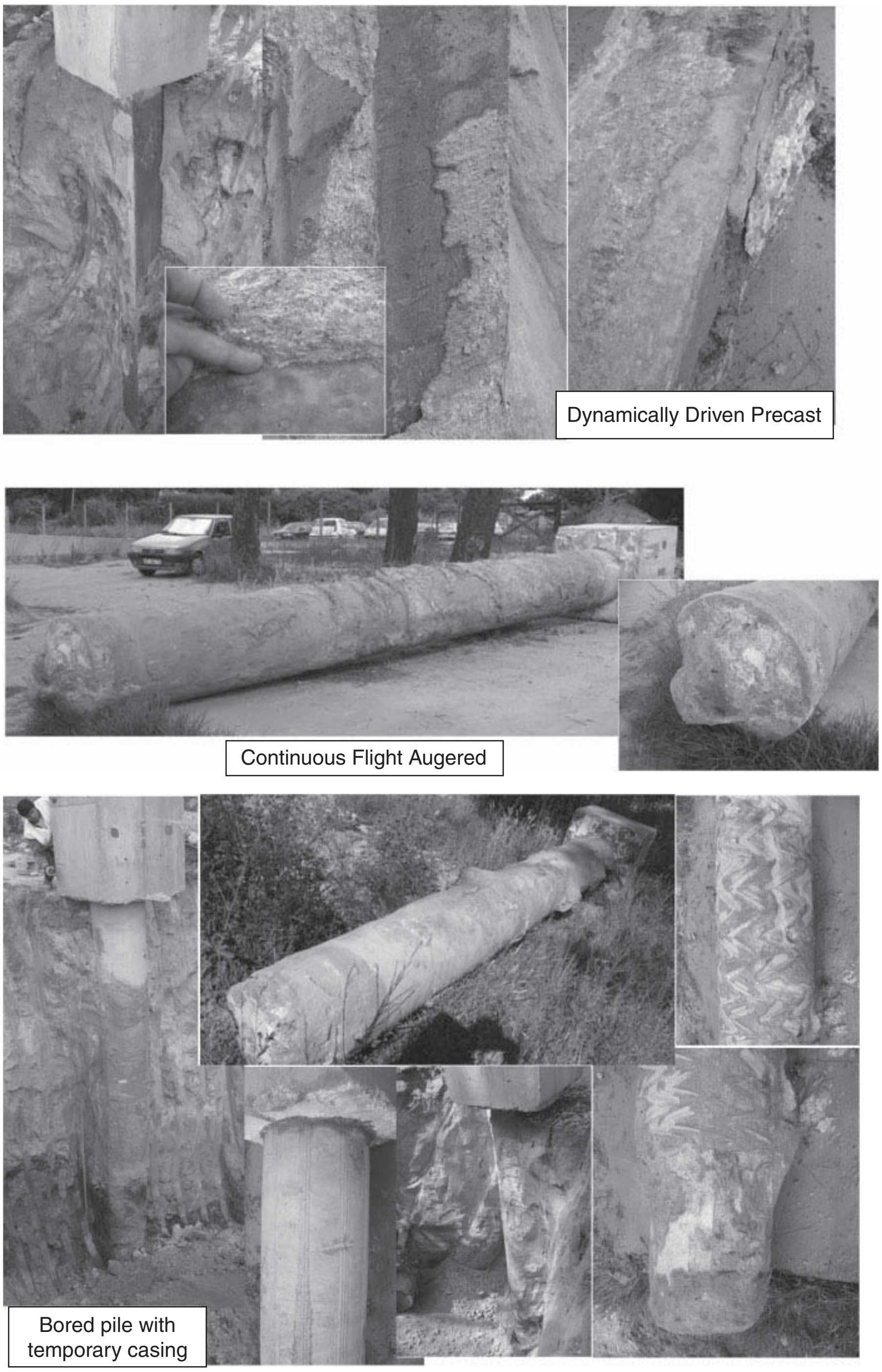

Figure 8.41 Some of the differences in the three types of piles after extraction

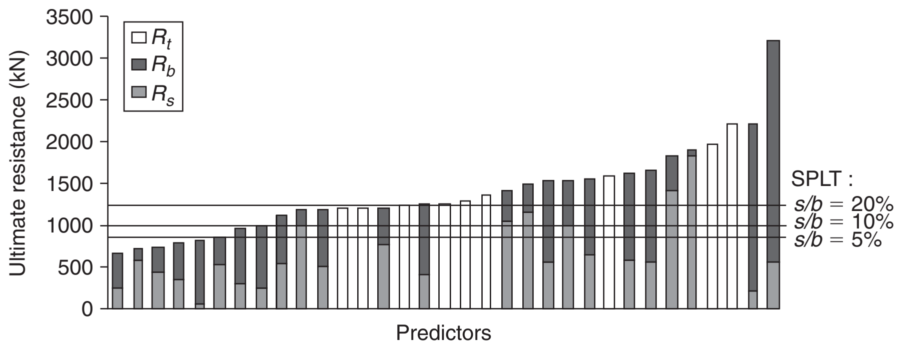

Figure 8.42 Ultimate resistance: predictions for bored pile E9

(iv) ultimate compressive resistance and indication of criteria used to determine this;
(v) allowable bearing capacity, and factor of safety, if applied, used to determine this;
(vi) explanation of the methods used to make the predictions.

In December 2003, a total of 33 persons from 17 countries submitted predictions, and static loading tests on piles E9, T1 and C1 were then performed in January 2004. A summary of the predictions and the test results is given in Viana da Fonseca and Santos (2008).

A compilation of the predictions for the ultimate compressive resistance is represented in Figures 8.42, 8.43 and 8.44 for piles E9, T1 and C1, respectively. The pile base resistance (R_b) and shaft resistance (R_s) are indicated separately when applied; otherwise the total resistance (R_t) is shown. The predictors applied different calculation methods, such as analytical or empirical methods, results of dynamic load tests or a combination of both. It is also important to note that different criteria or calculation approaches were used to define the ultimate compressive resistance.

The predictions presented in the figures are very scattered demonstrating that the accurate estimation of pile axial capacity is still a very difficult task in residual soils. For each pile type one prediction was optimistic, and the means and standard deviations of the remainder are shown in Table 8.23.

For the non-displacement piles (bored piles and CFA piles), most predictions have overestimated the ultimate capacity, probably because the settlements induced in the static tests have not mobilised the failure mechanism assumed in theoretical formulations for the evaluation of base resistance. On the other hand, the predictions for the displacement piles (precast driven piles) were conservative, probably because there was an underestimation of the strength gains due to pile installation effects.

Predictions based on analytical methods give a large scatter, since there is a great risk with such methods in using the input data with no judgement. It is generally preferable to use directly the results of *in situ* tests for prediction of ultimate resistance of piles. Synthesis of that data for the ISC'2 event site is presented in Viana da Fonseca and Santos (2008).

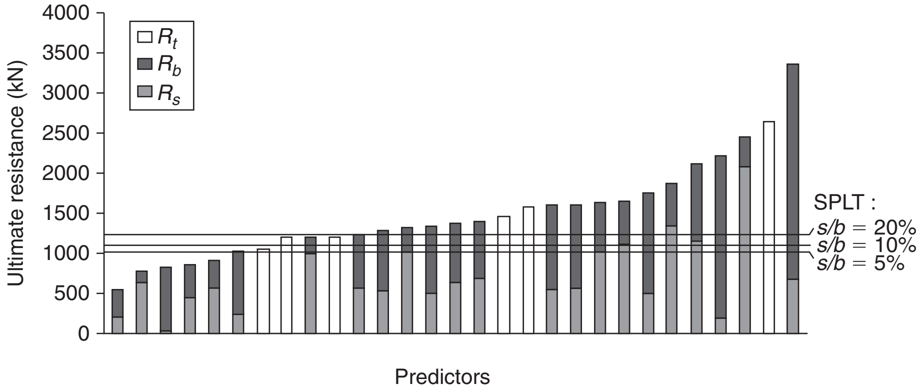

Figure 8.43 Ultimate resistance: predictions for CFA pile T1

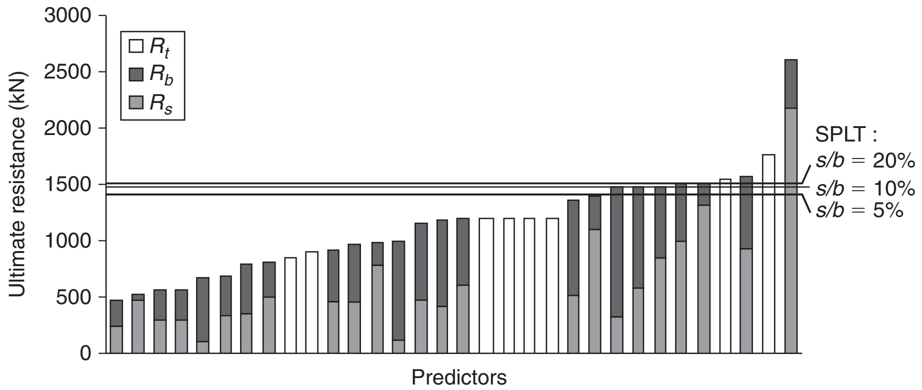

Figure 8.44 Ultimate resistance: predictions for driven pile C1

The SPT-based predictions performed fairly well for the non-displacement piles, being in fairly good agreement with the load test results for the bored pile (E9), while generally over-predicting the ultimate capacity of the CFA pile (T1). As for CPT based predictions, these show good agreement with the load test results for the bored pile (E9), with some scatter, but only reasonable agreement for the CFA pile (T1), for which there were fewer predictions. For the driven pile C1, the predicted ultimate capacity values, of which there were a large number, were very low when compared with the load test results, with a few exceptions (Viana da Fonseca and Santos, 2008).

The results of the PMT-based predictions and their interdependence with the pile construction process in residual soil are interesting. The results generally agree very well with the Q_{SPLT} ($s/b = 20\%$), being far better than the SPT and CPT based predictions, especially for the non-displacement bored pile (E9 see Figure 8.45a) and CFA pile (T1 see Figure 8.45b). For the displacement pile (C1 see Figure 8.45c), the agreement is good for ½ of the predictions.

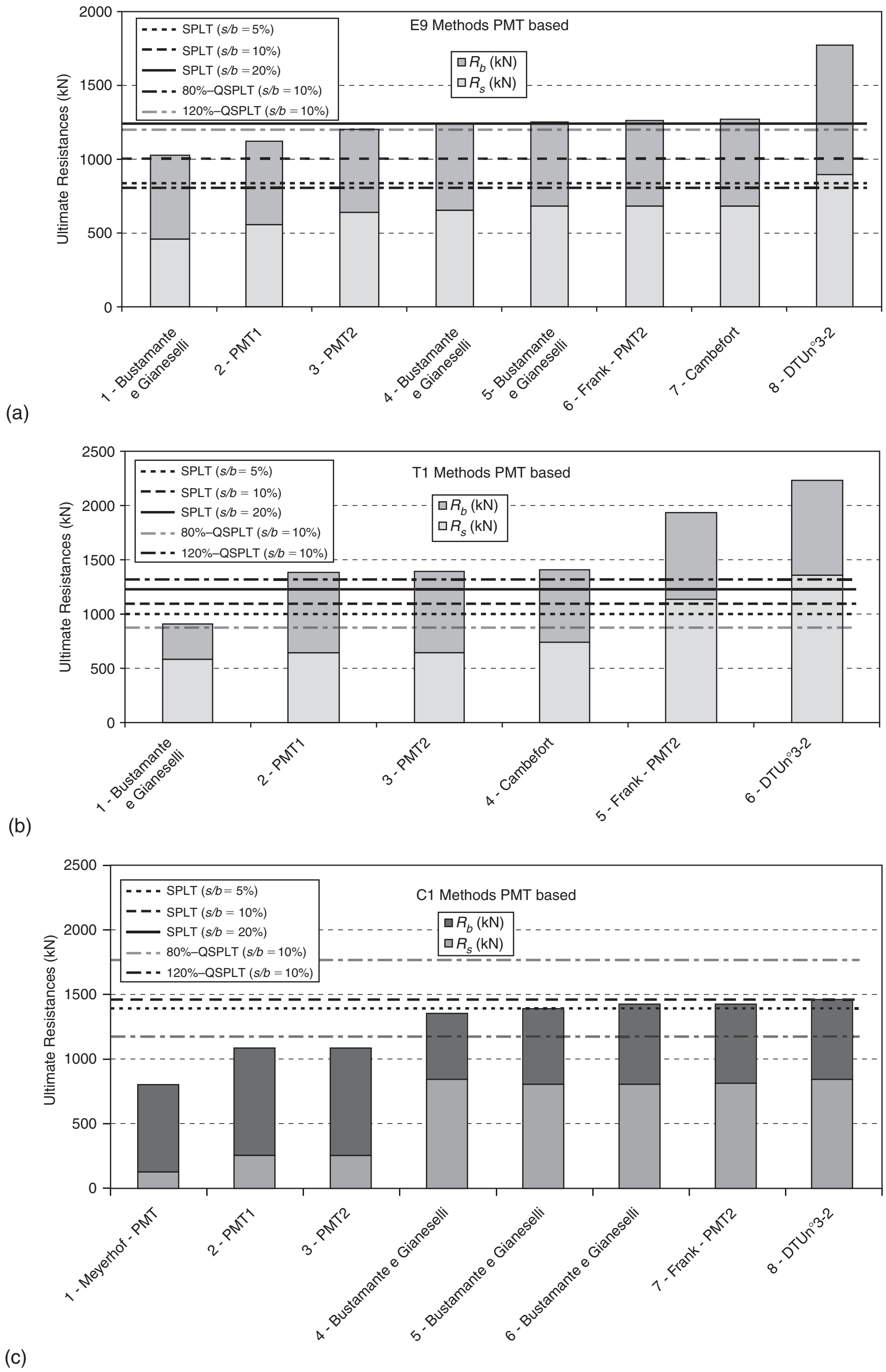

Figure 8.45 Predictions from PMT results of ultimate resistance of: (a) bored pile, E9; (b) CFA pile, T1; (c) precast driven pile, C1

The overall preliminary conclusion was that analytical methods generally are very scattered and potentially unsafe, and are therefore to be avoided. More specifically methods based on SPT are very scattered, and may be too unsafe for CFA piles, while too conservative for driven piles. CPT-based methods show less scatter than SPT-based methods, being generally reasonable for non-displacement piles, but grossly conservative for displacement piles. PMT methods, although not so numerous in the prediction exercise which is a sign of international practice, are clearly the most accurate, especially for bored piles and CFA piles.

Re-analysis of the results of the Static Pile Load Tests

Fellenius *et al.* (2007) re-analysed the load test data, and drew two main conclusions:

1 In these granular residual soils, analyses based on alpha method and undrained shear strength were not as suitable as the beta method in the well-drained conditions.
2 Preference was given to analysis based on CPTu data, for its continuous and representative scanning of the site spatial variations.

CPTU data includes the area correction of the cone tip resistance, q_c, for the pore pressure, u_2. Of the CPTU methods, the Dutch method (DeRuiter and Beringen, 1979), the method of Schmertmann (1978), the LCPC method (Bustamante and Gianeselli, 1982) as quoted by the CFEM 1992, all require a choice of soil type, between "clays" and "sands". In addition, the method of Meyerhof (1976), is limited to piles in sands, while the method of Tumay and Fakhroo (1981) is limited to piles in clay. On the other hand the Eslami-Fellenius or "E-F CPTU method" (Eslami, 1996; Eslami and Fellenius, 1997) differentiates more diverse types of geomechanical soil behaviour from the CPT/CPTU results, considering six main soil classes with some intermediate materials.

From some of the previous analysis of this study, reported in Santos *et al.* (2005) and Fellenius *et al.* (2007), the following conclusions were extracted:

- Extensometer measurements allowed for a very reliable estimation of load distribution. They showed that, for 1,200 kN/100 mm movement, Pile E9 had shaft and base resistances of 1,000 kN and 200 kN respectively, while T1 had 800 kN and 400 kN. However, the piles were expected to have some unknown residual loads, locked-in before the static loading test, as consequence of the installation process. A trial-and-error analysis of the data (as described by Fellenius *et al.*, 2007) indicated the presence of residual loads and estimated their values. However, it appeared that the method overestimated the shaft resistance by 300 kN and consequently underestimated the base resistance by the same amount. An effective stress analysis of the data, adjusted to these residual loads, correlates to a constant beta-coefficient (β) value of 1.0 and a base coefficient (N_b) equal of 16. These are not compatible, and the low N_b value is attributed to disturbance of the soil at the base during the construction process;
- A back-analysis of the loading test on Pile C1 using the same value of 1.0 for β as that derived from the load distribution of Piles E9 and T1, indicates total

shaft and base resistances of 520 kN and 980 kN, respectively. This base resistance corresponds to a N_b of 70, which is compatible with the β of 1.0.

A new analysis was carried out by Viana da Fonseca *et al.* (2007), with the purpose of having a more fundamental evaluation of the residual loads and, consequently, the load distribution between ultimate shaft resistance and tip resistance for 100 mm top settlement. This was possible by applying a mathematical model that allowed a back analysis of the top load-settlement curve.

A model to predict single pile performance under vertical loading was proposed by Massad (1995), which included many aspects of load transfer phenomena, considered previously by Baguelin and Venon (1971), such as pile compressibility and progressive failure. In addition, it takes into account the presence of residual stresses due to driving or subsequent cycling loadings. The solutions are analytical, in closed form, and were derived using load transfer functions based on Cambefort's Laws, accounting for the current knowledge of the shaft and tip displacements needed to mobilise the full resistances. They may be applied to bored, jacked or driven piles subjected to a preliminary monotonic loading and/or subsequent loading-unloading cycles. The soil is supposed to be homogeneous with depth, along the entire pile shaft. A thorough description of the model is given in Viana da Fonseca *et al.* (2007).

For the bored pile E9 and the CFA pile T1, a comparison was possible between the results of these analyses and the measurements from the extensometers installed within the piles. With these results, it was possible to evaluate the load distribution, for a reference top settlement of 100 mm, into an ultimate shaft resistance and base resistance, as shown in Table 8.23. These values are in close agreement with the ones from the previous analysis (Fellenius *et al.*, 2007), and the differences are due to the estimation of the residual loads. With this new numerical model, residual load values derived for the bored (E9) and CFA (T1) piles were around 150 kN, whereas Fellenius *et al.* (2007) had estimated them at 300 kN. The value of 150 kN for the base residual load was consistent with the measured value. In addition, for the driven pile (C1), the model defined an upper bound value for residual load of 500 kN. If the model is assumed to be valid, the ultimate unit shaft resistance for bored (E9) and CFA (T1) piles will be about 60 kPa. For the driven (C1) pile, this value may be taken as a lower limit.

Returning to the proposed relationships between SPT N value, shaft friction and end bearing in equations (33) and (34) results, in this case, in a K_s value of around 3.75, while K_b is around 70.

The K_s value of 3.75 is higher than the ranges previously reported (Table 8.24).

However, some caution is necessary. The higher values are measured values in only two tests, while some of the tabulated values are measured and some are proposed values to be used in design. The latter should always include a degree of conservatism.

Table 8.23 Load Distribution for 100 mm pile head settlement

Pile	*Shaft load (kN)*	*Base load (kN)*	*Total load (kN)*
E9 (Bored)	696	481	1177
T1 (CFA)	703	499	1202
C1 (Precast)	511 to 1021	1004 to 494	1515

Table 8.24 Values of K_s by different researchers

Author	K_s
Toh *et al.* (1989)	2.5–2.7
Phienwej *et al.* (1994)	2.3
Tan *et al.* (1998)	2
Chang and Broms (1991)	2
Chen and Hiew (2006) dry process	3
Chen and Hiew (2006) wet process	2

Table 8.25 Values of K_b by different researchers

Author	K_b
Toh *et al.* (1989)	27–60
Chang and Broms (1991)	30–45
Chen and Hiew (2006) preliminary	10
Chen and Hiew (2006) with good cleaning	30

The measured values for a dry process bored pile and a CFA pile are therefore compatible with the proposed design value.

The values of K_b are also much higher than those previously suggested (Table 8.25).

This would imply that the bored pile tested in the ISC'2 programme was subject to effective base cleaning, as would be expected for a dry process pile, and that the CFA pile was installed carefully without loosening of soil at the base.

Design of axially loaded piles using the LCPC method

The advantage of using pressuremeter tests when dealing with residual soils, but also the possibility of having piling design rules for a wide variety of construction methods, makes the LCPC method very interesting and quite universal. The method was developed by the Laboratoire Central des Ponts et Chaussées, the French Highway Agency, and is also known as the French Design Rules for Foundations, Fascicule 62-V. As described by Bustamante *et al.* (2009), this method is based on the results of 30 years of pile loading tests on prototype piles constructed by more than 20 different techniques, mostly in Europe, the soil having been previously subjected to a site investigation using the Ménard pressuremeter (MPM). The study looked at the analysis of 550 load tests, of which 350 piles were instrumented to record the shaft friction of each soil layer and the base pressure; so as to compare these with the MPM design rules initiated by Louis Ménard in the 1960s, based on both the theory of cavity expansion in soils and his own experiments. Recently, additional experimental data, including comprehensive site investigations with PMT, CPT and SPT, have been gathered about full-scale pile load tests on deep foundations with instrumentation to:

(i) include the most recent installation/construction techniques used in common practice; and
(ii) refine the values of the limiting shaft friction q_s and the pile tip bearing factor K_p.

The principles

The principles of the PMT method used for designing foundations for civil engineering works in France are given by Gambin and Frank (2009). During most pile load tests, the end of the test occurs when the pile head starts to sink rapidly. The load related to this particular threshold is called the limit load Q_L. Conventionally, Q_L is defined as being the load for which the head settlement s_L is given by:

$$s_L \geq \frac{D}{10} + \Delta e \tag{8.37}$$

where D is the diameter of the pile, and Δe is the pile elastic shortening. The bearing capacity of a pile is expressed by:

$$Q = AK_p[(p_{LM} - p_0)_e] + P\sum(q_{si} \cdot z_i) \tag{8.38}$$

where
A = pile tip area
K_p = tip bearing factor
$[(p_{LM} - p_o)_e]$ = net equivalent Ménard limit pressure under the pile tip
P = pile perimeter
z_i = thickness of soil layer "i"
q_{si} = uniform shaft friction of soil layer "i".

The parameters K_p and q_s, which are essential in this equation, are measured on prototype piles load tested to failure with strain gauges.

The universality of this method has enabled it to be cited as a "common method to calculate the ultimate compressive resistance, Q, of piles" in the European standard for geotechnical design, EN 1997-1. In the future French standard to complement Eurocode 7, the factors are being readjusted to take into account the additional full scale tests available. The adaptation of these rules to the action and material factors of Eurocode 7 requires, in particular, having a precise knowledge of the scatter of the ratio of predicted bearing capacity to the measured bearing capacity.

The types of piles and the construction methods included in the design rules for axially loaded piles recommended by the French code covers all types of bored cast-in-place and driven piles, of any cross section (circular, polygonal, barrette, etc.); steel sheet piles and reinforced concrete diaphragm walls, when used as bearing elements (i.e. carrying vertical loads), are considered to belong to "piling".

Applicability of the method

The range of deep foundations to which this method may be applied is particularly varied including: pre-manufactured or cast-in-place; driven, jacked, jetted, screwed, bored or excavated; supplemented by grouting; piles with cylindrical section, but also H-section steel piles and sheet piles, as well as bored bearing elements (barrettes) of any shape; constitutive materials of concrete, grout, mortar, steel, or combinations thereof (timber piles are very rare in Europe).

The classification system for the design methods, presented by Bustamante and Frank (1999), is as follows:

Preformed piles:	*driven precast concrete*
	driven steel (caisson, H, tube)
	prestressed tube
	concreted driven steel (H, tube)
Rotary bored or excavated piles:	*bored without casing*
	bored with casing
	flush bored (including barrettes)
	continuous flight auger
	cast-in-place screwed
Micropiles:	*micropile types I, II, III and IV*
Piers	
Jacked piles:	*concrete jacked*
	steel jacked
Driven cast-in-place piles:	*internal drop hammer driving*
	with a sacrificial shoe

Basis of the method

There are some definitions in this method for design of axially loaded piles:

for compression piles	Q_c : creep load
and	Q_u : limit load
for tension piles	Q_{tc} : tension creep load
and	Q_{tu} : tension limit load.

The creep load Q_c may be used to characterise the axial behaviour of piles. ISSMFE (1985) defines the creep load as "a critical experimental load beyond which the rate of settlement under constant load takes place with a notably increased increment". In case of a static load test performed using the maintained load procedure, it is easily determined by a simple graphic construction (for instance AFNORNFP94-150).

The limit load is defined as the load at which the displacement of the head of the pile is 10% of the width or diameter of the pile. When deriving Q_c, Q_u, Q_{tc} or Q_{tu} from static load test(s), a reduction is applied to the measured value(s), related to the uncertainty of the result.

1 According to the Frenchstandard Fascicule 62-V, if only one single pile load test is performed:

$$Q = \frac{Q_m}{1.2} \tag{8.39}$$

where Q_m is the measured value.

If several load tests are performed:

$$Q_k = Q_{\min}\left(\frac{Q_{\min}}{Q_{\max}}\right)^{\xi'} \tag{8.40}$$

Table 8.26 Values of factor ξ' (Fascicule 62-V, 1993)

Number of load tests	2	3	4	5
ξ'	0.55	0.20	0.07	0.00

Table 8.27 Correlation factors ξ to derive characteristic values from static pile loadtests (n – number of tested piles)

ξ *for n*	*1*	*2*	*3*	*4*	*≥5*
ξ_1	1.40	1.30	1.20	1.10	1.00
ξ_2	1.40	1.20	1.05	1.00	1.00

where $Q_{\min}$ and $Q_{\max}$ are the minimum and maximum measured values, and ξ' is given in Table 8.26.

2 EN 1997-1 adopts similar concepts by stating that, when deriving the characteristic ultimate compressive resistance $R_{c;k}$ from measured values $R_{c;m}$, from pile load tests and from comparable experience, including one or more site specific pile load tests, an allowance shall be made for the variability of the ground and the variability of the effect of pile installation, by applying correlation factors as follows:

$$R_{c;k} = \min\left\{\frac{(R_{c;m})_{\text{mean}}}{\xi_1}; \frac{(R_{c;m})_{\min}}{\xi_2}\right\} \tag{8.41}$$

where ξ_1 and ξ_2 are correlation factors that depend on the number of tests. The values of ξ_1 and ξ_2 are presented in Table 8.27.

On the limit states

Bustamante and Frank (1999), and Frank (2008) define Design Loads, Q_d, by the following:

ULS (ultimate limit state)

Under fundamental combinations: $Q_{tu}/1.4 \leq Q_d \leq Q_u/1.4$
Under accidental combinations: $Q_{tu}/1.3^{(1)} \leq Q_d \leq Q_u/1.2$
where

$Q_u = Q_{pu} + Q_{su}$ is the ultimate limit load in compression (end bearing + skin friction),

and

$Q_{tu} = Q_{su}$ is the ultimate limit load in tension (skin friction alone).

SLS (serviceability limit state)

Under rare combinations: $Q_{tc}/1.4^{(2)} \leq Q_d \leq Q_c/1.1$
Under quasi permanent combinations: $0^{(3)} \leq Q_d \leq Q_c/\ 1.4$

[1]For micropiles, $-Q_{tu}/1.2$; [2]For micropiles, $-Q_{tc}/1.1$; [3] For micropiles, $-Q_{tc}/1.4$

where Q_{cc} or Q_{tc} are the corresponding (compression and tension) creep loads:

$Q_{cc} = 0.5Q_{pu} + 0.7Q_{su}$ and $Q_{tc} = 0.7Q_{su}$ for non-displacement piles
$Q_{cc} = 0.7Q_{pu} + 0.7Q_{su} = 0.7Q_u$ and $Q_{tc} = 0.7Q_{su}$ for displacement piles

It should be noted that the way of treating serviceability limit states in the French standard is different from Eurocode 7. The former is based on the creep load, easily determined from bearing capacity approaches, while the latter relies essentially on settlement estimates.

The evaluation of Q_{pu} and Q_{su} is made by deriving the limiting values for the base pressure (q_u) and the shaft friction (q_{si}) by the formulae:

$$Q_{pu} = q_u \cdot A_p \tag{8.42}$$

$$Q_{su} = \sum_{0}^{i} q_{si} \cdot A_{si} \tag{8.43}$$

where A_p is the area of the base, A_{si} the shaft surface area in layer i. The values of q_u and q_{si} are derived by specific correlations to the *in situ* tests as described below. For tension piles, the limiting shaft friction is assumed to be the same as for compression piles.

PMT (MPM) method

The last update reported by Bustamante *et al.* (2009) included a total of 561 tests, of which 276 tests (or 49%) were taken to their limit load. For the remainder, the load was extrapolated up to this value by one of the analytical methods. Finally, 13% of the piles were subjected to tensile tests.

The Base Bearing Factor K_p
The K_p value can be chosen from Table 8.28.

Table 8.28 Direct design with PMT data in weathered rock

Group Code	K_p
1	1.6
2	2.0
3	2.3
4	2.4*
5	1.1*
6	1.4*
7	1.1*
8	1.5*

*If a higher K_p value is to be used, it must be proved by a load test.

Table 8.29 Description and characteristics of 138 analysed piles

Group Code	*Type No.*	*Piles (2) Qty*	*B(3) (mm)*	*D(4) (m)*	*Pile Description*
1	1	8	500–2,000	11.5–23	Pile or barrette bored in the dr
	2	64	270–1,800	6–78	Pile and barrette bored with slurry
	3	2	270–1,200	20–56	Bored and cased pile (permanent casing)
	4	28	420–1,100	5.5–29	Bored and cased piler (recoverable casing)
	5(1)	4	520–880	19–27	Dry bored piles/or slurr bored piles with grooved sockets/or piers (3 Types)
2	5(1)	50	410–980	4.5–30	Bored pile with a single or double-rotation CFA (2 types)
3	7	48	310–710	5–19.5	Screwed cast-in-place
	8	1	650	13.5	Screwed pile with casing
4	9(1)	30	280–520	6.5–72.5	Pre-cast or pre-stressed concrete driven pile (2 types)
	10	15	250–600	8.9–20	Coated driven pile (concrete, mortar, grout)
	11	19	330–610	4–29.5	Driven cast-in place pile
	12	27	170–810	4.5–45	Driven steel pile, closed tip
5	13	27	190–1,22	8–70	Driven steel pile, open end
6	14	23	260–600	6–64	Driven H pile
	15	4	260–430	9–15.5	Driven grouted(5) or (6) H Pile
7	16	15	—	3.5–2.5	Driven sheet pile
1	17		80–140	4–12	Micropile type I
	18	8	120–810	8.5–37	Micropile type II
8	19	23	100–1,220	8.5–67	SGP(5) micropile (type III) or SGP pile
	20	20	130–660	7–39	MRP(6) micropile (type IV) or MRP pile

The Ultimate Shaft Friction q_s
According to Bustamante *et al.* (2009), the parameter q_s is chosen as follows:

– select the pile type from Table 8.29 and get the applicable Q_i from Table 8.30
– use Figure 8.46 to obtain, on the selected Q_i curve, the q_s for the Ménard limit pressure (p_{LM}) measured at the appropriate depth.

Contrary to the set of discontinuous straight lines which are shown on the similar graph in the French codes, Fascicule 62-V and AFNOR DTU-13.2, it should be noticed that in Figure 8.46, the q_s lines are continuous, which avoids any ambiguity when choosing this parameter.

Application of CPT method to the results of ISC'2-PPE static pile load tests

For CPT values, the correlations with the unit shaft and base resistances may be expressed, following the same pattern as the French/LCPC method (Bustamante and Frank, 1999), as the following:

$$q_s = \min\left[\frac{q_c}{\beta}; q_{s\max}\right] \tag{8.44}$$

Table 8.30 Direct design with PMT Data in weathered rock

Pile Type No.	Q_i
1	Q6*
2	Q6*
3	Q1*
4	Q4*
5	Q6
6	Q5*
7	Q4*
8	Q2*
17	Q6*
18	Q6*
19	Q9*
20	Q10*

** Use of a higher value must be proved by a load test.

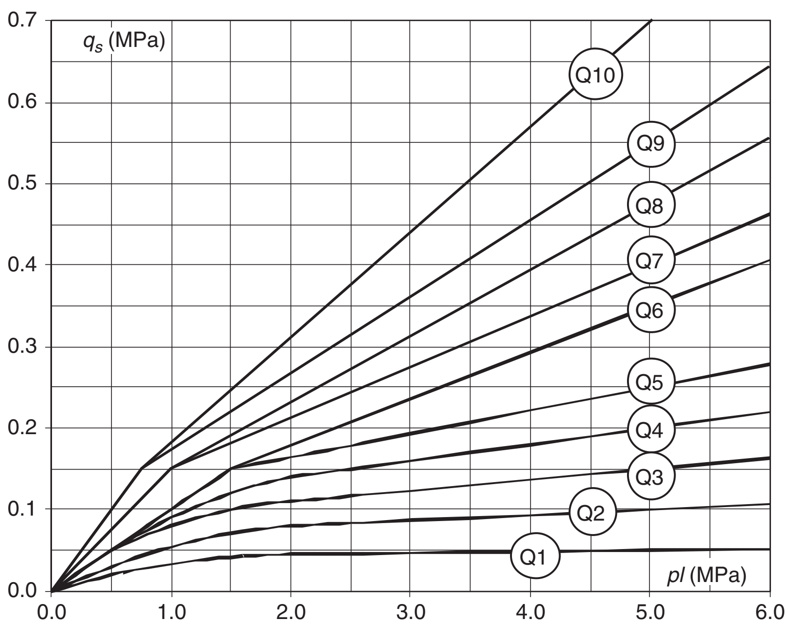

Figure 8.46 Direct design using PMT Data. Chart for shaft friction q_s

$$q_b = K_c \cdot q_{ce} \tag{8.45}$$

where q_c is the average CPT static cone resistance in each assumed layer and q_{ce} is the cone resistance around the base – measured between half a diameter above the base and one and a half diameters below); K_c is the base bearing factor, which is a function of the type of soils, and the pile type and method of execution (values are available for non-displacement piles and displacement piles); β is a correlation factor that depends

Table 8.31 Unit shaft friction from CPT data (*After* Bustamante and Frank, 1999)

	Soils	*Clays and Silts*					*Sands and Gravels*		
Type of piles	*Range of q_c (MPa)*	*<3*	*3–6*		*>6*		*<5*	*8–15*	*>20*
A: Bored without casing	β	—	—	75			200	200	200
(dry method)	$q_{s\,max}$(kPa)	15	40	80	40	80			120
B: Bored with temporary	β	–	100	100	—	100	250	250	300
casing	$q_{s\,max}$(kPa)	15	40	60	40	80	—	40	120
C: Driven precast	β	—	75		—		150	150	150
concrete	$q_{s\,max}$(kPa)	15	80		80		—	—	120

on the pile type and the soil; $q_{s\,max}$ is the limiting value of shaft friction, which again depends on the type of soil and the method of pile construction.

In the specific case of the non-displacement piles tested in the residual soil of Porto granite:

$$\beta \cong 55; K_c \cong 0.35$$

For the displacement piles, where the shaft friction is reduced by $\beta \cong 120$, then $K_c \cong 0.75$.

These may be compared to some reference values (Bustamante and Frank, 1999), which would suggest for sand or silty sand, the values for base resistance would be $K_c = 0.15$, for non-displacement piles, and $K_c = 0.50$, for displacement piles. For shaft resistance the patterns for β and $q_{s\,max}$ proposed in the LCPC method are given in Table 8.31 (considering the three classes closer to the three types of piles used in the experimental site).

These appear to show, considering that typical values of CPT are in the mid-range, that for the bored and CFA piles, the values of the shaft coefficient ($\beta \cong 55$) are more in agreement with the behaviour of silty soils, while for the driven piles, the values of the shaft coefficient ($\beta \cong 120$) are much more in agreement with the behaviour of sandy soils.

It must be noted that all the reported values were obtained for one static pile load test. Therefore, even considering the extensive *in situ* tests, the values of the design coefficients must be reduced, as required by French standards as well as in EN 1997-1.

Driving formulae and wave equation analysis

Since the early 20th century, many different dynamic formulae have been proposed as a simple means of determining pile capacity from measurements made on site, of hammer weight, drop height, final set (in mm per blow) and temporary compression. There are plenty of formulae (Poulos and Davis, 1980), including the Hiley, Janbu, Danish, Dutch, Crandall and modified Engineering News Record formulae. Not surprisingly, considering the range of soil types, of hammer types, and of pile types, none has proved to be sufficiently reliable in all situations. They are commonly used for harbour, water-front, canal and off-shore constructions for which driven steel profiles, i.e. pipes, H-sections and sheet piles, are employed. They are also very widely used in conjunction

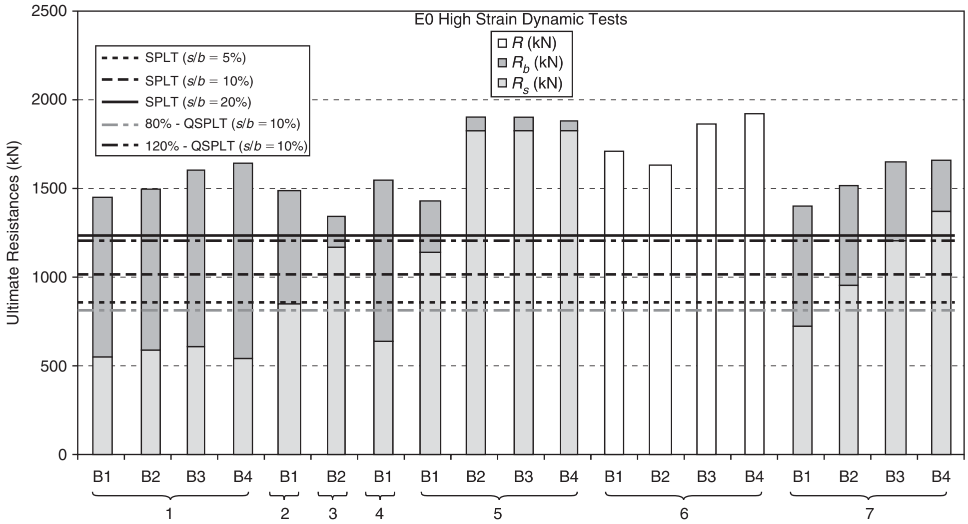

Figure 8.47 Predictions from HSDT to ultimate resistance of pile E0 (bored)

with other forms of testing, since it is generally not feasible to carry out a static or dynamic load test on every pile. Presently, there is an increasing trend to use dynamic load testing, in which the interpretation is generally made using methods based on wave propagation theory, such as the CASE method, CAPWAP analysis, TNO and Simbat. Whereas CASE, CAPWAP and TNO analyses are mainly used for displacement piles, Simbat has been developed for bored piles. A recommended procedure is to verify a static pile design by carrying out dynamic load tests on a suitable number of piles, depending on the size of the project. The French Code and EN 1997-1 give guidance on how many piles should be tested, by varying the correlation coefficient with the number of tests. The Australian Standard AS 2159:2009, introduces a geotechnical resistance reduction factor, within the range of 0.4 to 0.9, and the larger numbers are only possible with reasonable amounts of testing. While carrying out the dynamic testing, the chosen dynamic formula can be calibrated, and the values of set and temporary compression used to check the capacity of all other piles at time of driving through a dynamic formula. There are criticisms of dynamic pile testing and its correlation with static load testing because of the very short time during which the force is applied. Attempts have been made to overcome this with Statnamic testing, in which the force, while still dynamic, is applied over a longer time by the explosive expansion of gases which raise a heavy weight against the resistance of the pile. It is becoming popular, but is still expensive to set up and operate and is limited in availability.

State of the art of stress wave testing

From the ISC'2 event, Viana da Fonseca and Santos (2008) reported and analysed the contribution of participators that used High Strain Dynamic Tests (HSDT) for the prediction of the bored, CFA and precast driven piles. Figure 8.47 presents the 7

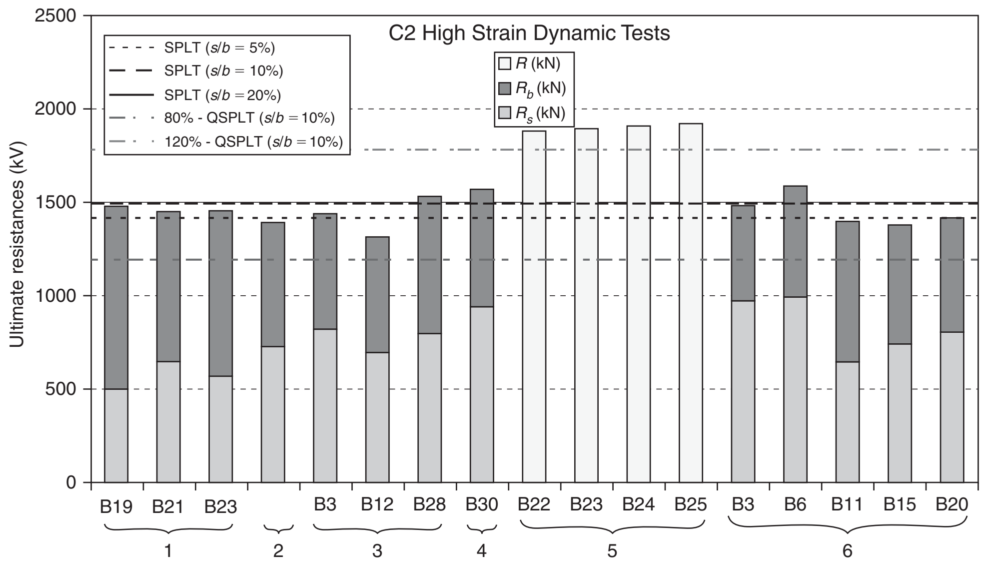

Figure 8.48 Comparison between HSDT on pile C2 and SPLT on pile C1 (driven)

predictions for the bored pile, E0, compared with the ultimate resistance obtained in the Static Pile Load Test (SPLT) on E9. There were four blows, and four predictors used all four, while three used only B1. It can seen that all the predicted values were higher than those obtained in the SPLT, at a settlement = 10% of diameter, by between 34 and 91%. It can also be seen that the predicted values are within quite a narrow range, about ±15%.

A similar analysis is presented for CFA piles. The HSDT predicted values were, generally, higher than those obtained from SPLT for a settlement = 10% of diameter. In this case, the predicted values cover a wider range, about ±33%, and were between 62 and 189% of the SPLT value.

Finally, the report presented the results of the application of HSDT to precast driven piles. Most of the results are in the range of 88–128% Q_{SPLT} (Figure 8.48). The exception is one predictor who proposed the highest capacity for all three types of pile. The values for the remaining predictors are similar, within a range of about ±15%. Clearly, the HSDT is best at predicting the capacity of driven piles, for which it was developed. This may be because the dynamic load test (with consecutive dynamic blows with increasing energy) can modify the subsequent pile resistance compared to the static "virgin resistance" of the pile, the "virgin resistance" being defined as the pile resistance obtained during its first loading. This is particularly true for the bored and CFA piles, in which the mobilisation of base resistance is highly affected by the load history and, as a consequence, the HDST with increasing energy can lead to unsafe predictions of the static "virgin resistance". The difference between the values of HSDT and SPLT can probably be attributed to differences of soil characteristics between piles C2 and C1.

Axial displacements in a single pile

The evaluation/prediction of settlements in piled foundations for support of large axial loads from buildings, towers, and bridges is usually separated from the determination of axial capacity. They should really be integrated, since the load transfer is a progressive mechanism which develops local failure along the shaft interface from the top down to the mobilisation of the ultimate base resistance (punching or local failure), accompanied by an overall movement.

To consider axial displacements, methods are available based on spring models, *t-z* curves, elastic continuum theory, and empirical relationships. Details of these approaches are summarised by O'Neill and Reese (1999). Mayne and Schneider (2001) note that, in reality, the axial response of deep foundations changes progressively from small strain behaviour that occurs elastically at initial stress states (corresponding to the non-destructive region and K_0 conditions), and develops to elastic-plastic states (corresponding to intermediate strains), eventually reaching plastic failure (as well as post-peak) conditions. Numerical approximations using finite elements, discrete elements, finite differences, and boundary elements can be used to follow the stress paths at points near, in the middle region, and far away from the pile-soil interface, although the interface conditions are highly dependent on the construction method.

Geomechanics characteristics of geomaterials

The practice of foundation analysis demands that even simplified analytical methods include key features of geomaterial behaviour. These features include the well established idea that soils and weathered rocks exhibit highly non-linear behaviour under load, with linear elastic behaviour observed only at very small strains in the vicinity of the operational $G_{\max}$ (G_0). This small-strain stiffness, which can be determined from shear wave velocity measurements ($G_0 = \rho \cdot V_s^2$, ρ being the mass density of the soil) applies to the initial static monotonic loading, as well as the dynamic loading of geomaterials (Burland, 1989; Tatsuoka and Shibuya, 1992; Lo Presti *et al.*, 1993). The equivalent elastic modulus is found from: $E_0 = 2 \cdot G_0(1+\nu)$, where ν is the value of Poisson's ratio of geomaterials at small strains. Mayne and Schneider (2001) illustrate this pattern of behaviour and tentatively suggest the relative position of the most common *in situ* tests in terms of the stress-strain curves (see Figure 8.49).

This highly nonlinear stress-strain-strength-time response of soils depends upon loading direction, anisotropy, rate effects, stress level, strain history, time effects, and other factors. So, as Mayne and Schneider (2001) commented, it is difficult to recommend a single test, or even a suite of tests, that directly obtains the relevant E_s for all possible types of analyses in every soil type. They admit that, in certain geomaterials, it has been possible to develop calibrated correlations between specific tests (e.g. PMT, DMT), since they generate the stress-strain-strength curve, generally at an intermediate level of strain, allowing a fair correlation with full-scale structures, including foundations and embankments, or with reference values from laboratory tests.

A more comprehensive analysis is proposed by some (Mayne *et al.*, 1999b; Mayne and Schneider, 2001, amongst others), which takes advantage of the significance the small-strain modulus (G_0) attains as a reference starting point, and makes it possible to use a generalised approach where the initial modulus (E_0, related to G_0) is degraded to an appropriate stress level for the desired FOS.

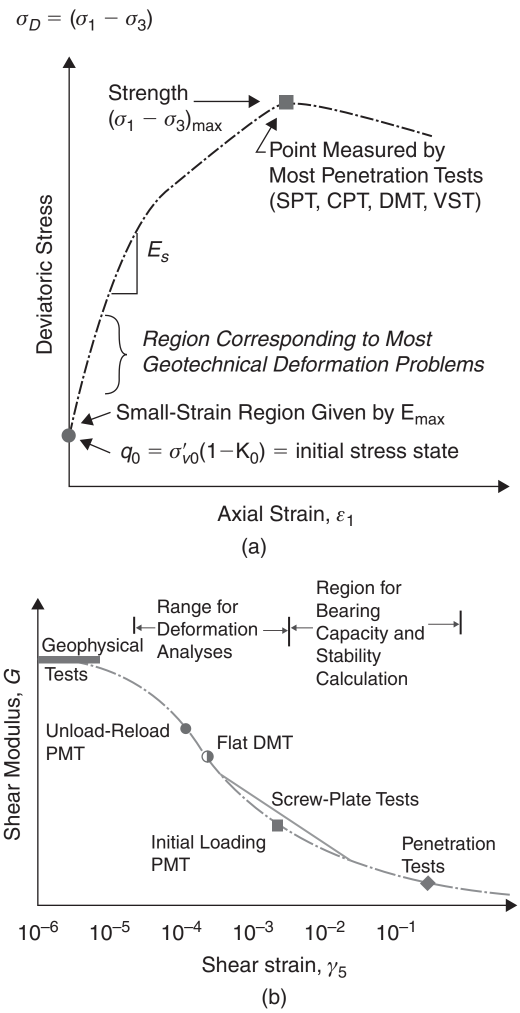

Figure 8.49 (a) Stresses and stiffnesses of soils at small and large strains, (b) Variation of shear modulus with strain level and relevance to *in situ* tests (*After* Mayne and Schneider, 2001)

There are several expressions that have been proposed to represent modulus degradation. Mayne (2000) presents a good overview of some of these proposals:

- the simple hyperbola (Kondner, 1963) requiring only two parameters: shear modulus, G_{max}, and maximum shear stress, or shear strength, τ_{max}; this fails to adequately model the complex behaviour of natural soils with other non-linearities;
- modified hyperbolic laws (Duncan and Chang, 1970; Hardin and Drnevich, 1972; Prevost and Keane, 1990; Fahey and Carter, 1993; Mayne, 1994; Fahey and Carter, 1993), which increase the number of required parameters to either 3 or 4;

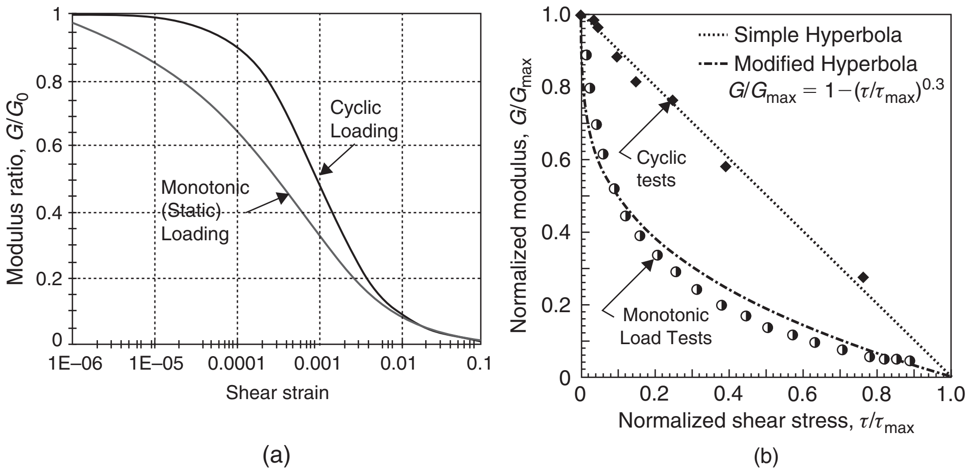

Figure 8.50 Modulus degradation: (a) with Log Shear Strain for Initial Monotonic (Static) and Dynamic (Cyclic) Loading Conditions (Mayne *et al.*, 1999b); (b) results for Toyoura sand (Teachavorasinskun *et al.*, 1991; also Mayne, 2000)

- a periodic logarithmic function which has been proposed by Jardine *et al.* (1986, 1991), relying on 5 curve-fitting parameters;
- a logarithmic stress-strain function for soils and rocks proposed by Puzrin and Burland (1998) using one, three, or four parameters, depending on available information.

Several authors have demonstrated that monotonic decay of stiffness is faster than in cyclic loading conditions (Figure 8.50a). Laboratory torsional shear tests on Toyoura sand, reported by Teachavorasinskun *et al.* (1991) are presented in Figure 8.50b in terms of mobilised stress level. Others from residuals soils from Porto Granite were presented by Viana da Fonseca and Coutinho (2008) and also included in Figure 8.51.

Even in normally consolidated soils, while the cyclic torsional shear tests show modulus degradation reasonably represented by a standard hyperbola, the monotonic tests lose stiffness morequickly (Figure 8.52). For monotonic torsional shearing of normally-consolidated sands, the modified hyperbola proposed by Fahey and Carter (1993) takes one of the two forms:

$$\frac{G}{G_0} = 1 - f\left(\frac{\tau}{\tau_{max}}\right)^g \quad \text{or} \quad \frac{E}{E_0} = 1 - f\left(\frac{q}{q_{ult}}\right)^g$$

where f and g are fitting parameters and q/q_{ult} is the reciprocal of the safety factor. Values of $f = 1$ and $g = 0.3$ appear reasonable first-order estimates for unstructured and uncemented geomaterials (Mayne *et al.*, 1999a).

Evaluating axial displacements

The axial load-displacement behaviour of single piles can be predicted by elastic continuum theory through the solutions developed by Poulos and Davis (1980), by

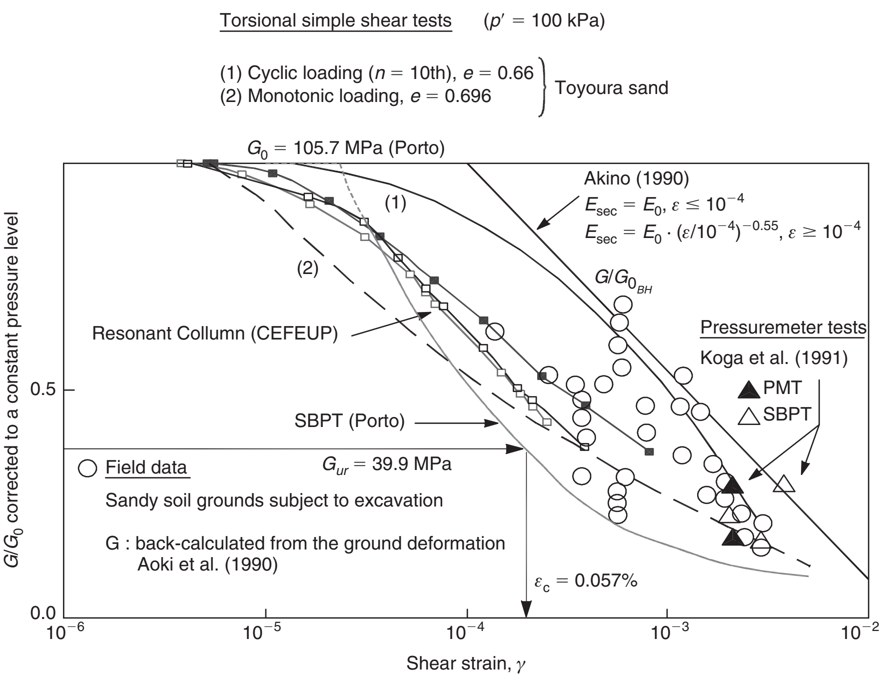

Figure 8.51 Comparison of secant shear modulus as a function of shear strain level: results of resonant column results in residual soils from granite of Porto with data from other testing conditions in sandy soils (*After* Aoki *et al*., 1990; Tatsuoka and Shibuya, 1992)

finite elements (Poulos, 1989), and by approximate closed-form analytical solutions (Randolph and Wroth, 1978, 1979; Fleming *et al*., 1985). Continuum theory characterises the soil stiffness by two elastic parameters: an equivalent elastic soil modulus (E_s) and Poisson's ratio (ν_s). Four generalised cases are considered: (1) a homogeneous case where E_s is constant with depth; (2) a Gibson-type condition where E_s is linearly-increasing with depth; (3) friction or floating-type piles; and (4) end-bearing type piles resting on a stiffer stratum.

The vertical displacement of a pile foundation subjected to axial compression can be expressed (Poulos, 1987, 1989) as:

$$s = \frac{P_t \cdot I_\rho}{(E_{sL} \cdot d)} \tag{8.46}$$

where P_t is the applied axial load at the top of the shaft, E_{sL} stands for the soil modulus along the sides at full depth ($z = L$), d = foundation diameter, and I_ρ = displacement influence factor. The factor I_ρ depends on the pile slenderness ratio (L/d), pile material, soil homogeneity, and relative soil-pile stiffness, and is given in chart solutions, tables,

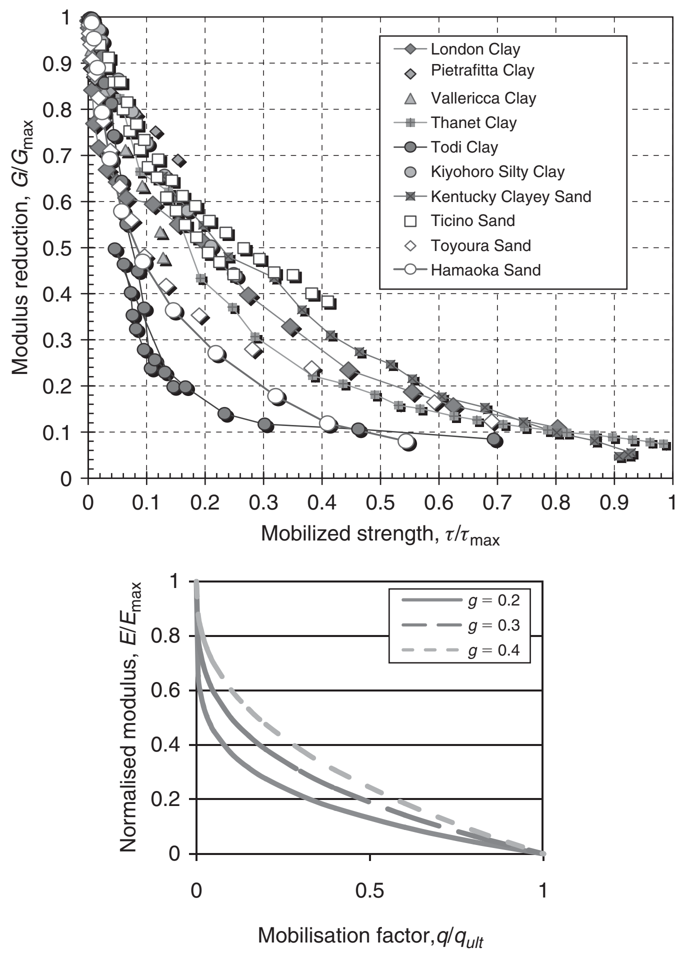

Figure 8.52 Modulus degradation in triaxial tests on uncemented and unstructured geomaterials and modified hyperbolae with $g = 0.2, 0.3$, and 0.4 (*After* Mayne *et al.*, 1999b)

or approximate closed-form. The last is given by the solutions of Randolph and Wroth (1978, 1979) and Poulos (1987):

$$I_\rho = 4(1 + \upsilon_s) \cdot \frac{\left[1 + 1/\pi\lambda \cdot 8/(1 - \upsilon_s) \cdot \eta_1/\xi \cdot \tanh(\mu_L)/\mu_L \cdot L/d\right]}{\left[4\eta/(1 - \upsilon_s)\xi + (4\pi \cdot \rho \cdot \tanh(\mu_L) \cdot L)/\zeta \cdot \mu_L \cdot d\right]} \tag{8.47}$$

where $\eta = d_b/d =$ eta factor ($d_b =$ diameter of base, so that $\eta = 1$ for straight shafts).
$\xi = E_{sL}/E_b =$ xi factor ($\xi = 1$ for floating pile; $\xi < 1$ for end-bearing).
$\rho^* = E_{sm}/E_{sL} =$ rho factor ($\rho^* = 1$ for uniform soil; $\rho^* = 0.5$ for simple Gibson soil).
$\lambda = 2 \cdot (1 + \nu_s) \cdot E_p/E_{sL} =$ lambda factor.

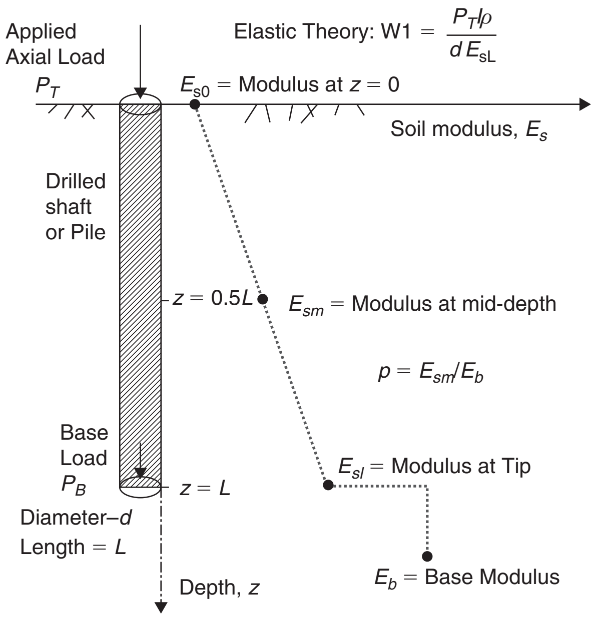

Figure 8.53 Terms used in elastic continuum model (*After* apud Mayne, 2000).

$\zeta = \ln\{[0.25 + (2.5\rho^*(1 - \nu_s) - 0.25) \cdot \xi]\ (2 \cdot L/d)\} =$ zeta factor.
$\mu_L = 2(2/(\zeta \cdot \lambda))^{0.5} \cdot (L/d) =$ mu factor.
$E_p =$ pile modulus (concrete plus reinforcing steel).
$E_{sL} =$ soil modulus value along pile shaft at level of base.
$E_{sm} =$ soil modulus value at mid-depth of pile shaft.
$E_b =$ soil modulus below foundation base (Note: $E_b = E_{sL}$ for floating pile).
$\nu_s =$ Poisson's ratio of soil.

Figure 8.53 shows the generalised stiffness profile for these cases, with corresponding definitions of moduli input for the analysis.

Elastic continuum methods also provide an evaluation of axial load transfer distribution. The fraction of load transferred to the pile base (P_b) is given by Mayne and Schneider (1999), based on the work of Fleming *et al.* (1985):

$$\frac{P_b}{P_t} = \frac{4/(1-\nu_s) \cdot \eta/\xi \cdot 1/\cosh(\mu_L)}{4/(1-\nu_s) \cdot \eta/\xi + 4\pi\rho/\zeta \cdot \tanh(\mu_L)/\mu_L \cdot L/d} \tag{8.48}$$

Additionally, a realistic non-linear load-settlement model of a pile can be determined by inserting a modified hyperbolic model, as introduced above, in the following expression:

$$s = \frac{Q \cdot I_\rho}{d \cdot E_{\max} \cdot [1 - f(Q/Q_{ult})]^g} \tag{8.49}$$

where Q = applied load and Q_{ult} = axial capacity for compression loading. Note that the displacement influence factor also depends on current reduced E_{sL}.

This simple model may be appropriate for many practical cases of foundations which are between the pure floating pile, and piles well toed in to stiff bases with a shaft through softer materials, either homogeneous or with stiffness linearly increasing in depth. This model was applied in the granitic residual soil which was thoroughly studied for ISC'2, applying it to the bored piles with temporary casing, CFA, and driven piles. Figure 8.54 shows the results of applying the model solely considering a shaft embedded in homogeneous soil to such diverse conditions, resulting in fairly reasonable reproduction of the observed load/settlement curves, but using very different parameters.

In other cases, however, the nonhomogeneity of the ground may require modelling of successive layers in depth, and recourse to other less simple models may be necessary. This may be particularly the case in residual soil profiles.

PMT method for predicting load-settlement curves of piles (Frank, 2008)

In this method shaft friction mobilisation "τ-z" curves and end load–end displacement curve (q-s_p curves) are used for the prediction of the load-settlement curve of single piles under axial loading. The pressuremeter approach uses a load transfer method developed by Gambin (1963) and Frank and Zhao (1982), where the pile is cut in a series of equal length elements (Figure 8.55).

According to Frank and Zhao (1982) the settlement s_p of the pile base is given by:

$$s_p = \left(\frac{B}{k_p}\right) q_p \tag{8.50}$$

where B is the diameter of the pile and q_p is the pile base pressure, while the skin friction q_{si} mobilised during the settlement of each pile shaft element i is then obtained as a function of z_{si} which is the local displacement of the i^{th} shaft element against the adjacent soil layer (Figure 8.55). k_t and k_q are functions of the pressuremeter modulus E_M and the diameter B of the pile, with models proposed by Frank and Zhao and shown in Figure 8.56:

$$k_t = 2.0E_M/B \quad \text{and} \quad k_q = 11.0E_M/B \quad \text{for fine soils}$$
$$k_t = 0.8E_M/B \quad \text{and} \quad k_q = 4.8E_M/B \quad \text{for granular soils}$$

Examples of the use of this PMT method for predicting load-settlement curves of piles are given in Frank (1984) or Bustamante and Gianeselli (1993), and one is reproduced in Figure 8.57.

Lateral pile loading

Piles are often subject to lateral loading, and should be designed considering the lateral interaction with the ground. The methods using the subgrade reaction modulus (or p-y reaction curves, where p = reaction pressure, and y = horizontal displacement) are well known for the design of piles under lateral loads. These methods, which

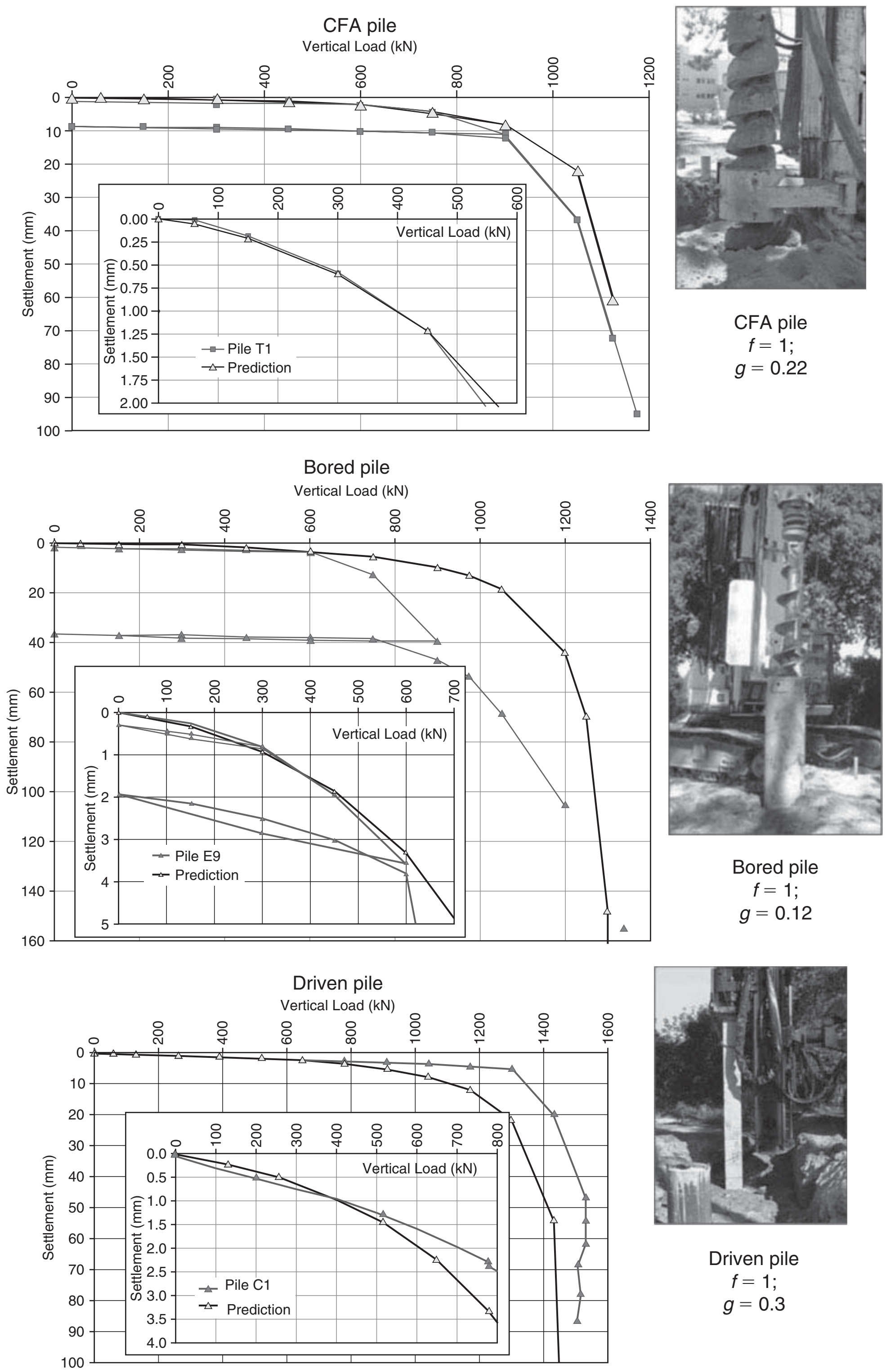

Figure 8.54 Axial load-displacement behaviour of single piles calculated by elastic continuum theory with non-linear stiffness integration (*After* Mayne and Schneider, 1999).

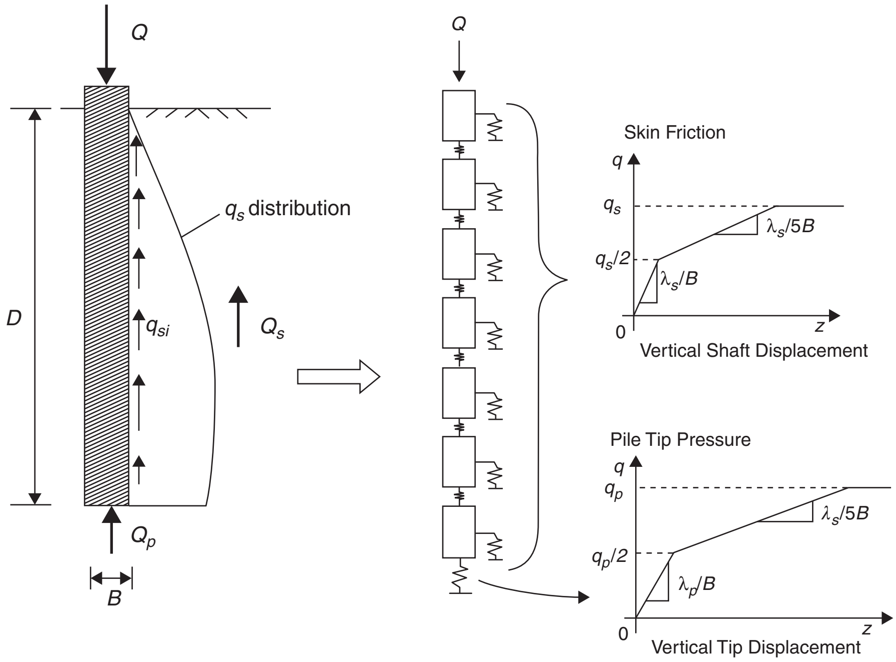

Figure 8.55 Load transfer method to estimate pile settlement (*After* Frank and Zhao, 1982)

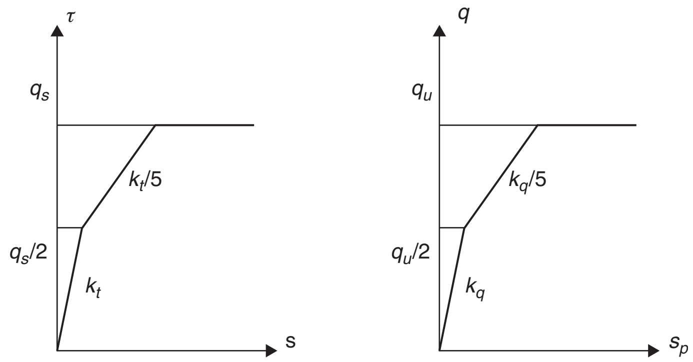

Figure 8.56 PMT τ-*s* and *q*-s_p curves after Frank and Zhao (1982)

consider the pile to be a beam on linear or non-linear elastic spring, are supported by the Winkler theory:

$$EI\frac{d^4y}{dz^4} + k \cdot B \cdot y = 0 \tag{8.51}$$

The value of k is readily obtained from the settlement equation $w = f(E_M)$ given by Ménard (1963) for an infinitely long strip footing, of width B, since $k \cdot B = p/w$.

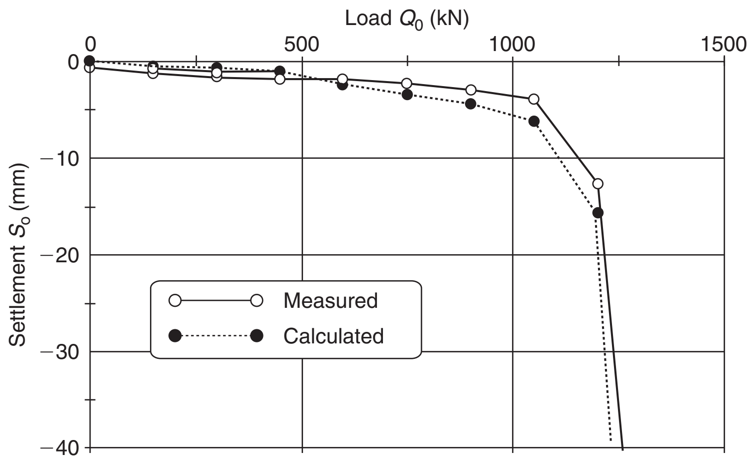

Figure 8.57 Comparison of measured and calculated load-settlement relationship for the Koekelare pile (*After* Bustamante and Gianeselli, 1993)

In this condition, the ground reaction is similar to that observed under a PMT borehole expansion (Gambin and Frank, 2009). When E_M values are averaged, for B larger than 0.6 m, below the critical depth:

$$k \cdot B = E_s = E_M \cdot \left\{ \frac{18}{[4 \cdot (2.65 \cdot B/B_0)^{\alpha} \cdot B_0/B + 3\alpha]} \right\} \tag{8.52}$$

where α is the Ménard rheological factor ($1/4 < \alpha < 2/3$) and B_o is a reference diameter equal to 0.6 m. According to Gambin and Frank (2009), this was checked as early as 1962 using PMT data on various laterally loaded prototype piles. The present design rules (Frank, 1999), using generalised p-y curves, include the decrease of k as y increases. In Figure 8.58, four different loading conditions are shown to be dependent on the creep (or yield) pressure p_c (which can be estimated as: $p_c = p_L/2$).

Gambin and Frank (2009) present a small modification to Equation (51) where a soil applies a horizontal thrust to a pile (Figure 8.59). The equation becomes:

$$EI \cdot \frac{d^4y}{dz^4} + k \cdot B \cdot [y(z) - g(z)] \tag{8.53}$$

where $y(z)$ is replaced by $[y(z) - g(z)]$, $g(z)$ being the free horizontal displacement of the soil without pile.

A description of the data interpretation and analysis of the behaviour of laterally loaded piles in ISC'2 experimental site using PMT and DMT based methods has been given by Tuna (2006) and Tuna *et al.* (2008).

The bored piles E0 and E9 had 6 m net embedment depth, and reaction piles E1 to E8, all 22 m long, were embedded in bedrock. They are described in detail in Tuna *et al.* (2008), as well as the CFA piles (T1 and T2), about 6 m depth and 60 cm diameter,

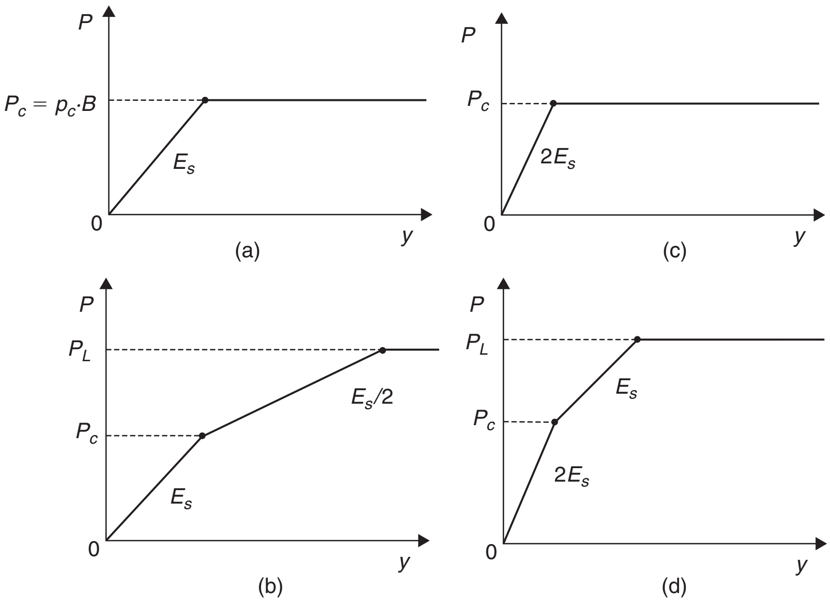

Figure 8.58 Soil reaction against lateral displacement for actions at head level (*After* Frank, 1999), for: (a) permanent actions at pile head; (b) soil lateral thrust; (c) short time actions at pile head; (d) unexpected instant actions at pile head

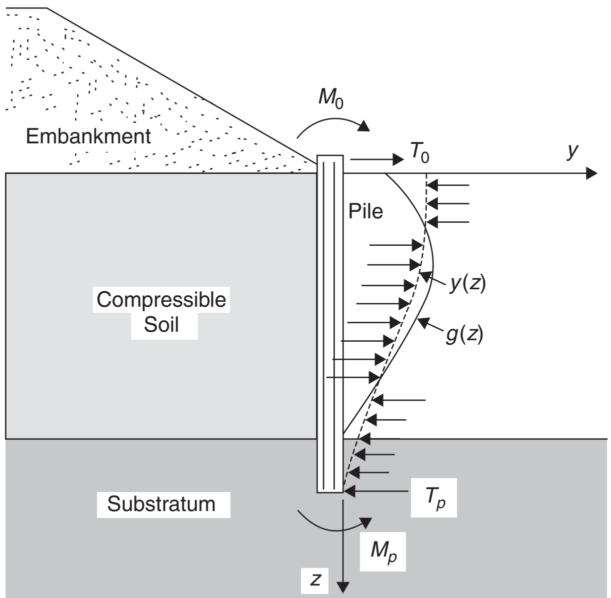

Figure 8.59 Example of a pile subjected to earth pressure (*After* Frank, 1999)

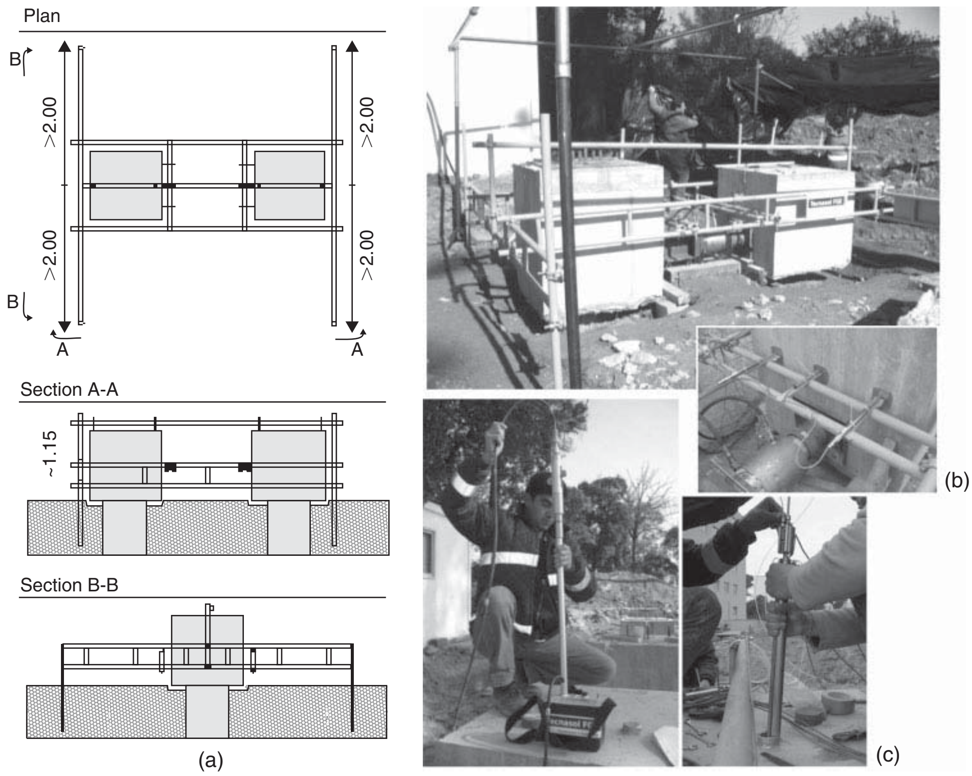

Figure 8.60 (a) Assemblage of the test with reference beam; (b) structure; (c) instrumentation: inclinometer, retrievable extensometer and LVDT mounted horizontally.

and the driven piles (350 mm square). The piles were laterally loaded by pushing each pair apart (E0-E1, E7-C2 and E8-T2) using a hydraulic jack. Measurement of displacements (vertical and horizontal) and rotations of pile heads were made using LVDTs. Detailed inclinometer measurements were made in piles E0, E1 and T2, to define the development of these displacements and rotations through the full length of the piles. In order to determine the bending moment in pile E0, strains in the concrete were measured using retrievable extensometers (Figure 8.60).

Pile head lateral displacements, as measured using the LVDT and also from inclinometer integration, are presented in Figure 8.61.

Tuna *et al*. (2008) used the *p-y* curve method based on PMT (MPM) parameters suggested by Ménard *et al*. (1969) (see Figure 8.62) through the following equations, where B is the pile diameter, B_0 is the diameter of the reference pile (taken equal to 0.6 m) and α is Ménard's rheological factor, varying between 0.25 and 1.

$$\text{For } B > B_0: \quad K = \frac{18E_M}{4\,(2.65(B/B_0))^a\, B_0/B + 3\alpha} \tag{8.54}$$

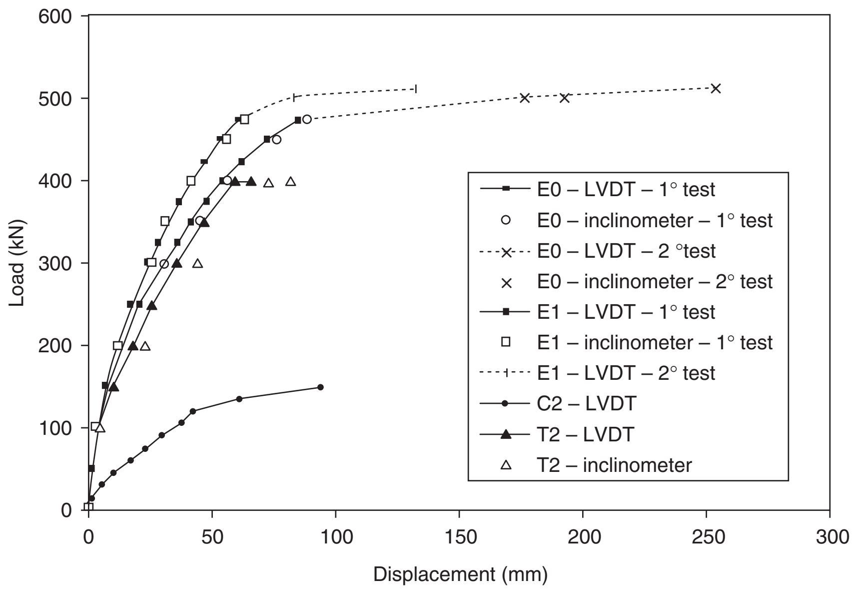

Figure 8.61 Load versus observed pile head lateral displacement

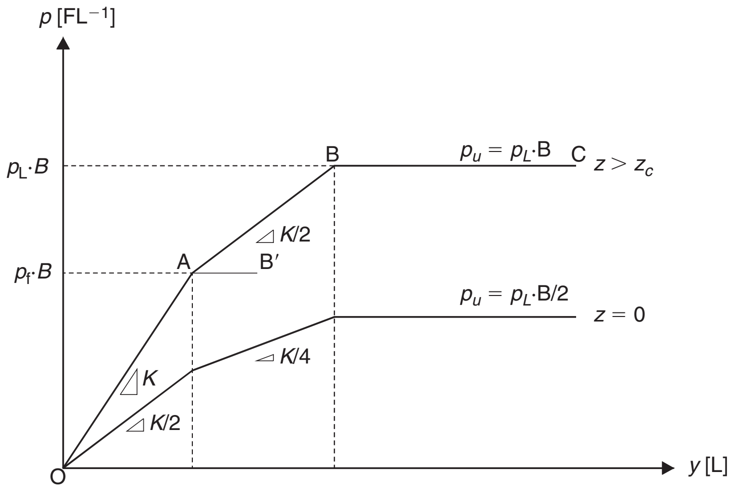

Figure 8.62 *P-y* curve by Ménard *et al.* (1969)

For $B < B_0$: $$K = \frac{18E_M}{4(2.65)^{\alpha} + 3\alpha} \tag{8.55}$$

The reaction curve is modified for depth values, z, less than a critical depth z_c, by multiplying the pressure by a coefficient equal to $0.5(1 + z/z_c)$. For cohesive soils, z_c is about $2 \cdot B$ and for granular soils about $4 \cdot B$.

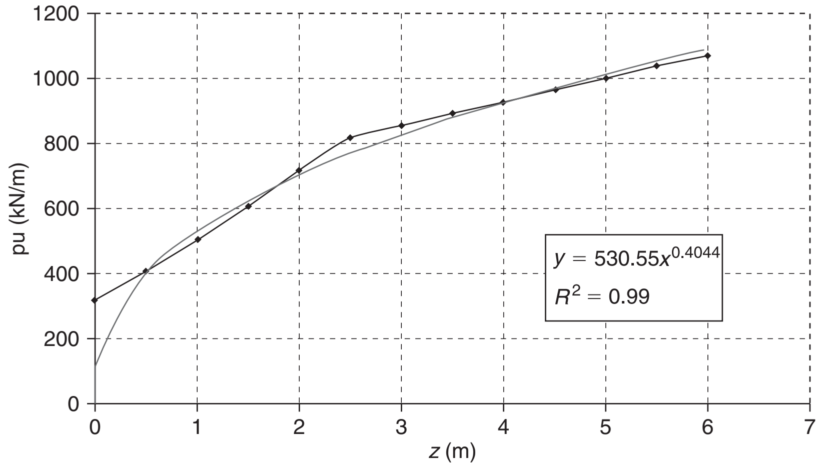

Figure 8.63 Pile E0 – linear relationship of p_u with depth, with power law and trend line

The development of limit pressure (p_L), creep pressure (p_F) and pressuremeter modulus (E_M), with vertical effective stress (depth), is defined by the following equations (a value of 0.33 was adopted for α):

$$p_L\,(\text{kPa}) = 6.4\sigma'_{v0}\,(\text{kPa}) + 1017.2 \tag{8.56}$$

$$p_F\,(\text{kPa}) = 2.4\sigma'_{v0}\,(\text{kPa}) + 365.3 \tag{8.57}$$

$$E_M\,(\text{kPa}) = 92.5\sigma'_{v0} + 12949 \tag{8.58}$$

Additionally, a study was made in order to adjust the soil strength to the points A and B (see Figure 8.62) by power laws. The main purpose was to decrease the high values of p_u, obtained for depths less than 0.5 m. For example, for the bored pile E0, p_u was approximated by a power law as shown in Figure 8.63.

Displacements of pile heads were calculated by the application of the original method proposed by Ménard *et al.* (model A) and by applying the power law approximation (model B). Figure 8.64 shows the calculated and observed displacements.

For the driven pile, the displacements by both methods are generally underestimated. For the bored and CFA piles, model A overestimates the calculated displacements for small loading levels, but underestimates then for higher loading levels. Model B overestimate the displacements for the bored piles, while it predicts fairly well for CFA piles.

In conclusion, this work has indicated that the PMT method, originally proposed by Ménard *et al.* (1969), generally underestimates horizontal displacements in residual soils, mostly at high loading levels, but this can be corrected by decreasing soil strength for shallow depths. Both the Ménard proposal and the one designated as "modified", overestimated displacements for very small loading levels, as a consequence of the excessively low value considered for the reaction modulus (K). Even so, it can be seen

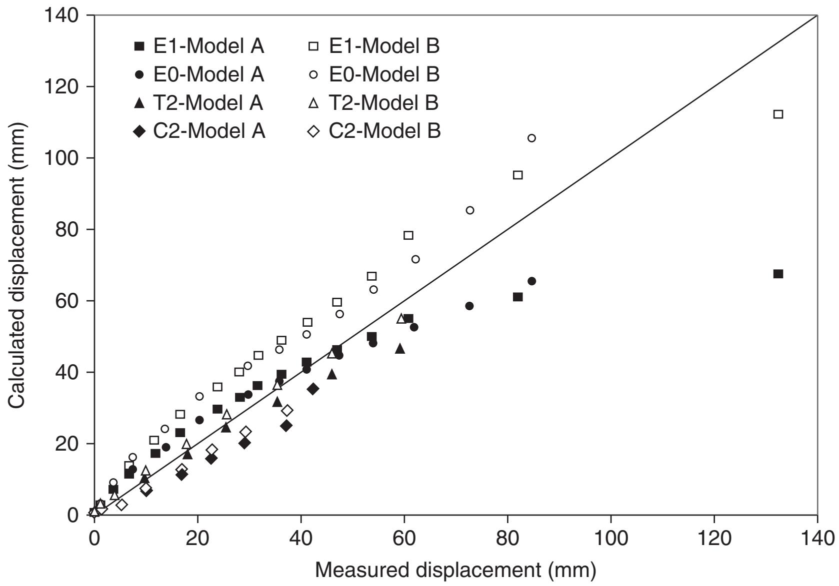

Figure 8.64 Measured and calculated displacements using Ménard *et al.* (1969) method

that this method leads to a reasonable simulation of the behaviour of bored (E0, E1) and CFA (T2) piles. For driven piles (C2) this method is unreliable, because the power law considered for the variation of p_u with depth, is inadequate to model the behaviour of this type of pile.

Quality control and monitoring

Piles normally provide an extremely important function, in supporting a structure such as a bridge or a building. They are also, generally speaking, out of sight once formed so that it is impossible to carry out a detailed inspection. It is therefore, commonly accepted in piling engineering, both by public authorities and by the private sector, that piles have to be subjected to very specific and demanding quality control processes. Two types of tests are in common use: (i) integrity tests (destructive or non-destructive); and (ii) load tests (static or dynamic). These can be done separately or in conjunction, depending on the type of piles, the ground conditions, the importance and the size of the project, the anticipated construction defects and workmanship of the piling contractor.

Integrity testing

The most commonly used methods of non-destructive integrity testing are the following:

a) low strain integrity tests (sometimes referred to as seismic tests);
b) sonic-logging (sometimes referred to as sonic coring);

c) vibration tests (referred to as impedance or transient dynamic response);
d) high strain integrity tests (PDA);
e) parallel sonic method (MSP).

Among these methods, the first four are the most frequently used, the last (MSP) being recommended in special cases when actual length of pile embedment is in dispute.

The most popular is the low strain integrity test, in which a small hammer, which can be fitted with an accelerometer, is used to strike the top of the prepared pile. Another accelerometer is used to record the passage of the stress wave as it travels down the pile and reflects back to the surface. This record can be used to make an assessment of the impedance of the pile at any section, and the impedance is a function of the stiffness and the area, both of which are affected by pile integrity. The test is very simply and quickly carried out, making about ten blows on each pile head which can be processed later, and more than 100 piles can be tested in one day if access is suitable. It is therefore very economical. With good data and experienced interpretation, it is possible to detect defects such as bulging, cracking, and low modulus concrete, possibly caused by honeycombing in bored piles, but it is hard to get signals from depth. Aspect ratios of 20 to 1 are normally good, and up to 30 to 1 may be acceptable. A commonly used apparatus is the Pile Integrity Tester (PIT) produced by Pile Dynamics Inc., but other similar devices are available. In special cases, this method can be augmented by down-hole tests as illustrated in Figure 8.65 (CIRIA, 1997) in which a signal is picked up at various levels though a piezo-electric receiver lowered into an adjacent hole.

In major projects (highway and bridges, railways, harbours, etc.) sonic coring is preferred, but this has two main disadvantages. The method requires access tubes, made from plastic or, more usually, steel to be cast into the pile or diaphragm wall, by fixing them to the reinforcing cage prior to concreting. This is an inconvenience during construction, and therefore a significant expense. It is also much less practical for CFA piling. As a result, it is normal to preselect piles for integrity testing, which takes away the random aspect which is an essential feature of quality control. Based on acoustic principles, one measures the propagation time of sonic transmission between two piezo-electric probes, which are simultaneously raised from the base of the pile to the top. The travel time of the signal is a function of velocity, and hence concrete modulus, and distance; so, if the two tubes being used are parallel, the arrival time of the first signal should be at a constant time interval. It is easy to detect depths at which signals are delayed. In spite of the cost it is a reliable method which gives results which are independent of depth, although it is very sensitive and has been found to detect lack of bond between sound concrete and plastic access tubes.

The impedance method was more popular in the seventies and seems to be hardly used now, having given way to the low strain integrity test. High strain integrity tests, or dynamic methods, are normally used as load testing. Some other methods are still applied to some particular problems and as supplementary tests: (a) echo method (usually limited to short piles, not exceeding 20 m); and, (b) gamma ray method (for detecting defects in bored piles and diaphragm walls and controlling proposed remedial works).

All the integrity tests described are non-destructive, and are indirect, requiring subjective interpretation. If possible defects are located it may be advisable to confirm them with direct integrity testing, by coring over the whole or part of pile length. This is

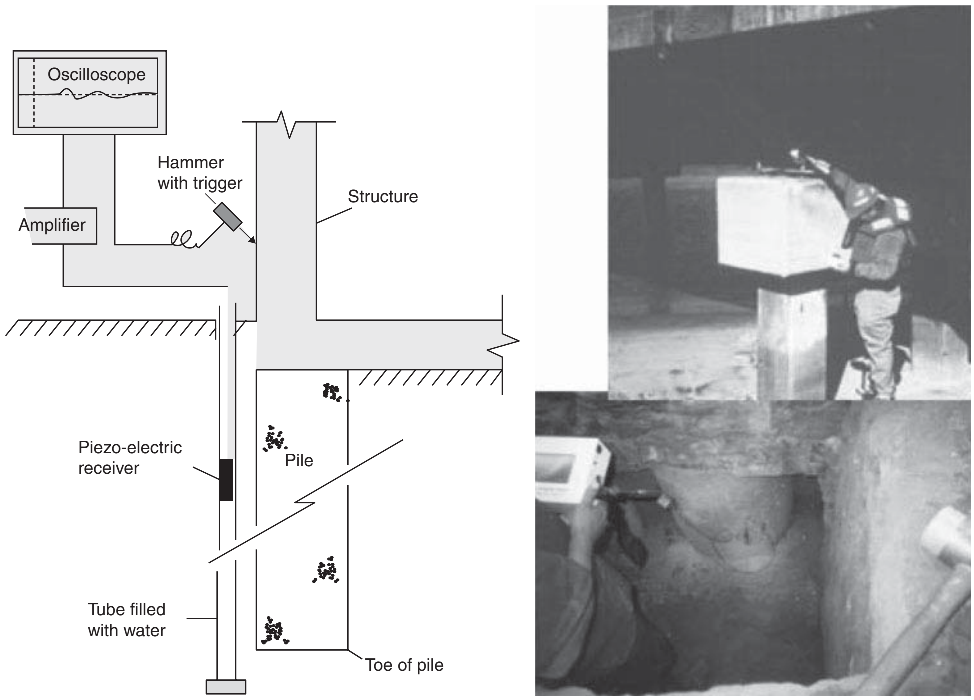

Figure 8.65 Down-hole low strain integrity tests (scheme CIRIA, 1997; pictures GEOMEC, 2004)

a costly method, but is often been prescribed in Europe for bored piles of large diameter and heavy loads (Bustamante and Frank, 1999). It allows the evaluation of concrete quality (homogeneity or segregation and discontinuity) and may show contact of the soil/concrete in the base, if the base material is of a similar strength and consistency to concrete. Coring of the pile shaft is usually imposed when non-destructive methods are not effective or the importance of the defect detected is high. In special cases a down-hole television camera may be used to allow the sides and the bottom of the core hole to be inspected.

Pile load tests

For major or complex projects, it is commonly accepted that, in addition to integrity tests, full scale (static) load tests have to be carried out to verify workmanship and, more importantly, design. Current structural codes, such as recent European Code for Geotechnical Design (CEN, 2004), are very clear in the indication that the design shall be based on one of the following approaches:

- *the results of static load tests, which have been demonstrated, by means of calculations or otherwise, to be consistent with other relevant experience;*
- *empirical or analytical calculation methods whose validity has been demonstrated by static load tests in comparable situations;*

- *the results of dynamic load tests whose validity has been demonstrated by static load tests in comparable situations;*
- *the observed performance of a comparable pile foundation, provided that this approach is supported by the results of site investigation and ground testing.*

The recent Australian Standard AS 2159-2009 "Piling – Design and installation" states in the Preface that the major changes from the previous version include:

a) *Requirement for some testing to be "normative";*
b) *Inclusion of new types of test including rapid pile testing.*

Further, when determining an ultimate geotechnical capacity from a calculated capacity using a "geotechnical resistance reduction factor", this value is restricted to 0.4 if no testing, even proof load testing, is carried out. However, it can be up to 0.9 if testing is used and all other conditions are favourable.

In Singapore, following a number of significant construction problems in the past, it has become compulsory to carry out static load testing unless very low prescribed strength values are used. As a result, about 500 to 550 static load tests are carried out each year in the island state alone, with capacities up to 6,000 tonnes.

Static load tests may be carried out on trial piles, installed for test purposes only, before the design is finalised, or on working piles which are part of the foundation. If on trial piles, they are usually taken to failure, to record the ultimate geotechnical capacity of the pile, but if on working piles they are normally restricted to less than $1.5 \times$ working load in order to verify performance. In terms of the EN 1997-1, these tests are to be carried out in the following situations: (i) when using a type of pile or installation method for which there is no comparable experience; (ii) when the piles have not been tested under comparable soil and loading conditions; or (iii) when the piles will be subject to loading for which theory and experience do not provide sufficient confidence in the design.

There are two main methods for carrying out pile tests: the Maintained Load (ML) and the Constant Rate of Penetration (CRP). In the first, loads are applied in increments, and maintained for a certain period of time. This method is generally preferred and widely used. Some recommendations that can be referenced include ISSMFE (1985), AFNOR NFP94-150, ASTM D1143-81and De Cock *et al.* (2003), and problems can arise with the definition of when a new load increment is to be applied. It is also conventional to hold the load for an extended period at some increments, such as the working load or some higher multiple of it, and this then makes it difficult to compare the settlement at different load increments. For piles and soil conditions where this is important such as in stiff clays, the CRP test is more effective, though it is more complex to carry out. A special gauge is used to measure settlement, and this is linked to a clock which drives a second pointer according to time. The load is then applied, and constantly increased and monitored, such that the actual settlement follows the clock pointer at a "constant rate of penetration". This continues until no significant increase in load is required to achieve further penetration.

The pile load test procedures, particularly with respect to the number of loading steps, the duration of these steps and the application of load cycles, should be such that conclusions can be drawn about the deformation behaviour, creep and rebound of a piled foundation from the measurements on the pile. For trial piles, the loading should be such that conclusions can also be drawn about the ultimate failure load.

Another variation which is gaining in popularity in certain parts of the world is the Bi-Directional test, better known as the Osterberg Cell or O-Cell test after its inventor, the late Jorge Osterberg. In this test, one or mare hydraulic jacks, or layers of jacks, is cast into a bored pile, along with a full array of instrumentation including extensometers and strain gauges. No surface reaction is needed since, during the test, one of the layers of jacks is expanded pushing part of the pile up against the reaction of the rest of the pile going down. In the most informative test, a lower layer of jacks near the base is expanded first, measuring the resistance of the base and some small amount of the shaft against the middle and upper shaft portions. Once ultimate resistance has been determined, the middle of the shaft is pushed downwards against the reaction of the upper section. Finally, the lower section is joined with the middle section, by closing the valves on the lower jacks, to provide reaction to raise the upper section. By suitable combining these results, the ultimate capacity of the whole pile can be estimated. This method is particularly suited to applications such as in rivers for major bridges, where conventional reaction systems are prohibitively expensive (Randolph, 2003).

High Strain Integrity Tests or Dynamic Load Tests may be used to estimate the compressive resistance of a pile. These were developed from the impact hammers and stress wave theory applied to driven piles, but has been widely extended to cover bored and CFA piles by the use of special drop hammers. The two leading exponents are probably Pile Dynamic Inc. from USA and TNO from the Netherlands. They can give very useful results, because the post-processing of the signal can model the behaviour of a layered soil, and allow reasonable estimates of shaft friction, end bearing, and even load/settlement behaviour. For best results, an adequate site investigation is needed and the method should be calibrated against Static Load Tests, see ASTMD4945.

The results of full scale static load tests with instrumentation by means of extensometer system and strain gauges in a large number of piles have been collected in Europe over more than 30 years. This has allowed the creation of a database with the measured values of unit shaft friction and base resistance values which could then be used in design charts such as those developed by LCPC in France, for the PMT and CPT methods referred above (Frank, 2008; Bustamante and Frank, 2009).

REFERENCES

Amar, S., Baguelin, F., Canépa, Y. & Frank, R. (1994). Experimental study of the settlement of shallow foundations. In: *Vertical and Horizontal Deformation of Foundation and Embankments*, ASCE Geotechnical Special Publication No. 40. ASCE, New York, 2, 1602–1610.

Anagnastopoulos, A.G., Papadopoulos, B.P. & Kawadas, M.J. (1991). Direct estimation of settlements on sand, based on SPT results. In: *Proceedings of the 10th European Conference on Soil Mechanics & Foundation Engineering*, Firenze, Italy. Balkema, Rotterdam. 1, 293–296.

Aoki, M., Shibata, Y. & Maruoka, M. (1990). Estimation of ground deformation during construction period (part 1), *Proceedings of the Annual Conference of AIJ*. B, 1649–1650 (In Japanese).

Babenderde, S., Hoek, E., Marinos, P. & Cardoso, A.S. (2004). Characterization of Granite and the Underground Construction in Metro do Porto, Portugal. In: Viana da Fonseca, A. & Mayne, P.W. (eds) *Geotechnical & Geophysical Site Characterization*. Rotterdam, Millpress. 1, 39–47.

Baguelin, F., Jézéquel, J.F. & Shields, D.H. (1978). *The Pressuremeter and Foundation Engineering*. Clausthal, Germany, Trans Tech Publications.

Baguelin, F. & Venon, V.P. (1971). The influence of piles' compressibility on the resistant stress mobilization.In: '*Le Comportement des Sols Avant la Roture*'. Special number of the Bulletin Liaison de Laboratoire des Ponts et Chaussés. Paris, LPC.

Balakrishnan, E.G., Balasubramaniam, A.S. & Phienwej, N. (1999). Load deformation analysis of bored piles in residual weathered formation. *ASCE Journal of Geotechnical and Geoenvironmental Engineering*, 125(GT2), 122–131.

Bellotti, R., Fretti, C., Jamiolkowski, M. & Tanizawa, F. (1994). Flat dilatometer tests in Toyoura sand. In: *Proceedings of the 13th International Conference on Soil Mechanics & Foundation Engineering, New Delhi*. Rotterdam, Balkema. 4, 1779–1782.

Berardi, R., Jamiolkowski, M. & Lancellotta, R. (1991). Settlement on shallow foundations in sands.Selection of stiffness on the basis of penetration resistance. *Geotechnical Special Publication* 27. ASCE, New York. 1, 185–200.

Bjerrum, L. & Eggestad, A. (1963). Interpretation of loading test on sand. In: *Proceedings of the 1st European Conference on Soil Mechanics & Foundation Engineering*, Wiesbaden. 1, 199–203.

Briaud, J.L. (1992). *The Pressuremeter.* Rotterdam, Trans Tech Publications.

Brown, D.A. (2002). Effect of Construction on Axial Capacity of Drilled Foundations in Piedmont Soils, *ASCE Journal of Geotechnical and Geoenvironmental Engineering*, 128 (GT12), 967–973.

Burland, J.B. (1989). Small is beautiful: The stiffness of soils at small strains. *Canadian Geotechnical Journal*, 26 (4), 499–516.

Burland, J.B. & Burbidge, M.C. (1985). Settlement of foundations on sand and gravel. *Proceedings of the Institution of Civil Engineers.* 78, 1325–1381.

Bustamante, M. & Doix, B. (1985). Design method for ground anchors and grouted micropiles. *Bulletin Liaison Laboratoire Central des Ponts et Chaussées*, 140, 75–92 (in French).

Bustamante, M. & Frank, R. (1999). Current French design practice for axially loaded piles. *Ground Engineering*, 32 (3), 38–44.

Bustamante, M. & Gianeselli, L. (1982). Pile bearing capacity predictions by means of static penetrometer CPT. In: *Proceedings of the 2nd European Symposium on Penetration Testing, ESOPT II, 24–27 May 1982, Amsterdam.* Rotterdam, A. A. Balkema. 2, 493–500.

Bustamante, M., Gambin, M. & Gianeselli, M. (2009). Pile design at failure using the Ménard pressuremeter: an up-date. In: Iskander M., Debra F., Laefer D.F. & Hussein M.H. (eds), *Contemporary Topics in In situ Testing, Analysis, and Reliability of Foundations, Proceedings of the International Foundation Congress and Equipment Expo'09, IFCEE'09, 15–19 March 2009, Orlando, Florida.* ASCE Geotechnical Special Publication No. 186.

Buttling, S. (1986). Instrumentation and testing of bored piles. In: *4th International Geotechnical Seminar: Field Instrumentation and In situ Measurements.* Singapore, Nanyang Technological Institute.

Buttling, S. (1990). The calibration and use of a finite difference model of single axially loaded piles. In: *International Symposium on Developments in Laboratory and Field Tests in Geotechnical Engineering Practice*, South East Asian Geotechnical Society, Bangkok.

Buttling, S. & Robinson, S.A. (1987). Bored piles – design and testing. In: *Singapore Mass Rapid Transit Conference*, Singapore.

Buttling, S. & Lam, T.S.K. (1988). Behaviour of some rock-socketed piles. In: *5th Australia-New Zealand Conference on Geomechanics*, Australian Geomechanics Society, Sydney.

Camp, W.M., Brown, D.A. & Mayne, P.W. (2002). Construction methods effects on drilled shaft axial performance. In: O'Neill, M.W. & Townsend, F.C. (eds), *Deep foundations 2002*, Geotechnical Special Publication No. 116, ASCE, Reston, Va., 193–208.

Campos e Matos, A., Pimenta, P. & Marques, H. (2004). Structural conception of the Dragon Stadium, Porto. In: Figueiras, Faria, Samento, Pipa, Henriques & Cachim (eds) *Proceedings of the Portuguese Congress of Strctural Concrete*. FEUP (in Portuguese).

Carrier, W.D. & Christian, J.T. (1973). Rigid circular plate resting on a non-homogeneous elastic half-space. *Géotechnique*, 23 (1), 67–84.

Cassan, M. (1978). *Les Essais In situ en Mécanique des Sols. Vol. 1: Realization et Interpretation*. Editions Eyrolles, Paris.

Chang, M.F. & Broms, B.B. (1991). Design of bored piles in residual soils based on field-performance data. *Canadian Geotechnical Journal*, 28 (2), 200–209.

Chen, F.H. (1965). The use of piers to preventing the uplifting of lightly structured founded on expansive soils. In: *Proceedings of the Engineering Effects of Moisture Changes in Soils International Research on Engineering Conference on Expansive Clay Soils, College Station*, 108–119.

Chen, F.H (1988). *Foundations on Expansive Soils*. 2nd edition, Elsevier Science Publications, New York.

Chen, C.S. & Hiew, L.C. (2006). Performance of bored piles with different construction methods. *Geotechnical Engineering*. 159 (3), 227–232.

Clarke, B.G. (1995). *The Pressuremeter in Geotechnical Design*. Glasgow, Blackie Academic and Professional.

Clarke, B.G. & Gambin, M.P. (1998). Pressuremeter testing in onshore ground investigations: A report by the ISSMGE Committee TC 16. In: Robertson, P.K. & Mayne P.W. (eds) *Geotechnical Site Characterisation (ISC'98)* Rotterdam, Balkema. 1429–1468.

Clarke, B.G. & Smith, A. (1993). Self-boring pressuremeter tests in weak rocks. In: Cripps *et al.* (eds) *The Engineering Geology of Weak Rocks*. Rotterdam, A.A. Balkema.

Clayton, C.R.I. & Serratrice, J.F. (1997), General report session 2: The mechanical properties of hard soils and soft rocks. In: Anagnastopoulos *et al.* (eds) *Geotechnical Engineering of Hard Soils and Soft Rocks*. Rotterdam, Balkema. 3, pp. 1839–1877.

Costa Filho, L.M., Döbereiner, L., De Campos, T.M.P. & Vargas, E. Jr. (1989). Fabric and engineering properties of saprolites and laterites. *Session 6 – Invited lecture. Proceedings of the 12th International Conference on Soil Mechanics & Foundation Engineering. Rio de Janeiro*. 4, 2463–2476.

Coutinho, R.Q., Castro, B.P.F. & Dourado, K.C.A. (2010). Identification, characterization and analysis of deep foundation in collapsible soil – Regional prison of Eunápolis, Bahia, Brazil. In: *Fifth International Conference on Unsaturated Soils, Barcelona*, 1161–1167.

Coutinho, R.Q., Dourado, K.C.A. & Souza Neto, J.B. (2004a). Evaluation of effective cohesion intercept on residual soils by DMT and CPT. In: *Proceedings of ISC-2 on Geotechnical and Geophysical Site Characterization, September 2004, Porto, Portugal*.

Coutinho, R.Q., Souza Neto, J.B. & Dourado, K.C.A. (2004b). General report: Characterization of non-textbook geomaterials. In: *Proceedings of ISC-2 on Geotechnical and Geophysical Site Characterization, Porto, Portugal*. 2, 1233–1257.

Davies, R.V. & Chan, A.K.C. (1981). Pile design in Hong Kong. *Hong Kong Engineer*. 9 (3), 21–28.

Day, R., Johnston, I. & Yang, D.Q. (2009). Design of foundations to Second Gateway Bridge – Brisbane. *Proceedings of the 7th Austroads Bridge Conference: Bridges Linking Communities*.

De Cock, F., Legrand, C. & Huybrechts, N. (2003). Axial Static Piles Load Test (ASPLT) in compression or in tension – Recommendations from International Society for Soil Mechanics & Geotechnical Engineering Subcommittee ERTC3-Piles. In: Vanicek *et al.* (eds) *Proceedings* *of the 13th European Conference on Soil Mechanics & Geotechnical Engineering, Prague*. 3, 717–741.

De Ruiter, J. & Beringen, F.L. (1979). Pile foundation for large North Sea structures. *Marine Geotechnology*, 3 (3), 267–314.

Dearman, W.R. (1976) Weathering classification in the characterisation of rock: A revision. *Bulletin International Association of Engineering Geologists*, 13, 373–381.

Décourt, L. (1992). SPT in non classical material. In: Lima, Nieto, Viotti, Buena (eds.) *Applicability of Classical Soil Mechanics Principles in Structured Soils, Proceedings of the US/Brazil Geotechnical Workshop, November 1992, Belo Horizonte, Brazil*. Mato Grosso, Univ. Fed. Viçosa. pp. 67–100.

Décourt, L. (1996). Foundation failures assessed on basis of the concept of stiffness (in Portuguese) *SEFE III* São Paulo. 1, 215–224.

Décourt, L. (2002). Capacidade de carga de estacas executadas no campo experimental de engenharia geotécnica da U.E. de Londrina. Algumas Ponderações (in Portuguese). *Proceedings of the 12th Congresso Brasileiro de Mecânica dos Solos e Engenharia Geoténcica, São Paulo/SP, Brasil*, 3, 1545–1555.

Décourt, L. & Quaresma, A.R. (1978). Bearing capacity of piles from SPT values, *5th Panamerican Congress of Soil Mechanics and Foundations Engineering, Buenos Aires*. 1, 45–54.

Dourado, K.C.A. & Coutinho, R.Q. (2007). Identification, classification and evaluation of soil collapsibility by Ménard pressuremeter. *Proceedings of the 13th Panamerican Conference on Soil Mechanics & Foundation Engineering. Isla de Margarita, Venezuela*. 724–730.

Duncan, J.M. & Chang, C.Y. (1970). Nonlinear analysis of stress and strains in soils. *ASCE Journal of the Soil Mechanics & Foundations Division*. 96 (SM5), 1629–1653.

Eslami, A. (1996). *Bearing Capacity of Piles from Cone Penetrometer Test Data*. Ph.D. Thesis, University of Ottawa, Department of Civil Engineering.

Eslami, A. & Fellenius, B.H. (1997). Pile capacity by direct CPT and CPTu methods applied to 102 case histories. *Canadian Geotechnical Journal*. 34 (6), 886–904.

Fahey M. & Carter J.P. (1993). A finite element study of the pressuremeter test in sand using a non-linear elastic plastic model. *Canadian Geotechnical Journal*, 30 (2), 348–362.

Fearenside, O.R. & Cooke, R.W. (1978). *The skin friction of bored piles formed in clay under bentonite, CIRIA Report No 77*. London, Construction Industry Research and Information Association.

Fellenius, B.H., Altaee, A., Kulesza, R. & Hayes, J. (1999). O-cell testing and FE analysis of 28-m-deep barrette in Manila, Philippines. *ASCE Journal of Geotechnical and Geoenvironmental Engineering*, 125 (GT7), 566–575.

Fellenius, B.H., Santos, J.A. & Viana da Fonseca, A. (2007). Analysis of piles in a residual soil – The ISC'2 prediction. *Canadian Geotechnical Journal*. 44, 201–220.

Ferreira, C., Mendonça, A.A. & Viana da Fonseca, A. (2004). Assessment of sampling quality in experimental sites on residual soils from Porto granite. *Proceedings of the 9th Portuguese Conference on Geotechnics, Aveiro, Portugal*. Lisbon, SPG. 1, 27–38.

Fleming, W.G.K., Weltman, A.J., Randolph, M.F. & Elson, W.K. (1985). *Piling Engineering*, New York, Wiley & Sons.

Fleming, W.G.K. & Sliwinski, Z.J. (1977).*The use and influence of bentonite in bored piles*. London, Construction Indsutry Research and Information Association (CIRIA).

Frank, R. (1984). *Theoretical Studies of Deep Foundations and Selfboring in situ Tests in LPC and Practical Results (1972-1983)* Research Report LPC No. 128, Laboratoire Central des Ponts et Chaussées, Paris (in French).

Frank, R. (1999). *Design of Shallow and Deep Foundations*. Paris, Presses de l'Ecole Nationale des Ponts et Chaussées et Techniques de l'Ingénieur, ENPC (in French).

Frank, R. (2008). *Design of foundations in France with the use of Ménard pessuremeter tests*. Invited lecture, Jornada el ensayo presiométrico en el proyecto geotécnico, 24 June 2008, Madrid, CEDEX-UPC, pp. 1–16.

Frank, R. & Zhao, S.R. (1982). Estimation par les paramètres pressiométriques de l'enfoncement sous charge axiale de pieux forés dans des sols fins. *Bulletin Liaison Laboratoire Central des Ponts et Chaussées*. 119, 17–24 (in French).

Fredlund, D.G. & Rahardjo, H. (1993). *Soil Mechanics for Unsaturated Soils*. New York, John Wiley & Sons Inc.

Gaba, A., Pickles, A. & Oliveira, R., (2004). Casa da Música do Porto: site characterisation. In: Viana da Fonseca, A. & Mayne, P.W. (eds) *Geotechnical and Geophysical Site Characterization. ISC'2*. Rotterdam, Millpress. 2, 1089–1096.

Gambin, M. (1963).The Ménard Pressuremeter and the Design of Foundations. *Actes Journées des Fondations*, Paris, Laboratoire Central des Ponts et Chaussées. (in French).

Gambin, M. & Frank, R. (2009). Direct design rules for piles using Ménard pressuremeter test. Contemporary Topics in *In situ* Testing, Analysis, and Reliability of Foundations. In: Iskander M., Debra F. Laefer D. F. & Hussein M.H. (eds.), *Proceedings of the International Foundation Congress and Equipment Expo'09 (IFCEE'09), 15–19 March 2009, Orlando, Florida*. ASCE Geotechnical Special Publication No. 186. Reston, Va, pp. 111–118.

GEOMEC (2004). *P.I.T., Pile Integrity Testing; L.S.T., Low Strain Dynamic Pile Integrity Testing*.Notes on FUNDEC Short Course, IST. Technical University of Lisbon.

GSEGWP (1990). Report on tropical residual soils – Geological Society Engineering Group Working Party. *The Quarterly Journal of Engineering Geology*, 23 (1), 1–101.

Ghionna, V.N., Manassero, M., & Peisino, V. (1991). Settlement of large shallow foundations on partially cemented gravely sand deposit using PLT data. *Proceedings of the 10th European Conference on Soil Mechanics & Foundation Engineering*, *Firenze*. Rotterdam, Balkema. 1, 1417–1422.

Gomes Correia, A., Viana da Fonseca, A. & Gambin, M. (2004). Routine and advanced analysis of mechanical *in situ* tests. Keynote lecture in Viana da Fonseca, A. & Mayne, P.W. (eds) *Geotechnical and Geophysical Site Characterization*, *ISC'2*. Rotterdam, Millpress. 1, 75–95.

Gustmão Filho, J.A., Gusmão, A.D. & Veloso, D.A. (2002). Case Records Involving Foundation in Swelling Unsaturated Soils in Brazil. In: Jucá, de Campos & Marinho (eds) *Unsaturated Soils, Lisse, Swets & Zeitlinger*. 877–882.

Hardin, B.O. & Drnevich, V.P. (1972). Shear modulus and damping in soils. *ASCE Journal of the Soil Mechanics & Foundations Division*. 98 (SM7), 667–692.

Hight, D.W. (2000). Sampling methods: evaluation of disturbance and new practical techniques for high quality sampling in soils. Keynote lecture in *7th National Congress of the Portuguese Society of Geotechnics*. Lisbon, SPG.

Holtz, W.G. & Gibbs, H.J. (1953). Engineering properties of expansive clays. *Reprinted in Award Winning ASCE Papers in Geotechnical Engineering, 1977, ASCE, New York*, 1950–1959.

Holtz, W.G. & Gibbs, H.J. (1956). Engineering properties of expansive clays. *Transactions of the American Society of Civil Engineers*, 121 (1), 641–663.

Houston, S.L. (1996). Foundations and pavements on unsaturated soils – Part 1: Collapsible soils. *Proceedings of the 1st International Conference on Unsaturated Soils – Unsat' 95, Paris – France*, 1421–1437.

Irfan, T.Y. (1988). Fabric variability and index testing of a granitic saprolite. *Proceedings 2nd International Conference on Geomechanics in Tropical Soils, Singapore*. Rotterdam, A.A. Balkema. 1, 25–35.

Jamiolkowski, M., Lancellotta, R., LoPresti, D.C.F. & Pallara, O. (1994). Stiffness of Toyoura sand at small and intermediate strain, *Proceedings of the 13th International Conference on Soil Mechanics & Foundation Engineering, New Delhi*. 3, 169–173.

Jardine, R.J., Potts, D.M., Fourie, A.B. & Burland, J.B. (1986).Studies of the influence of non-linear stress-strain characteristics in soil-structure interaction. *Géotechnique*, 36 (3), 377–396.

Jardine, R.J., Potts, D.M., St. John, H.D. & Hight, D.W. (1991). Some practical applications of a non-linear ground model. *Proceedings of the 10th European Conference on Soil Mechanics & Foundation Engineering, Firenze*, Rotterdam, Balkema. 1, 223–228.

Kahle, J.G. (1983). Predicting Settlement in Piedmont Residual Soil with the Pressuremeter Test. *Transportation Research Board Meeting.* Washington.

King, P., Stuzyk, K., Lara, O. & Steiben, G. (2001). Under slab in situ moisture content. *Proceedings, ASCE Texas Chapter Meeting*, San Antonio, Texas, 99–108.

Kondner, R. (1963). Hyperbolic stress-strain response: cohesive soils. *ASCE Journal of the Soil Mechanics & Foundations Division*. SM1, 115–143.

Konstantinidis, B., Schneider, J.P. & Van Reissen, G. (1986). *Structural Settlement of Shallow Foundations on Cohesionless Soils: Design and Performance.* Geotechnical Special Publication No 5. New York, ASCE.

Lacerda, W.A. & Almeida, M.S.S. (1995). Engineering properties of regional soils: residual soils and soft clays. *Lecture at the 10th Panamerican Conference on Soil Mechanics and Foundation Engineering, International Society for Soil Mechanics & Geotechnical Engineering, México*, 4.

Ladd, C.C. & Lambe, T.E. (1961). The identification and behavior of compacted expansive clays. *Proceedings of the 5th International Conference on Soil Mechanics and Foundation Engineering. Paris*, 1, 201–205.

Lei, G.H. & Ng, C.W.W. (2007). Rectangular barrettes and circular bored piles in saprolites. *ICE Journal of Geotechnical Engineering.* 160 (4), 237–242.

Leonards, G.A. & Frost, J.D. (1988). Settlement of shallow foundations on granular soils. *ASCE Journal of the Geotechnical Engineering Division.* 114 (GT7), 791–809.

Leroueil, S. & Vaughan, P.R. (1990). The general and congruent effects of structure in natural clays and weak rocks. *Géotechnique*, 40, 467–488.

Lo Presti, D.C.F., Pallara, O., Lancellotta, R., Armandi, M. & Maniscalco, R. (1993). Monotonic and cyclic loading behavior of two sands at small strains, *ASTM Geotechnical Testing Journal* 16 (4), 409–424.

Marchetti, S. (1980). *In situ* tests by flat dilatometer. *ASCE Journal of the Geotechnical Engineering Division.* 106 (GT3), 299–321.

Marques, E.A.G., Viana da Fonseca, A., Carvalho, P. & Gaspar, A. (2004). Example of erratic distribution of weathering patterns of Porto granite masses and its implication on site investigation and ground modelling. In: Viana da Fonseca, A. & Mayne, P.W. (eds) *Proceedings of ISC-2 on Geotechnical and Geophysical Site Characterization, Porto, Portugal*. Rotterdam, Millpress. 2, 1293–1299.

Massad, F. (1995). Pile analysis taking into account soil rigidity and residual stresses. *Proceedings 10th Pan-American Congress on Soil Mechanics and Foundation Engineering, November 1995, Guadalahara, México.* 2, 1199–1210.

Mayne, P.W. (1994). CPT-based prediction of footing response. *Measured & Predicted Behavior of Five Spread Footings on Sand (GSP 41)* Reston, Va, ASCE. 214–218.

Mayne, P.W. (2000). Geotechnical site characterization by seismic piezocone tests, *Proceedings of the 4th International Geotechnical Conference*, Soil Mechanics & Foundations Research Laboratory, Cairo University, Giza, January 24–27, 2000. 91–120.

Mayne, P.W. & Brown, D.A. (2003). Site characterization of Piedmont residuum of North America. *Characterization and Engineering Properties of Natural Soils.* Lisse, Swets & Zeitlinger. 2, pp. 1323–1339.

Mayne, P.W. & Frost, D.D. (1988). Dilatometer experience in Washington, D.C. *Transportation Research Record 1169*, Washington, D.C., National Academy Press. 122 (10), 813–821.

Mayne, P.W., Martin, G.K. & Schneider, J.A. (1999a). Flat dilatometer modulus applied to drilled shafts in the Piedmont residuum. *Behavioral Characteristics of Residual Soils, Geotechnical Special Publication No. 92*, ASCE, Reston, Va, pp. 101–112.

Mayne, P.W. & Schneider, J.A. (2001). Evaluating axial drilled shaft response by seismic cone modulus. In: Brandon, T.L. (ed.) *Foundations & Ground Improvement, Geotechnical Special Publication No 113*, GeoInstitute – ASCE, Reston, Va, pp. 655–669.

Mayne, P.W., Schneider, J.A. & Martin, G.K. (1999b). Small- and large-strain soil properties from seismic flat plate dilatometer tests. *Pre-Failure Deformation Characteristics of Geomaterials, Torino*. Rotterdam, Balkema. 1, 419–426.

McKeen, G.R. (1992). A model for predicting expansive soil behavior. *Proceedings of 7th International Conference on Expansive Soils, Dallas, Texas*, 1–6.

Ménard, L. (1955). *Pressuremeter*. French patentof invention. No 1.117.983 (in French).

Ménard, L. (1963). Estimation of load bearing capacity of foundations from pressuremeter test results. *Sols Soils* 5, 9–32 (in French).

Ménard, L. (1965). Rules for the estimation of load bearing capacity and settlements of foundations from pressuremeter test results. *Proceedings of the 6th International Conference on Soil Mechanics & Foundation Engineering*, Montreal. 295–299 (in French).

Ménard, L., Bourdon, G. & Gambin, M. (1969). Méthode générale de calcul d'un rideau ou d'un pieu sollicité horizontalement en fonction des résultats pressiomètriques. *Sols Soils No* 22/23 (6), 16–29.

Ménard, L. & Rousseau, J. (1962). L'évaluation des tassements. Tendances Nouvelles. *Sols Soils 1 (1)*, 13–30. Paris (in French).

Meyerhof, G.G. (1976). Bearing capacity and settlement of pile foundations. The 11th Terzaghi Lecture, November 5 1975, *ASCE Journal of Geotechnical Engineering*, 102 (GT3), 195–228.

Milititsky, J., Consoli, N. & Schnaid, F. (2005). *Pathologiesof Foundations*. Edições Oficina de Textos, S. Paulo, Brasil (in Portuguese).

Mitchell, J.K. & Coutinho, R.Q. (1991). Occurrence, geotechnical properties, and special problems of some soils of America. *Proceedings of the 9th Pan-American Conference on Soil Mechanics and Foundation Engineering, Viña del Mar, Chile*, 4, 1651–1741.

Ng, C.W.W. & Leung, E.H.Y. (2007a). Small-strain stiffness of granitic and volcanic saprolites in Hong Kong. In: Tan, Phoon, Hight & Leroueil (eds.) *Characterization and Engineering Properties of Natural Soils*. London, Taylor & Francis. 4, 2507–2538.

Ng, C.W.W. & Leung, E.H.Y. (2007b). Determination of Shear-Wave Velocities and Shear Moduli of Completely Decomposed Tuff. *ASCE Journal of Geotechnical and Geoenvironmental Engineering*. 133 (GT6), 630–640.

Ng, C.W.W., Li, J.H.M. & Yau, T.L.Y. (2001a). Behaviour of large diameter floating bored piles in saprolitic soils. *Soils and Foundations*, 41 (6), 37–52.

Ng, C.W.W., Yau, T.L.Y., Li, J.H.M. & Tang, W.H. (2001b). New failure load criterion for large diameter bored piles in weathered geomaterials. *ASCE Journal of Geotechnical and Geoenvironmental Engineering*, 127 (GT6), 488–498.

Oasys (2001).*VDISP – Vertical Displacement Analysis computer program*. London: Oasys Ltd.

O' Neill, M.W. & Poormoayed, N. (1980). Methodology for foundations on expansive clays. *Journal of the Geotechnical Emgineering Division*, ASCE, 106 (GT12).

O'Neill, M.W. & Reese, L.C. (1999). *Drilled Shafts: Construction Procedures & Design Methods*, Volumes I & II, Publication No. FHWA-IF-99-025, U.S. Dept. of Transportation. Dallas, ADSC.

Parry, R.H.G. (1978). Estimating foundation settlements in sand from plate bearing tests. *Géotechnique*. 28(1), 107–118.

Phienwej, N., Balakrishnan, E.G. & Balasubramaniam, A.S. (1994). Performance of bored piles in weathered meta-sedimentary rocks in Kuala Lumpur, Malaysia. *Proceedings of the Symposium on Geotextiles, Geomembranes and other Geosynthetics in Ground Improvement* *on Deep Foundations and Ground Improvement Schemes, Bangkok*. Rotterdam, Balkema. 251–260.

Poulos, H.G. (1987). From theory to practice in pile design (E.H. Davis Memorial Lecture) *Transactions of the Australian Geomechanics Society*, Sydney, 1–31.

Poulos, H.G. (1989). Pile behavior: theory and application, 29th Rankine Lecture, *Géotechnique*, 39 (3), 363–416.

Poulos, H.G. & Davis, E.H. (1980). *Pile Foundation Analysis and Design*. New York, Wiley & Sons.

Prevost, J.H. & Keane, C.M. (1990). Shear stress-strain curve generation from simple material parameters. *ASCE Journal of Geotechnical Engineering* 116 (GT8), 1255–1263.

Puppala, A.J., Enayatpour, S., Vanapalli, S., and Intharasombat, N. (2004). Review of current methods for swell characterization of subsoils for transportation infrastructure design. *ASCE, Geotechnical Special Publication No. 126 – Geotechnical Engineering for Transportation Projects*. 1, 1105–1114.

Puzrin, A.M. & Burland, J.B. (1998). Nonlinear model of small-strain behavior of soils. *Géotechnique*, 46 (1), 157–164.

Randolph, M.F. (2003). Science and empiricism in pile foundation design, 43rd Rankine Lecture, *Géotechnique*, 53 (10), 847–875.

Randolph, M.F. & Wroth, C.P. (1978). Analysis of deformation of vertically loaded piles. *ASCE Journal of the Geotechnical Engineering Division*, 104 (GT12), 1465–1488.

Randolph, M.F. & Wroth, C.P. (1979). A simple approach to pile design and the evaluation of pile tests. *Behavior of Deep Foundations*, ASTM STP 670, 484–499.

Robertson, P.K. (1990). Soil classification using the cone penetration test. *Canadian Geotechnical Journal*, 27 (1), 151–158.

Robertson, P.K. (1991). Estimation of foundation settlements in sand from CPT. In: *Vertical and Horizontal Deformation of Foundation and Embankments, ASCE Geotechnical Special Publication No* 40. 2 (27), 764–778.

Robertson, P.K., Campanella, R.G., Davies, M.P. & Sy, A. (1988). Axial capacity of driven piles in deltaic soils using CPT. *Penetration Testing 1988*. Rotterdam, Balkema. 2, 919–928.

Rocha Filho, P. (1986). Discussion on "Settlement of foundations on sand and gravel" by Burland J.B. & Burbidge, M.C. 1985, *Proceedings of Institution of Civil Engineers*. 79, 1633–1635.

Sabatini, P.J., Bachus, R.C., Mayne, P.W., Schneider, J.A. & Zettler, T.E. (2002). Evaluation of Soil and Rock Properties. *Technical Manual. FHWA-IF-02-034*. Washington, Federal Highway Administration.

Santos, J.A., Duarte, R.J.L, Viana da Fonseca, A.& Costa Esteves, E. (2005). ISC'2 experimental site – Prediction and performance of instrumented axially loaded piles. *Proceedings of the 16th International Conference on Soil Mechanics & Geotechnical Engineering, September 21 – 25 2005, Osaka, Japan*. 2, 2171–2174.

Schmertmann, J.H. (1970). Static cone to compute static settlement over sand. *ASCE Journal of the Soil Mechanics and Foundation Division*. 96(3), 1011–1043.

Schmertmann, J.H. (1978). *Guidelines for Cone Test, Performance and Design*. Federal Highway Administration, Report FHWA-TS-78209, Washington.

Schmertmann, J.H. (1986). Dilatometer to compute foundation settlement, *Proceedings of the ASCE Specialty Conference, In situ '86, VPI, Blacksburg, Virginia*, 303–321.

Schmertmann, J.H., Hartman, J.P. & Brown, P.R. (1978). Improved strain influence factor diagram. *ASCE Journal of the Geotechnical Engineering Division*. 104 (8), 1131–1135.

Schnaid, F. (2005). Geo-characterisation and properties of natural soils by *in situ* tests. *Keynote Lecture. 16th International Conference on Soil Mechanics & Geotechnical Engineering, Osaka*. Rotterdam, Millpress. 1, 3–45.

Schnaid, F., Lehane, B.M. & Fahey, M. (2004). *In situ* test characterisation of unusual geomaterials. In: Viana da Fonseca, A. & Mayne, P.W. (eds) *Proceedings of ISC-2 on Geotechnical and Geophysical Site Characterization, Porto, Portugal*. Rotterdam, Millpress. 1, 49–74.

Schneider, R.L., Muhlram, H., Tommasi, E., Medeiros, R.A., Daemon, R.F. & Nogueira, A.A. (1974). Revisão Estratigráfica da Bacia do Paraná (in Portuguese). *Congresso Brasileiro de Geologia, 1974, Porto Alegre, Sociedade Brasileira de Geologia*, 1, 41–65.

Seed, H.B. & Idriss, I.M. (1982). *Ground motion and soil liquefaction during earthquakes*, Monograph, Earthquake Engineering Research Institute, Oakland, Ca.

Seed, H.B., Woodward, R.J., Jr. & Lundgren, R. (1962). Prediction of swelling potential for compacted clays: *ASCE Journal of the Soil Mechanics and Foundation Division*. 88, (SM3), Part I, 53–87.

Singh, H., Omar, H. & Huat, B.B.K. (2006). Geological investigations for foundations. In: Huat, B.B.K., Ali, F.H., Omar, H. & Singh, H. (eds) *Foundation Engineering: Design and Construction in Tropical Soils*. London, Taylor & Francis.

Snethen, R.R. (1984). Evaluation of expedient methods for identification and classification of potentially expansive soils. *Proceedings of 5th International Conference on Expansive Soils*, Australia, 22–26.

Snethen, D.R., Johnson, L.D. & Patrick, D.M. (1977). *An Evaluation of Expedient Methodology for Identification of Potentially Expansive Soils*. Soil and Pavements Laboratory, US Army Engineering Waterway Experiment Station, Vicksburg, MS. Rep. No FHWA-RE-77-94, NTIS, PB-289-164.

Stroud, M.A. (1974). The Standard Penetration Test in insensitive clays and soft rocks. *Proceedings of the European Seminar on Penetration Testing 1*, **2** (2), 367–375.

Stroud, M.A. (1988). The Standard Penetration Test – Its application and interpretation, *Proceedings of Penetration Testing in the UK*. London, Thomas Telford. 29–48.

Tan, Y.C., Chen, C.S. & Liew, S.S. (1998). Load transfer behavior of cast-in-place bored piles in tropical residual soils of Malaysia. *Proceedings of the 13th Southeast Asian Geotechnical Conference, Taipei*, 563–571.

Tatsuoka, F. & Kohata, Y. (1995). Stiffness of hard soils and soft rocks in engineering applications. *Proceedings 1st International Conference on Pre-failure Deformation Characteristics of Geomaterials, Sapporo*. 2, 947–1063.

Tatsuoka, F. & Shibuya, S. (1992). Deformation Characteristics of Soils and Rocks from Field and Laboratory Tests. Keynote lecture in: Proceedings of the *9th Asian Regional Conference on Soil Mechanics & Foundation Engineering, Bangkok*. Rotterdam, A.A. Balkema. 2, 101–170.

Terzaghi, K. & Peck, R.B. (1967). *Soil Mechanics in Engineering Practice*. 2nd Edition, New York, John Wiley & Sons.

Toh, C.T., Ooi, T.A., Chiu, H.K. Chee, S.K. & Ting, W.H. (1989). Design parameters for bored piles in a weathered sedimentary formation. *Proceedings of the 12th International Conference on Soil Mechanics and Foundation Engineering, Rio de Janeiro*. Rotterdam, Balkema. 2, 1073–1078.

Topa Gomes, A. (2009). *Elliptical Shafts by the Sequential Method of Excavation on Vertical Direction*. The Case of Metro do Porto. PhD Thesis, Faculdade de Engenharia, University do Porto. (In Portuguese).

Touma, F.T. & Reese, L.C. (1972). *Drilled Shafts; Construction Procedures and Design Methods*. U.S. Department of Transportation, FHWA-HI-88-042, Dallas, Texas.

Tumay, M.T. & Fakhroo, M. (1981). Pile capacity in soft clays using electric QCPT data. *ASCE, Cone Penetration Testing and Experience, October 26–30, 1981, St. Louis*, 434–455.

Tuna, C. (2006). *Tests and Analysis of the Behaviour of Laterally Loaded Piles in Residual Soils from Granite*. MSc Thesis. FEUP, University of Porto (in Portuguese).

Tuna, C., Viana da Fonseca, A. & Santos, J.A. (2008). Data interpretation and analysis of the behavior of laterally loaded piles in ISC'2 experimental site by recourse of PMT and DMT based methods. In: Huang, A-B. & Mayne, P., (eds) *Proceedings of the 3rd International Conference on Site Characterization (ISC'3), 1–4 April 2008, Taiwan*. London, Taylor & Francis.

Van Der Veen, C. (1953). The bearing capacity of a pile. *Proceedings of the 3rd International Conference Soil Mechanics & Foundation Engineering, Zurich*. 2, 84–90.

Vargas, M. (1971). Geotechnics of residual soils. *Solos & Rochas. Latin-American Journal of Geotechnics*. 1, 20–41.

Vargas, M. (1985). The concept of tropical soils. *Proceedings of the 1st International Conference on Geomechanics in Tropical Lateritic and Saprolitic Soils, February 1985, Brasília, Brazil*. International Society for Soil Mechanics & Foundation Engineering. 3, 101–134.

Vaughan, P.R. (1985). Mechanical and hydraulic properties, particularly as related to their structure and mineral components. General Report. *Proceedings of the 1st International Conference on Geomechanics in Tropical Lateritic and Saprolitic Soils. February 1985, Brasília, Brazil*. International Society for Soil Mechanics & Foundation Engineering. 3, 231–336.

Vaughan, P.R., Maccarini, M. & Mokhtar, S.M. (1988). Indexing the engineering properties of residual soils. *Quarterly Journal of Engineering Geology*. 21, 69–84.

Viana da Fonseca, A. (1996). *Geomechanics in Residual Soils from Porto Granite. Criteria for the Design of Shallow Foundations*. Ph.D. Thesis, University of Porto. (In Portuguese).

Viana da Fonseca, A. (1998). Identifying the reserve of strength and stiffness characteristics due to cemented structure of a saprolitic soil from granite. *Proceedings of the 2nd International Symposium on Hard Soils – Soft Rocks, Naples*. Rotterdam, Balkema. 1, 361–372.

Viana da Fonseca, A. (1999). Surface loading tests for mechanical characterisation of a saprolitic soil from granite of Porto. *Proceedingsof the 9th Pan-American Conference on Soil Mechanics and Geotechnical Engineering*, *Foz do Iguassu, Brasil*. 1, 403–409.

Viana da Fonseca, A. (2001). Load Tests on residual soil and settlement prediction on shallow foundation. *ASCE Journal of Geotechnical and Geoenvironmental Engineering*. 127 (10), 869–883.

Viana da Fonseca, A. (2003). Characterizing and deriving engineering properties of a saprolitic soil from granite, in Porto. In: Tan et al. (eds) *Characterization and Engineering Properties of Natural Soils*. Lisse, Swets & Zeitlinger. 1341–1378.

Viana da Fonseca, A. (2006). *Ground Investigations and Soil Characterization by In situ Testing*. DVD – Multimedia (Films, Pictures and Technical Notes) Reg. Assoft N. 1329/D/06. Pub. Univ. of Porto (IC-FEUP).

Viana da Fonseca, A. & Almeida e Sousa, J. (2001). At rest coefficient of earth pressure in saprolitic soils from granite. *Proceedings of the 15th International Conference on Soil Mechanics & Geotechnical Engineering, Istanbul*. 1, 397–400.

Viana da Fonseca, A. & Almeida e Sousa, J. (2002). Hyperbolic model parameters for FEM analysis of a footing load test on a residual soil from granite. In: J.-P. Magnan (ed.) *PARAM 2002: International Symposium on Identification and Determination of Soil and Rock Parameters for Geotechnical Design*. Paris, Presses L'ENPC. 1, 429–443.

Viana da Fonseca, A. & Cardoso, A.S. (1999). Linearly increasing elastic analysis of surface loading tests on a saprolitic soil from granite. *Proceedings 9th Panamerican Conference on Soil Mechanics and Geotechnical Engineering*, *Foz do Iguassu, Brasil*. 3, 1527–1535.

Viana da Fonseca, A., Carvalho, J., Ferreira, C., Santos, J.A., Almeida, F., Pereira, E., Feliciano, J., Grade, J. & Oliveira, A. (2006) Characterization of a profile of residual soil from granite combining geological, geophysical, and mechanical testing techniques. *International Journal of Geotechnical and Geological Engineering*, 24 (5), 1307–1348.

Viana da Fonseca, A. & Coutinho R.Q. (2008). Characterization of residual soils. Keynote Lecture, in: Huang, A-B. & Mayne, P. (eds) *Proceedings of the 3rd International Conference on Site Characterization (ISC'3), 1–4 April 2008, Taiwan*. London, Taylor & Francis. 195–248.

Viana da Fonseca, A., Marques, E.A.G., Carvalho, P. & Gaspar, A. (2003). Implication of heterogeneity of Porto granite in the site investigation and classification options. Design parameters definitions for cut-and-cover stations design in Metro do Porto. *I Jornadas Luso-Espanholas de Geotecnia, CEDEX, Madrid*. (in Portuguese).

Viana da Fonseca, A., Matos Fernandes, M. & Cardoso, A.S. (1997). Interpretation of a footing load test on a saprolitic soil from granite. *Géotechnique*, 47(3), 633–651.

Viana da Fonseca, A., Matos Fernandes, M. & Cardoso, A.S. (1998). Characterization of a saprolitic soil from Porto granite by *in situ* testing. *Proceedings of the 1st International Conference on Site Characterization – ISC'98, Atlanta*. Rotterdam, Balkema. 2, 1381–1388.

Viana da Fonseca, A. & Santos, J. (2008). *International Prediction Event. Behaviour of Bored, CFA and Driven Piles in Residual Soil. ISC'2 experimental site*. University of Porto (FEUP) & Technical University of Lisbon (IST-UTL) www.fe.up.pt/sgwww/labgeo/pdf/Book-IppE-Piles-ISC2.pdf.

Viana da Fonseca, A., Santos, J.A., Massad, F. & Costa Esteves, E. (2007). Analysis of piles in residual soil from granite considering residual loads. *International Journal* "*Soil and Rocks*". 30 (1), 63–80.

Viana da Fonseca, A., Vieira de Sousa, J.F. & Cruz, N. (2001). Correlations between SPT, CPT, DPL, PMT, DMT, CH, SP and PLT Tests Results on Typical Profiles of Saprolitic Soils from Granite. *Proceedingsof the International Conference on In situ Measurement of Soil Properties and Case Histories, 21–23 May 2001, Bali, Indonesia*. Parayangan Catholic University. *1, 577–584*.

Vijayvergiya, V.N. & Ghazzaly, O.I. (1973). Prediction of swell potential for natural clays. *Proceedings of the 3rd International Research and Engineering Conference on Expansive Clay Soils*.

Wahls, H.E. & Gupta, M. (1994). Settlement of shallow foundations on sand. In: *Vertical and Horizontal Deformation of Foundation and Embankments*, Geotechnical Special Publication, No 40. New York, ASCE. 1, 190–206.

Wray, W.K. (1995). So your home is built on expansible soils: a discussion of how expansive soils affect buildings. *Shallow Foundations Committee of the Geotechnical Engineering Division of the American Society of Civil Engineers, ASCE*.

Wroth, C.P. (1982). British experience with the self-boring pressuremeter. *Proceedings of the International Symposium on the Pressuremeter and its Marine Application*, Paris. 143–164.

Yogeswaran, M. (1995). Geological considerations in the development of the Kuching area. *Proceedings of the Dialogue Session on Geological and Geotechnical Considerations in Civil Works*. Geological Survey of Malaysia. Kuala Lumpur. 59–101.

STANDARDS, GOVERNMENT AND OFFICIAL PUBLICATIONS

AFNORNFP94-150 (1991). *Essai Statique de Pieu Isolé Sous Compression Axiale*. Norme Française (in French).

AFNOR DTU-13.2 (1992). *Deep Foundations for the Building Industry P11-212* (in French).

ASTM D1143-81 (1994). *Piles Under Static Axial Compressive Load. Standard Test Method*.

ASTM D420-D5779 (2004). *Standard Test Method for Prebored Pressuremeter Testing in Soils*.

ASTM D4945 (2008). *Standard Test Method for High-Strain Dynamic Testing of Deep Foundations*.

Canadian Geotechnical Society (1992) *Canadian Foundation Engineering Manual* (CFEM) 3rd Edition, Vancouver, BiTech Publishers.

EN1997-1 (2004). *Eurocode 7: Geotechnical Design – General Rules*.

FASCICULE No 62 – Titre V(1993) *Technical Rules for the Design of Foundations of Civil Engineering Structures*. Technical Manuals for Public Construction Works, Textes Officiels No 93–3 T.O. (in French).

GCO Geoguide 2 (1987). *Guide to Site Investigation*.

GEO Publication No 1/2006 (2006). *Foundation Design and Construction*.

ISSMFE (1985). Axial pile loading test – Part 1: Static loading. *Geotechnical Testing Journal*. 8(2): 79–90.

BIBLIOGRAPHY

Aoki, N. & Velloso, D.A. (1975). An approximate method to estimate the bearing capacity of piles. In: *5th Pan-American Congress of Soil Mechanics and Foundations Engineering, Buenos Aires*, 1, 367–376.

Briaud, J.L. & Tucker, L.M. (1988). Measured and predicted axial response of 98 piles. *ASCE Journal of Geotechnical Engineering,* 114 (GT9), 984–1001.

Burns, S.E. & Mayne, P.W. (1996). Small- and high-strain soil properties using the seismic piezocone. *Transportation Research Record 1548*, Washington, D.C., National Academy Press. 81–88.

Bustamante, M. & Gianeselli L. (1981). Prévision de la capacité portante des pieux isolés sous charge verticale. Règles pressiométriques et pénétrométriques. *Bulletin Liaison Laboratoire Central des Ponts et Chaussées,* 113, 83–108 (in French).

Bustamante, M. & Gianeselli, L. (1993). Design of auger displacement piles from *in situ* tests. In: *2nd International Geotechnical Seminar: Deep Foundations on Bored and Auger Piles,* Rotterdam, Balkema.

Fellenius B.H. (1989). Tangent modulus of piles determined from strain data. In: Kulhawy, F.H. (ed.) *ASCE, Geotechnical Engineering Division, The 1989 Foundation Congress*. 1, 500–510.

Fellenius, B.H., (1999). Bearing capacity – A delusion? *Proceedings of the Deep Foundation Institute Annual Meeting, October 14–16, 1999, Dearborn, Michigan*.

Fellenius, B.H. (2001a). *What capacity value to choose from the results a static loading test*. Deep Foundations Institute, Fulcrum, May 2001.

Fellenius, B.H. (2001b). Where to plot average loads from telltale measurements in piles. *Geotechnical News Magazine*. 19 (2), 32–34.

Fellenius, B.H. (2001c). From strain measurements to load in an instrumented pile. *Geotechnical News Magazine*. 19 (1), 35–38.

Fellenius, B.H. (2002a). *Basics of Foundation Design*. Electronic Edition [www.Geoforum.com].

Fellenius, B.H. (2002b). Determining the true distribution of load in piles. In: O'Neill, M.W., Townsend, F.C. (eds) *ASCE International Deep Foundation Congress: An International Perspective on Theory, Design, Construction, and Performance, February 14–16, 2002, Orlando, Florida,* Geotechnical Special Publication No. 116 (2), 1455–1470.

Fellenius, B.H. (2002c). Determining the resistance distribution in piles. Part 1: Notes on shift of no-load reading and residual load. Part 2: Method for determining the residual load. *Geotechnical News Magazine*. 20 (2), 35–38, and (3), 25–29.

Fellenius, B.H. & Altaee, A. (1995). The critical depth – How it came into being and why it does not exist. *Proceedings of the Institution of Civil Engineers, Journal of Geotechnical Engineering*. 113 (2), 107–111.

Fellenius, B.H. & Eslami, A. (2000). Soil profile interpreted from CPTu data. In: Balasubramaniam, A.S., *et al.* (eds) *Proceedings of Year 2000 Geotechnics Conference, Southeast Asian Geotechnical Society, November 27–30, 2000, Asian Institute of Technology, Bangkok, Thailand*. 1, 163–171.

Fellenius, B.H., Hussein, M., Mayne, P. & McGillivray, R. T. (2004). Murphy's law and the pile prediction event at the 2002 ASCE Geo Institute's Deep Foundation Conference. *Proceedings of the Deep Foundation Institute 29th Annual Conference on Deep Foundations, Vancouver*, 29–43.

Fellenius, B.H. & Salem, H. (2003). Prediction of response to static loading of three piles at the ISC'2 Experimental Site. *Second International Conference on Site Characterization*, *Porto, Portugal*.

Ferreira, C. (2009). *The Use of Seismic Wave Velocities in the Measurement of Stiffness of a Residual Soil*. Ph.D. Thesis, University of Porto, Portugal.

Ferreira, C., Viana da Fonseca, A. & Nash, D. (2011). Shear wave velocities for sample quality assessment on a residual soil. *Soils and Foundations*. 51 (4), 683–692.

Finke, K.A., Mayne, P.W. & Klopp, R.A. (1999). Characteristic piezocone response in Piedmont residual soils. *Behavioral Characteristics of Residual Soils*. *ASCE Geotechnical Special Publication No. 92*. Reston, Va, pp. 1–11.

Fioravante, V., Ghionna, V.N., Jamiolkowski, M. & Pedroni, S. (1995). Load carrying capacity of large diameter bored piles in sand and gravel. *Proceedings of the 10th Asian Regional Conference on Soil Mechanics and Foundation Conference, Beijing*.

Lee, J.H. & Salgado, R. (1999). Determination of pile base resistance in sands. *ASCE Journal of Geotechnical & Geoenvironmental Engineering*. 125 (GT8), 673–683.

Mayne, P.W., Brown, D.A., Vinson, J., Schneider, J.A. & Finke, K.A. (2000). Site characterization of Piedmont residual soils at the NGES, Opelika, AL. *National Geotechnical Experimentation Sites, Geotechnical Special Publication No. 93*, ASCE, Reston, Va, pp. 160–185.

Philipponnat, G. (1980). Calculus Practical Method of a single pile using SPT. *Revue Française de Géotechnique*, 10, 55–64.

Puppala, A.J., Hanchanloet, S., Jadeja, M. & Burkart, B. (1999). Evaluation of Sulfate Induced Heave by Mineralogical and Swell Tests. *Proceedings of the 11th Pan-American Conference on Soil Mechanics and Geotechnical Engineering, Foz do Iguaçu, Brazil*.

Rollins, K.M., Clayton, R.G., Mikesell, R.C., & Blaise, B.C. (2005). Drilled shaft side friction in gravelly soils. *ASCE Journal of Geotechnical and Geoenvironmental Engineering*, 131 (8), 987–1003.

Santos, J.A. (1999). *Soil Characterization by Dynamic and Cyclic Torsional Shear Tests. Application to the Study of Piles under Lateral Static and Dynamic Loadings*. Ph.D. Thesis, Technical University of Lisbon, Portugal (in Portuguese).

Sousa, C.T. (2006). *Tests and Response Analysis of Piles in Granite Residual Soil under Horizontal Actions*. M.Sc. Thesis, Faculty of Engineering of the University of Porto, Portugal (in Portuguese).

Sowers, G.F. (1994). Residual soil settlement related to the weathering profile. In: *Vertical and horizontal deformation of foundation and embankments, ASCE Geotechnical Special Publication No* 40. ASCE, New York. 2, 1689–1702.

Takesue, K., Sasao, H. & Matsumoto, T. (1998).Correlation between ultimate pile skin friction and CPT data. *Geotechnical Site Characterization* (2), Rotterdam, Balkema. 1177–1182.

Viana da Fonseca, A. (1999). Surface loading tests for mechanical characterisation of a saprolitic soil from granite of Porto. *Proceedingsof the 9th Pan-American Conference on Soil Mechanics and Geotechnical Engineering*, *Foz do Iguassu, Brasil*. 1, 403–409.

Viana da Fonseca, A. & Quintela, J. (2010). Modelling the behaviour of a retaining wall monitored during the excavation for deep station in Metro do Porto. Submitted to *Geomechanics and Geoengineering: An International Journal*.

Vucetic, M. & Dobry, R. (1991). Effect of soil plasticity on cyclic response. *ASCE Journal of Geotechnical Engineering* 117 (GT1), 89–107.